Towards Elucidation of the Phenazine Biosynthesis Pathway of *Pseudomonas* with the Structural and Functional Analysis of the enzymes PhzA, B, G and BcepA

DISSERTATION

zur Erlangung des akademischen Grades
eines Doktors der Naturwissenschaften (Dr. rer. nat.)
des Fachbereichs Chemie der Universität Dortmund

Angefertigt am Max-Planck-Institüt für Molekulare Physiologie
In Dortmund

Eingereicht von

Ekta G. Ahuja (Niki)
Aus Ahmedabad/Indien

Dortmund, 2006

1. Gutachter : Prof. Dr. R.S.Goody
2. Gutachter : Prof. Dr. R. Winter

Towards Elucidation of the Phenazine Biosynthesis Pathway of *Pseudomonas* with the Structural and Functional Analysis of the enzymes PhzA, B, G and BcepA

DISSERTATION

Submitted towards partial fulfillment of requirement
for the degree of

DOKTOR DER NATURWISSENCHAFTEN
(DR. RER. NAT.)

in the Department of Chemistry,
University of Dortmund, Germany

By

Ekta G. Ahuja (Niki)
Max Planck Institute for Molecular Physiology
&
Department of Chemistry, University of Dortmund

2006

Die vorliegende Arbeit wurde in der Zeit von Januar 2003 bis September 2006 am Max-Planck-Institut für Molekulare physiologie in Dortmund unter der Anleitung von Prof. Dr. Roger S Goody, Dr. Wulf Blankenfeldt und Prof. Dr. Roland Winter durchgeführt.

Hermit versichere ich an Eides statt, dass ich die vorliegende Arbeit selbständig und nur mit den angegeben Hilfsmitteln angefertigt habe.

Dortmund, 2006 Ekta G Ahuja (Niki)

CONTENTS

SYMBOLS AND ABBREVIATIONS

Å	Ångstrom (0.1nm)
ADP	Adenosinediphosphate
APCI	Atmospheric pressure controlled ionisation
ATP	Adenisinetriphosphate
BSA	*Bovine Serum Albumin*
bp	base pair
cAMP	cyclic adenosine 5' phosphate
CCD	Charge coupled devices
C-terminus	Carboxyterminus
Da	Dalton
DNA	Desoxyribonucleic acid
EDTA	Ehtylendiamintetraacetate
ESRF	European Synchrotron Radiation Facility
E. coli	*Escherichia coli*
ESI-MS	electrospray ionisation mass spectroscopy
F_{calc}, F_{obs}	Structure-factor amplitudes (calc:calculated, obs: observed)
FMN	flavin mononucleotide
FPLC	Fast Performance Liquid Chromatography
g	gram
h	hour
HEPES	4-(2-Hydroxyethyl)-piperazin-1-ethan-sulfonsäure
HPLC	*High Performance Liquid Chromatography*
IPTG	Isopropyl-β-D-1-thiogalactopyranosid
kb	kilo-base pair
kDa	kilo-Dalton
kJ	kilo-Joule
λ	wavelength, Lambda
MAD	multiple wavelength anomalous dispersion
MALDI	matrix assisted Laser desorption/ionization
MES	
min	minute
MIR	multiple isomorphous replacement
mM	milimolar
MR	molecular replacement
NCS	non-crystallographic symmetry
nm	Nanometer
NMR	nuclear magnetic resonance
N-terminus	Aminoterminus
PCA	Phenazine-1-carboxylate acid
PCR	*Polymerase Chain Reaction*
PDB	Protein Data Bank
PDC	Phenazine-1,6-dicarboxylate acid
PEG	Polyetheleneglycol

PMSF	phenylemethylsulphonylfluoride
RNA	Ribonucleic acid
rmsd	root mean square deviations
rpm	revolution per minute
RT	room temperature
s	second
Se	Selinium
SAD	Single-wavelength anomalous dispersion
SDS-PAGE	Sodiumdodecylsulphate-Polyacrylamide gel electrophoresis
SeMet	Seleno-L-Methionine
TEMED	N,N,N,N -Tetramethyl-Ethylenediamine
TRIS	Tris-(hydroxymethyl)-aminomethane
U	Units
UV	Ultraviolet
V	Volt
µl	microliter
µM	micromolar

Amino Acids Abbreviations

Name	3-letter code	1-letter code
Alanine	Ala	A
Argenine	Arg	R
Asparagine	Asn	N
Aspartate	Asp	D
Cysteine	Cys	C
Glutamine	Glu	E
Glutamate	Gln	Q
Glycine	Gly	G
Histidine	His	H
Isoleucine	Ile	I
Leucine	Leu	L
Lysine	Lys	K
Phenylalanine	Phe	F
Methionine	Met	M
Proline	Pro	P
Serine	Ser	S
Threonine	Thr	T
Tryptophane	Trp	W
Tyrosine	Tyr	Y
Valine	Val	V

Introduction

Begin at the beginning and go on
till you come to the end: then stop.
- The King (Alice in wonderland, Lewis Carroll)

1.0 Introduction

Microorganisms produce an array of low molecular weight organic compounds with a wide range of biological activities. These compounds have interested chemists for more than a century and a versatile gamut has been isolated, analyzed and characterised. However, this process is by no means complete and the inventory of newly discovered compounds increases with each passing year. The compounds discovered so far have diverse chemical structures with intricate, idiosyncratic molecular frameworks displaying a remarkable variety and subtlety (Vining, 1990). They were recognised as products of specialised metabolism and the reason for their existence though not immediately apparent, was speculated on ever since their discovery more than a century ago. 'Secondary metabolites' was the name given to these compounds by plant phytologists (Barger, 1907) and this term was brought into common use by J. D. Bu'Lock (Bu'Lock, 1961).

The biosynthesis of all secondary metabolites has been found to arise from intermediates or products of primary metabolism (Vining, 1990). Unlike intermediates and cofactors which participate in cell-structure syntheses, energy transduction and other cellular processes, secondary metabolites do not seem to be essential either for growth or reproductive metabolism of the organism. These compounds are usually distinctive products of a particular group of organisms, sometimes even of a single strain and require a particular set of physiological conditions for the initiation of their synthesis. Prior to the antibiotic era, relatively few microbial products were discovered based on biological activity. However, in the late nineteenth century, the biochemical basis of microbial antagonism of secondary metabolites was discovered and since then these metabolites have been intensely investigated and a plethora of these compounds has been isolated and examined.

Phenazines produced under quorum-sensing control in pseudomonads have long been categorised as 'secondary metabolites' (Leisinger et al., 1979; Vining 1990; Kerr 2000). They satisfy the paradigms of secondary metabolites, namely, they are natural products synthesised by cells after reaching the stationary phase, display no obvious effects on cell growth and have highly sensitive requirements

of media, pH and temperature for their biosynthesis. However, recently, phenazines have been discovered to play more essential roles namely, as biocontrol agents and facilitators of root colonisation in plants (Lugtenberg et al., 1999; Haas et al., 2000; Lee et al., 2000), in transcriptional modulation (Goh et al., 2002), mineral reduction and scavenging (Hernandez et al., 2004) etc, all of which have far-reaching consequences not only for the well-being but also ultimately survival of the organism. Therefore, this notion of phenazines being secondary metabolites, indeed the phenomenon of secondary metabolism, is now being questioned and revised (Price-Whelan et al., 2005).

1.1 Discovery of phenazines

As early as the 1860s, a blue colouration was observed in the pus of injured soldiers, which on microscopic examination, was found to be caused by a rod-shaped micro-organism, named *Bacillus pyocyaneus* (later *Pseudomonas aeruginosa*) (Villavicencio et al., 1998). Again, in 1889, it was discovered that the concentrated cell-free culture fluid of the same *Pseudomonas aeruginosa* was capable of killing several different kinds of bacteria. This concentrate was used as therapy for meningitis, influenza and diphtheria until the first few decades of the last century (Leisinger *et al.,* 1979). The active compound in this culture-concentrate was isolated and this blue-coloured organic molecule named 'pyocyanin' (Fordos, 1859; Emmerich & Low, 1899). The discovery of antimicrobial properties of this compound aroused further interest and instigated deeper investigation into the 'secondary metabolites' of pseudomonads and of other micro-organisms in general (Woodruff, 1966; Aoyagi et al., 1978) . This led to the discovery of a range of compounds of bacterial origin, similar to pyocyanin, which were collectively designated as 'phenazines'.

1.2 Prevalence of phenazine producers

As mentioned in the preceding paragraph, the earliest known phenazines were discovered from the species *Pseudomonas aeruginosa.* These included, first, the blue-coloured pyocyanin and later the green chlororaphine (Leisinger *et al.,*

1979). For a long time, it was thought that this organism was the sole synthesiser of phenazines in nature. However, in the second half of the 20th century a range of micro-organisms capable of synthesising phenazines were discovered. It is now known that micro-organisms are the exclusive source of phenazines in nature and phenazine producers are widely distributed in the biosphere.

Phenazine producers have been identified as organisms belonging to a range of species like *Methanosarcina maze* (Archebacterium) (Abken et al., 1998), *Pantoea agglomerans* Eh1087 (Enterobacteriaceae) (Giddens, 2002), members of *Streptomyces* genus (Actinobacteria) (Umezawa et al., 1951; Turner, 1986; Maul et al., 1999), *Pseudomonads*, *Burkholderia cepacia* and *B. phenazinium* (Proteobacteria) (Arima et al., 1964; Chang et al., 1969; Byng, 1976; Brisbane et al., 1987; Thomashow et al., 1995; Chin-A-Woeng et al., 1998), *Pelagobacter variabilis* and *Vibrio* (marine bacteria) (Laursen et al., 2004; Turner, 1986; Chin-A-Woeng et al., 2003; Giddens et al., 2002) etc.

This long, albeit incomprehensive list also serves to highlight the fact that phenazine producers are spread over both gram-positive and gram-negative proteobacteria. Overall, phenazine producing species are more abundant among gram-negative bacteria with a high G+C genomic content. There is a considerable overlap in phenazine derivatives produced by these organisms; several different organisms are found to produce the same compound as are individual species known which produce a variety of phenazines in a growth-condition-dependent manner. Most intensively studied phenazine producers are the members of the fluorescent *Pseudomonas* species, in which these compounds were first identified (Thomashow et al., 1998). Fluorescent pseudomonads include organisms like *Pseudomonas aeruginosa, P. fluorescens, P. chloraraphis, P. putida* etc. which are gram negative, strictly aerobic, polar flagellated and rod-shaped.

1.3 Chemical properties of phenazines

Chemically, phenazines belong to the alkaloid class of compounds which contain a basic amino group in their structure. Phenazines are water-soluble and are secreted into media at concentrations as high as grams per litre of bacterial culture (Kerr, 2000; Smirnov, 1990). Most species synthesise two or more species-specific phenazines except *Pseudomonas fluorescens* which, so far, is known to produce only phenazine-1-carboxylic acid (PCA) (Mavrodi et al., 1992). The relative amount of phenazines produced by a species is directly co-related with growth-conditions (van Rij et al., 2004).

These nitrogen-containing heterocyclic compounds are substituted at different points around their rings, which alters their solubility and biological activity to suit environmental demands of phenazine producing species. (Table 1.1; overleaf).

Phenazines have a characteristic absorption spectrum which includes two intense peaks in the UV range (between 250-290 nm and 350-400 nm) and at least one more in the visible range (400-600 nm) (Britton, 1983). This peak in the visible range varies, depending on the aforementioned modifications of the core phenazine structure and gives rise to a range of brilliant colours, from bright blue of 1-hydroxy-5-methylphenazine (pyocyanin (PYO)), lemon yellow of phenazine-1-carboxylic acid (PCA) to the bright orange of 2-hydroxy phenazine (2-OHPCA) (Figure 1.1).

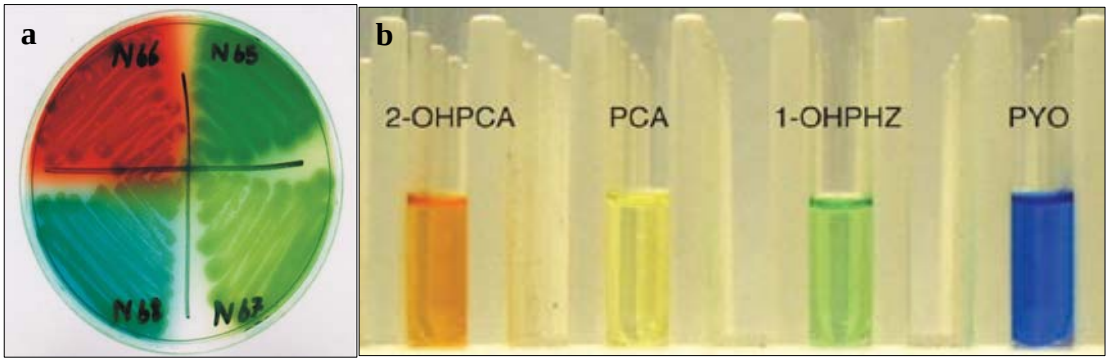

Figure 1.1: Streak plate of various phenazine-producing *Pseudomonads.* ('a'; From Kerr *et al* 2000) and aqueous solution of phenazines. ('b'; From Price- Whelan *et al*. 2005)

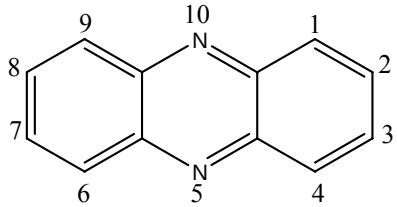

Name of phenazine compound	Position of substituents										Species of Origin
	1	2	3	4	5	6	7	8	9	10	
Phenazines with no carbon substituents on the heterocyclic ring system											
1-Hydroxyphenazine	OH										*P.aureofaciens*
1,6-Dihydroxyphenazine	OH					OH					*P.phenazinium; P.iodinium*
2,3-Dihydroxyphenazine		OH	OH								*P.aureofaciens*
Phenazines with one carbon substituent on the heterocyclic ring system											
Phenazine-1-carboxylic acid	COOH										*P.fluorescens; P.aeruginosa; P.aureofaciens; P.phenazinium; P.chlororaphis*
Phenazine-1-carboxamide	$COO.NH_3$										*P.aeruginosa; P.chlororaphis*
2,3-Dihydroxyphenazine-1-carboxylic acid	COOH	OH	OH						OH		*P.phenazinium*
Phenazines with two carbon substituent on the heterocyclic ring system											
Phenazine-1,6-dicarboxylic acid	COOH					COOH					*P.aureofaciens; P.phenazinium;*
2-Hydroxyphenazine-1,6-dicarboxylic acid	COOH	OH				COOH					*P.aureofaciens*
2,3,7-Trihydroxyphenazine-1,6-dicarboxylic acid	COOH	OH	OH			COOH	OH				*P.aureofaciens*

Table 1.1: Some of the phenazines synthesised by various species of *Pseudomonas*. (From Turner & Messenger, 1986)

Till date more than 50 phenazine compounds of bacterial origin have been identified (Laursen & Neilson, 2004). The *Pseudomonas* species synthesise simple phenazines, (Table 1.1) whereas other, more complex phenazine aldehydes, thioesters, ester and amides are made by *Streptomyces* and other phenazine producers. This work focuses on the phenazines associated with pseudomonads.

1.4 Biological significance of phenazines

The highlight of biological significance of phenazines is their ability to act as broad-spectrum antimicrobial, antiparasite, antimalarial agents affecting a vast range of organisms (Yang et al*.,* 2005; Cerecetto et al*.,* 2004; Turner et al*.,* 1986; Budziekiewicz, 1993; Hollstein et al*.,* 1973; Handelsmann et al*.,* 1996; Mavrodi et al., 2001; Kitahara et al., 1982; Baron et al*.,* 1989).

The root-associated soilborne pseudomonads - *P. fluorescens, P. chlororaphis* and *P. aureofaciens* produce PCA, phenazine-1-carboxamide (PCN), and hydroxyphenzaine-1-carboxylic acid (OH-PCA) respectively, which inhibit infection by soilborne phytopathogenic fungi (Chin-A-Woeng et al 2003) and bacterial root diseases ('take-all decline' disease), thus securing survival of the host in the rhizosphere and acting as potent biocontrol agents (Giddens et al., 2002; Thomashow et al., 1988).

The opportunistic pathogen *P.aeruginosa* produces an array of phenazines including pyocyanin (PYO), PCA, 1-hydroxyphenazine and aerugenosin A and B (Byng et al., 1979; Hassan et al., 1980, Holliman, 1969). Of these, the phenazines pyocyanin (PYO) and PCA are implicated in a number of instances of disease pathogenesis. PYO generates pathogenic symptoms leading to the effective killing of the nematode *Caenorhabditis elegans* by *P. aeruginosa* Rahme et al., 1997; Mahajan-Miklos et al., 1999). It is also found to be essential for lung infection in mice and the pathogenicity of *P. aeruginosa* in 'burned mouse' model (Cao et al., 2001; Lau, 2004; Ran et al., 2003). In case of cystic fibrosis patients, where lung infection by *P. aeruginosa* is highly prevalent and results in a high rate of mortality, phenazine compounds have been detected at

concentrations as high as 10^{-4} M (Wilson, 1988). Both PCA and PYO alter expression of immunomodulatory proteins of human airway epithelial cells (Denning et al., 2003; Lau et al., 2005), lead to neutrophil inflammation (Look et al. 2005), induce apoptosis of neutrophils (Usher et al., 2002) and thus among other factors, contribute towards the persistence of *P. aeruginosa* infections (Lau et al., 2004).

Phenazines are capable of mineral reduction and iron sequestering (Hernandez et al., 2004; Schroth et al., 1982), enabling accessibility of these essential minerals not only to phenazine producing species, but also other organisms present in soil, thus ultimately influencing the micro flora in a given environment. Finally, the phenazines produced by *P. agglomerans* on the stigmas of apple flowers contribute towards the ability of this bacterium to suppress colonization by phytopathogenic *Erwinia amylovora* which causes fire-blight disease in apples (Giddens et al., 2003). These examples clearly emphasise the role of phenazines as broad, host-nonspecific pathogenicity factors which contribute towards the ecological fitness of phenazine-producing strains in their natural habitats.

1.5 Mode of action of phenazines

The biological activities of phenazines have interested chemists for a long time and an estimated 6000 phenazine compounds have been synthesised or modified after their discovery from biological sources. These include chemically synthesised phenazines which play an important role in physical and electrochemical research e.g. construction of microbial fuel cells for generation of green and renewable energy (Rabaey et al., 2005). Additionally, phenazines were designed to exploit their DNA intercalative properties, e.g. [5,4-*ab*]-phenazine and phenazine-5,10-dioxide to investigate their antiproliferative, thus anti-tumour and anti-cancer activities (Fernandez et al., 2001; Gamage et al., 2002; Phillips et al., 2004; Yang et al., 2005). Although the exact mechanism or effect of intercalation of DNA by phenazines is not well understood, it is thought that phenazines act by hindering DNA biosynthesis, replication or processing (Cerecetto et al., 2004);

These examples clearly indicate that phenazines, rather than performing one dedicated purpose, seem to be capable of performing multiple roles. This has led to intensification in research towards understanding the mode of action of phenazines. The evident non-selective toxicity of phenazines was thought to arise from a mode of action directed against one of the more universal primary metabolic pathway reactions (Vining, 1991). In 1934, Friedheim and co-workers showed through potentiometric studies, that PYO in mixture with its reduced derivative acted as a reversible redox system. The same group also reported that PYO was capable of increasing the rate of respiration of both mammalian and bacterial cells.

Almost all the effects of phenazines mentioned in the previous paragraph (except DNA intercalation) can be attributed to this one essential feature of phenazines - their capacity for undergoing redox transformations (Hassan et al., 1980; Muller, 1995; Gardner, 1996; Denning et al., 1998). Phenazines are thought to diffuse across, or insert into membranes and readily undergo redox-cycling in the presence of molecular oxygen, resulting in the uncoupling of oxidative phosphorylation and generating reactive oxygen species like superoxide (O_2^-) hydroxyl (OH^-) and hydrogen peroxide (H_2O_2) (Hassan et al., 1980; Turner, 1986). The accumulation of these radicals is toxic not only to bacterial but also fungal and eukaryotic cells (Toohey et al., 1965; Hasset et al., 1992; Mahajan et al., 1999) thus conferring host-nonspecific pathogenicity to organisms producing phenazines. The finding of Friedheim about increased rates of respiration has been reiterated by O'Malley et al., (2003) and Lau et al., (2004) who showed that the effects of PCA and PYO on both bacterial and eukaryotic host cells result from oxidative activity and the inactivation of proteins involved in oxidative stress responses. Moreover, Hassett and co-workers (Hassett et al., 1992, 1995) have found that the superoxide dismutases of pyocyanin producing *P. aeruginosa* possess a higher activity than other known dismutases, which would protect this organism from the harmful effects of phenazines.

Though the redox activity of phenazines is well known and the mode of action is hypothesised, the exact mechanism of how phenazines generate these species

is not well understood. A more detailed understanding of mode of action of various phenazines, their influence on the molecular level and their metabolism is only just emerging (Hernandez et al., 2001; Rabaney et al., 2005; Look et al. 2005).

1.6 Biosynthesis of phenazines

1.6.1 The Shikimate pathway

As mentioned earlier, all secondary metabolites are known to arise from some modification of the primary metabolic pathways of cells. The discovery of the Shikimic acid pathway for the biosynthesis of aromatic amino acids - tryptophan, tyrosine and phenylalanine in the 1960s (Balinsky and Davis, 1961) and the availability of isotopically labelled compounds resulted in the investigation of some metabolic intermediates of the shikimate pathway as a possible precursor of phenazines.

Three important studies in the 1960-70 period established beyond doubt that the Shikimic acid pathway was indeed the primary metabolic pathway which branched into the phenazine biosynthesis. The first of these studies was carried out in 1963 by Millican (Millican, 1963) and showed that biosynthetically prepared [U^{14}C] shikimic acid was the precursor of pyocyanin synthesised by *P. aeruginosa;* with the recovery of around 16% of this radiolabelled shikimate in pyocyanin. A second set of experiments using isotope-competition technique (MacDonald, 1963; Levitch et al., 1964, 1966; Chang et al., 1968) confirmed that shikimic acid was the precursor for biosynthesis not only of pyocyanin but also phenazine-1-carboxylic acid and oxychlororaphin. Lastly, experiments by Longley et al. and Calhoun et al., (1972) used mutants unable to degrade shikimic acid and blocked at various points on the branched pathway to aromatic amino acids. Their experiments not only validated the conclusions by the previous two sets of experiments, but went further and identified chorismic acid as the branching point of the shikimic acid pathway to phenazine biosynthesis (Figure 1.2; overleaf). The next question in elucidating the phenazine biosynthesis pathway was the identification of the compound that led to the formation of the tricyclic scaffold of phenazines.

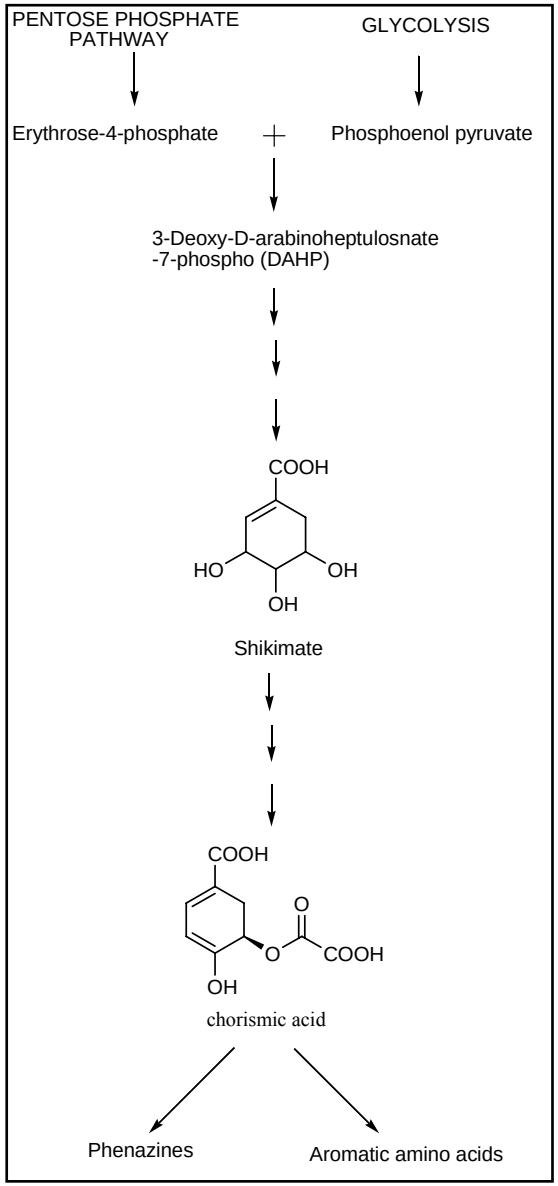

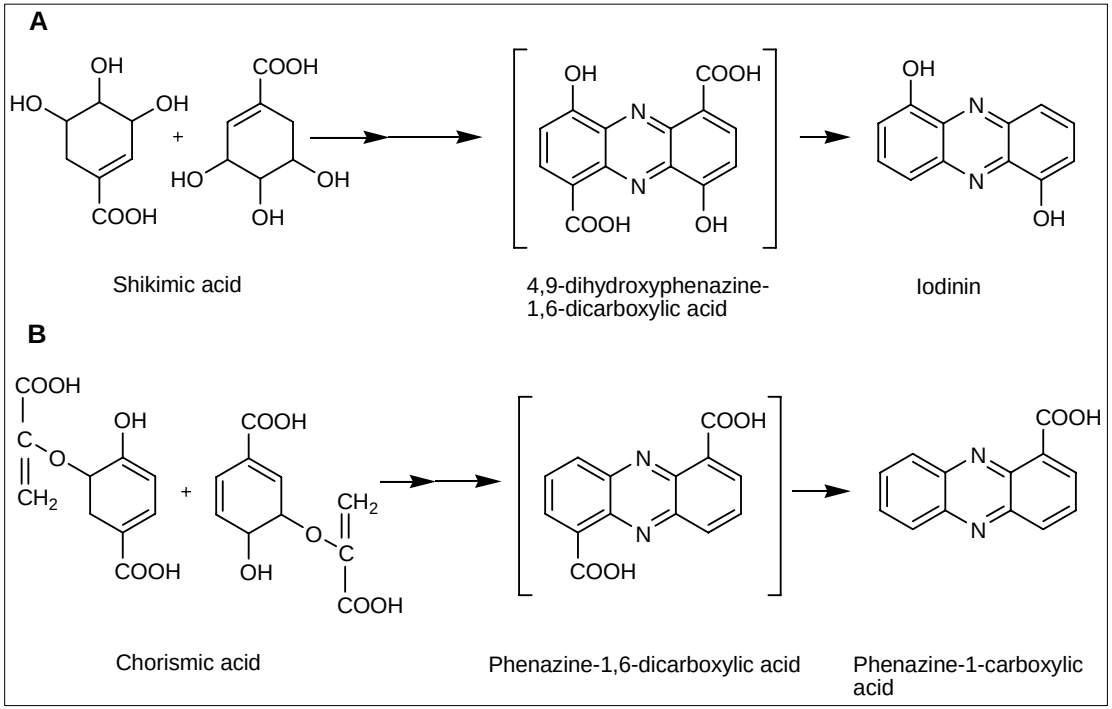

Figure 1.3: The proposed intermediates of the phenazine biosynthesis pathway.

Figure 1.2: The shikimic acid pathway and the two compounds investigated as the potential branching points for the biosynthesis of phenazines.

1.6.2 Assembly of the tricyclic phenazine ring scaffold

To further understand the mechanism of phenazine ring assembly, initial studies on Iodinin were initiated, which led to the hypothesis that the phenazine moiety was formed by the diagonal, asymmetrical incorporation of two shikimic acid units. 4,9-dihydroxyphenazine-1,6-dicarboxylic acid was hence proposed as the key intermediate in the biosynthesis of all phenazines (Podojil et al., 1970). However, studies on phenazine ring assembly of pyocyanin and phenazine-1-carboxylic acid by Herbert et al., (1972) and Hollstein et al., (1972 & 1973) led to a different hypothesis - that of diagonal, symmetric incorporation of two chorismic acid units leading to formation of the phenazine scaffold, with phenazine-1,6-dicarboxylic acid (PDC) as the common precursor of all phenazines (Herbert et al., 1976; Etherington et al., 1979) (Figure 1.3). This paradigm was accepted, despite lack of any significant incorporation of [$U^{14}C$] chorismic acid into phenazines observed by Hollstein (Hollstein et al., 1972, 1973). Meanwhile, search continued for more evidence for chorismic acid being the compound that dimerises to form the phenazine ring system, with anthranilic acid also being considered. The discovery of two sets of anthranilate synthase genes in pyocyanin producing strains of *P. aeruginosa* by Essar et al., (1990) gave some credence to this hypothesis; although all previous attempts to demonstrate incorporation of isotopically labelled anthranilate into phenazine were unsuccessful (Carter et al., 1961; Millican, 1962).

Thus, although the shikimic acid pathway was accepted as the primary metabolic pathway which branched off into phenazine biosynthesis, the mechanism of assembly of the tricyclic scaffold of phenazines and identity of the intermediate formed in this process remained unclear.

1.6.3 Genetic basis of phenazine biosynthesis in pseudomonads.

Further progress in understanding the phenazine biosynthesis pathway came in 1995, when Pierson and co-workers identified the biosynthetic genes responsible for the production of phenazine in *P. aureofaciens* (Pierson et al., 1995). Soon, a

phenazine biosynthesis locus was also identified, cloned and sequenced in *P. fluorescens* (Mavrodi et al., 1998) and *P. aeruginosa* (Mavrodi et al., 2001). This locus comprised of a conserved seven-gene operon *phzABCDEFG* which was found to be sufficient for the production of PCA from chorismic acid. (Figure 1.4). Both *P. aureofaciens* and *P. fluorescens* contain one, whereas *P. aeruginosa* possesses two copies of the phenazine biosynthesis operon. PCA is the end-product of this 'core' phenazine biosynthesis pathway.

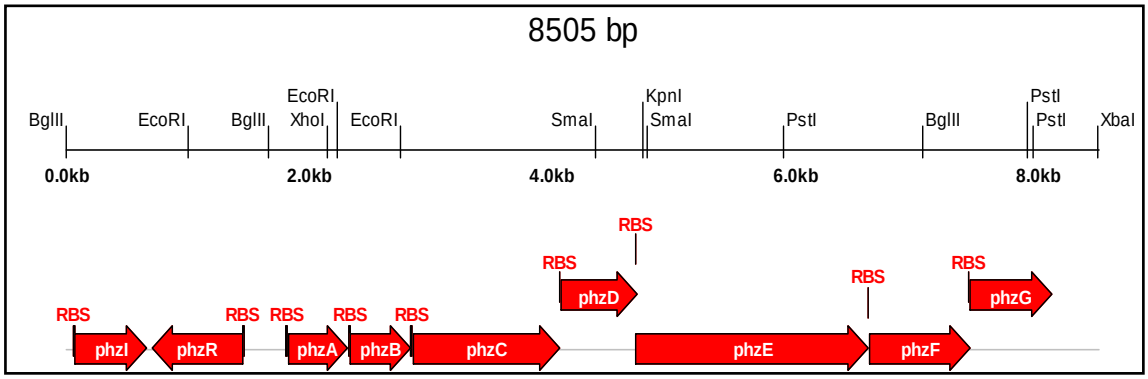

Figure 1.4: Phenazine biosynthesis operon from *P.fluorescens*.

The nucleotide sequences of the phenazine biosynthetic operon of these organisms were found to be very homologous, with an identity of 70-95%. This implies that the manner of phenazine biosynthesis and the functions of enzymes involved in these organisms are identical.

The discovery of this 'core' phenazine biosynthesis operon in *Pseudomonas* led to further investigation into the presence of this operon in other phenazine producing species.

1.6.4 Phenazine biosynthesis operon in other organisms

The seven-gene sequence from *Pseudomonas* was used as a probe to find similar genes in other phenazine-producing organisms. However, this probe yielded no results in case of *Burkholderia cepacia, Burkholderia phenazinium* (formerly, *Pseudomonas cepacia* and *P. phenazinium* respectively), and *Brevibacterium iodinum.* This led to the conclusion that although the phenazine biosynthesis operon is conserved in the *Pseudomonal* species, other phenazine producing species might utilise a modified or different operon for phenazine

biosynthesis. To test this hypothesis, further sequence comparison between the newly sequenced genomes of various microorganisms were initiated using only five of the seven enzymes i.e. PhzA, D, E, F and G. This probe found matches in the genomes of *B. cepacia, Erwinia carotovora* and the first gram positive bacteria *Brevibacterium lingens*.

B. cepacia was previously called *Pseudomonas cepacia* (Ballard et al., 1970) and was known to produce the phenazines shown in the figure below:

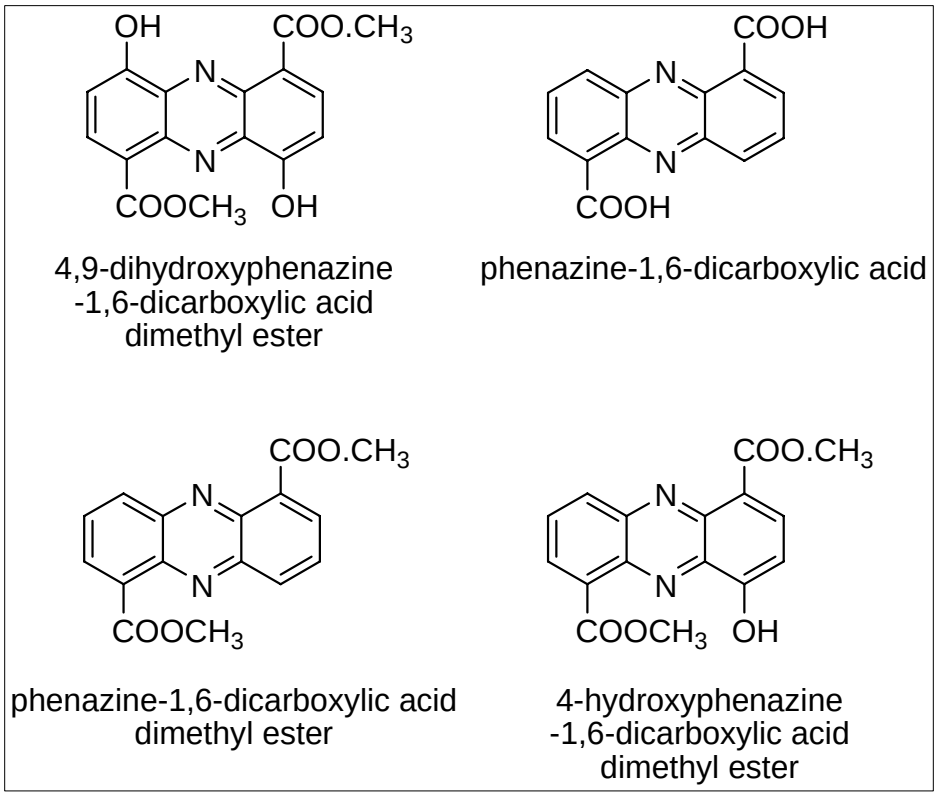

Figure 1.5: Phenazines produced by *B. cepacia.*

On further investigation, the phenazine cluster of *B. cepacia* was found to consist six instead of seven genes, with only one copy of the highly identical *phzA-B* genes of *Pseudomonas*.

Investigation into this *phzA/B*-like gene from *Burkholderia cepacia* (named BcepA in this work) was initiated, to gain further insight into the structure and function of *phzA/B*-like genes of *Pseudomonas*. This study is the first to undertake the investigation of an enzyme of the phenazine biosynthesis operon of *B. cepacia*

and no other information is available at this point regarding the specific details of how this pathway operates, the substrates, intermediates involved etc.

This, however, is not the case for the phenazine biosynthesis operon of *Pseudomonas*, for which a comprehensive study was undertaken by MacDonald and co-workers (MacDonald et al. 2001).

1.6.5 Phenazine biosynthesis in *Pseudomonas.*

MacDonald et al., (2001) expressed all or a subset of seven genes of the phenazine biosynthesis operon of *P. fluorescens* in *Escherichia coli*. Feeding experiments were then carried out using exclusively, chorismic acid, anthranilic acid or 2-amino-2-deoxychorismic acid (ADIC), to re-examine the branching point of phenazine biosynthesis from shikimic acid pathway and the process of phenazine ring assembly.

Their results proved conclusively that chorismic acid was the branching point and it was converted to ADIC by the enzyme PhzE. Also, neither anthranilic acid (no conversion to PCA) nor chorismic acid (conversion to ADIC by PhzE, but no PCA formation) were utilised for the assembly of the phenazine scaffold. ADIC however, was completely converted to PCA. Moreover, incubation of ADIC with the enzyme PhzD yielded trans-2, 3-dihydro-3-hydroxyanthranilic acid (DHHA) and incubation of DHHA with PhzA-G showed complete conversion to PCA. Both these compounds were thus confirmed as intermediates of phenazine biosynthesis pathway.

PDC, the previously hypothesised intermediated, was not detected in these experiments. To further explore the possibility of PDC formation, [11-C^{13}]-labelled PDC was incubated with PhzA-G extract. Less than 1% of this labelled PDC was found to be converted into PCA. Moreover, the incubation of radiolabelled PDC in the presence of radiolabelled ADIC with the same set of enzymes (PhzA-G) yielded no conversion of labelled PDC to PCA. Thus, PDC was ruled out as an intermediated of the phenazine biosynthesis pathway of *P. fluorescens*. Instead, the dimerisation of two molecules of oxidised DHHA was suggested as a possible mode of phenazine scaffold assembly.

These observations were collated and presented in the form of a scheme for the biosynthesis of PCA from chorismic acid by MacDonald and co-workers (shown overleaf) which included the newly identified intermediates and the role of enzymes involved.

1.6.6 Enzymes of the phenazine biosynthesis operon

While studying the various enzymes involved in the phenazine biosynthesis operon of *P. fluorescens*, MacDonald et al. compared the sequences of these seven enzymes with proteins of known function. Their results are tabulated in table below.

Gene	Size(amino acids)	Similar Enzymes
PhzA	163	PhzB
PhzB	162	PhzA
PhzC	400	Plant 3-deoxy-D-*arabino*-heptulosonate-7-phosphate (DAHP) synthase.
PhzD	207	Bacterial Isochorismate
PhzE	637	Bacterial Anthranilate synthase
PhzF	278	Unknown
PhzG	222	Bacterial pyridoxyamine 5'-phosphate oxidase

Table 1.2: Enzymes similar to those of the phenazine biosynthesis pathway.

There is more than 70% similarity between the genes *phzA* and *B*, which were found to be important for quantitative synthesis, but not essential for the biosynthesis of PCA (MacDonald et al. 2001). Both these enzymes however, are conserved in the phenazine biosynthesis operons of all *Pseudomonas* species. The enzymes PhzA-B were thought to act past the formation of DHHA, but no further information, either structural or biochemical was available, since these enzymes showed no similarity to any enzymes of known function in the NCBI database.

Of the rest of the enzymes PhzC, D, E, F and G, which are essential for PCA production, PhzC, D, E and G were found to have counterparts in the bacterial

world. PhzC is a 3-deoxy-arabino-heptulosonate-7-phosphate (DAHP) synthase and acts more upstream (prior to formation of chorismic acid), ensuring adequate availability of chorismate for phenazine biosynthesis. PhzE, which acts after PhzC, shows similarity to bacterial anthranilate synthase and catalyses the conversion of chorismate to ADIC. This enzyme is followed by PhzD, an isochorismatase, which catalyses the conversion of ADIC to DHHA. This conclusion was recently confirmed by the crystal structural analysis of PhzD by Parson et al., (2003).

Recently, Blankenfeldt et al., (2004) shed more light on the mode of action of the homodimeric enzyme PhzF through structural and biochemical analysis. They showed that PhzF acts as an isomerase, converting DHHA to its highly reactive ketone form - 1,2,4-trihydro-3-oxo-anthranilic acid. Blankenfeldt and co-workers also hypothesised that PhzF is an enzyme with dual functions and also catalyses the condensation of two molecules of this ketone to form the phenazine ring scaffold. This role was formerly thought to be performed by PhzG (MacDonald et al., 2001). The modified scheme proposed by Blankenfeldt et al is depicted in the Figure 1.6, overleaf.

The last of the seven enzymes, PhzG, is similar to bacterial pyridoxyamine-5-phosphatase. It was thought to act in steps past the formation of 2,3-dihydro-3-oxo anthranilic acid, but its exact role in PCA biosynthesis could not be deduced.

The functions of the enzymes PhzC, D, E and F were thus known or could be accurately surmised. However, no such conclusion could be drawn for PhzA, B and G. The clarification of the structure and roles of these three enzymes was one of the goals of this investigation.

As mentioned previously, the end product of core phenazine biosynthesis operon, *phzABCDEFG*, is PCA, which is the only phenazine compound synthesised by *P. fluorescens.* PCA however, is modified to other phenazine derivatives in case of *Pseudomonas* strains like *P. aeruginosa, P. chlororaphis* etc. The genetic basis of generation of phenazine diversity and the organisation of phenazine biosynthesis operon in other organisms is described herewith.

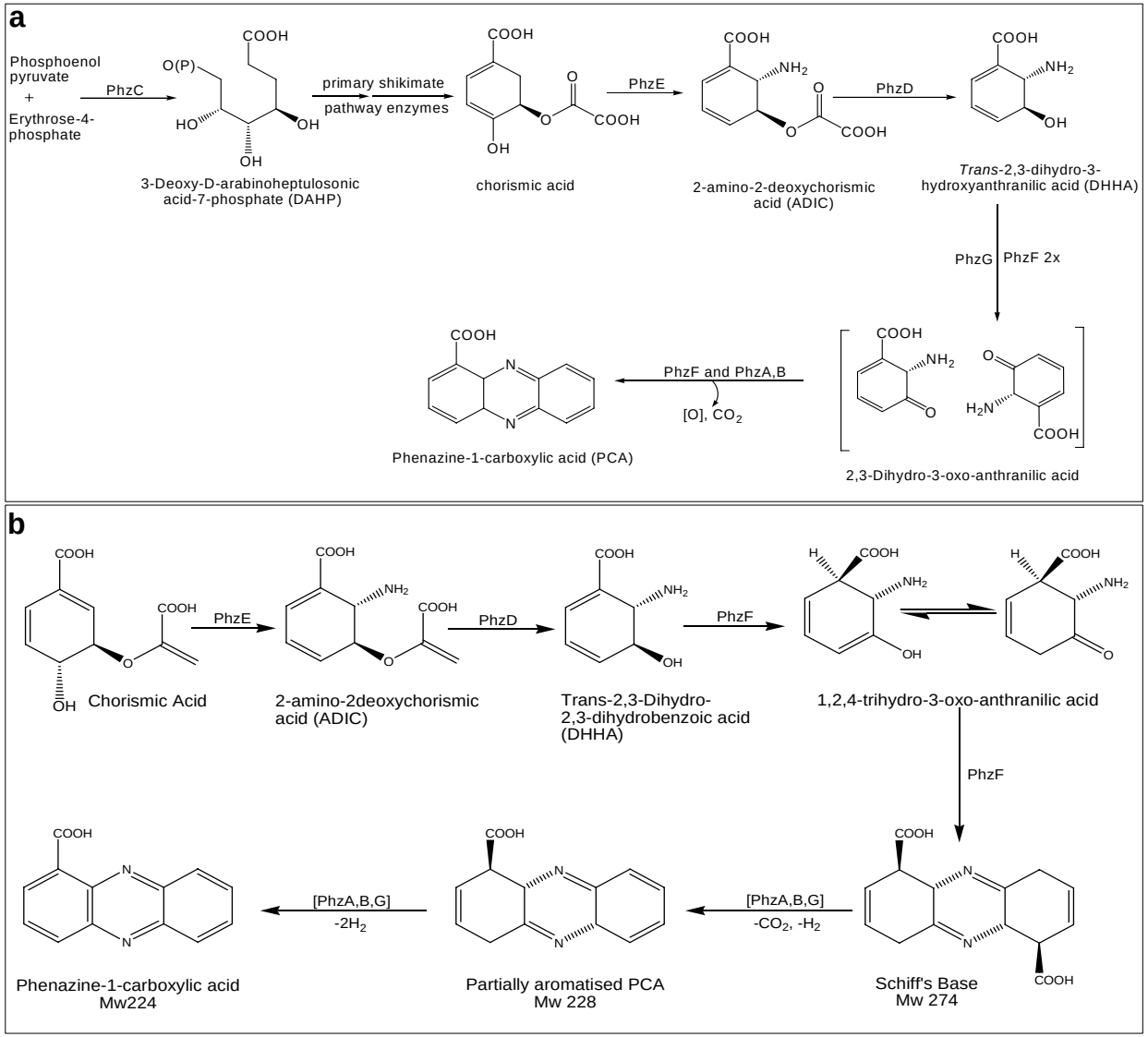

Figure 1.6: (a) Scheme of Phenazine biosynthesis proposed by MacDonald et al., (2001) & (b) modified by Blankenfeldt et al., (2004)

1.6 Generation of phenazine diversity.

Diversity in phenazine biosynthesis is achieved by the presence of other genes, associated with the core phenazine biosynthesis operon, which are capable of a wide range of modifications of PCA. Such genes were identified in *P. chlororaphis*, *P. aeruginosa* and *P. aureofaciens* and the organisation of phenazine biosynthesis operon in these organisms is compared to that of *P. fluorescens* in the figure below:

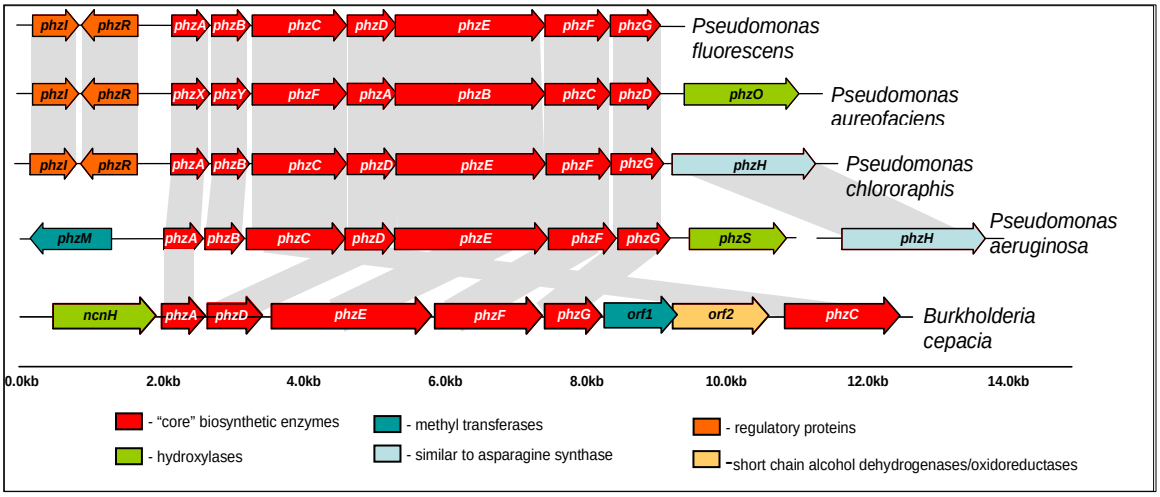

Figure 1.7 The organisation of the phenazine biosynthetic operon from various organisms (From Mavrodi et. al., 2005)

In case of *P. chlororaphis*, the biosynthetic gene phzH is found downstream of phzG. PhzH belongs to the asparagine snythase enzyme family and catalyses the conversion of PCA to PCN via a transamidase reaction. The transfer of phzH gene to the phenazine biosynthetic operon of *P. fluorescens* and *P. aureofaciens* enabled these strains to produce PCN and to act as biocontrol agents in tomato (Chin-A-Woeng et al., 2001). Thus, validating the observation that PCA is not only the end product of the enzymes PhzABCDEFG, but it is the compound that is produced in all phenazine synthesising *Pseudomonas.*

In *P. aureofaciens*, the gene phzO is localised immediately downstream of the core biosynthetic operon as well. Belonging to the family of two-component non-haem, flavin-diffusible bacterial aromatic monooxygenases, *phzO* catalyses the conversion of PCA to 2-OHPCA.

P. aeruginosa in addition to phzH contains two other genes – *phzM* and *phzS* associated with this pathway. *phzM* is located upstream of the operon and catalyses the formation of PYO. PhzS is a protein similar to bacterial monooxygenases and catalyses the conversion of PCA to both PYO and 1-hydroxyphenazine. Figure 1.8 summarises the conversion of PCA to different derivates.

The current knowledge of the enzymes involved in phenazine biosynthesis and modification is still not complete and it is expected that further research into this field will result in the identification of more such enzymes. This also holds true about the regulation of phenazine biosynthesis, which, though not yet fully understood, is known to be regulated by the mechanism of quorum sensing in *Pseudomonas*.

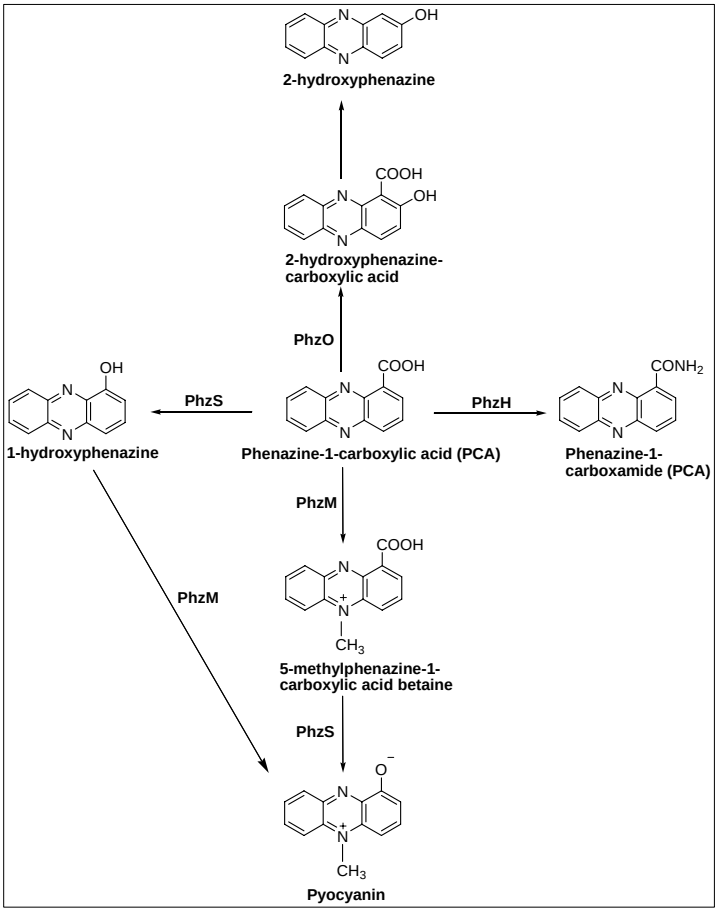

Figure 1.8: Derivatives of PCA and the enzymes involved in its modification.

1.8 Regulation of phenazine production

Quorum sensing is a mechanism that enables bacteria to regulate their gene expression in a population-density-dependent manner, thus adjusting various metabolic processes according to environmental conditions. In this process, autoinducer signal molecules convey population density information from neighbouring sister cells. These autoinducer molecules are diffusible across cell membranes and belong to N-acyl-L-homoserine lactone (N-AHLs) class of molecules in gram negative bacteria like pseudomonas.

In *P. fluorescens*, *P. aureofaciens* and *P. chlororaphis*, two genes, phzI and phzR, located directly upstream to the phenazine biosynthesis operon function as regulators of N-acyl-homoserine lactone mediated gene expression of the 'phz' operon. Thus, these two genes link quorum sensing to phenazine biosynthesis and act as regulating sub-circuit in these *Pseudomonas* strains. However, this is not the only mode of regulation. In *P. aeruginosa*, the genes regulating phenazine biosynthesis are not located upstream of the core biosynthetic pathway, but elsewhere in the genome. In this organism, the expression of phenazine biosynthesis is thought to be regulated in a more complex manner, by not one, but two sets of hierarchically organised quorum sensing cascades '*las'* and '*rhl*'. Thus, the regulation of phenazine biosynthesis is varied and the current knowledge still incomplete. However, a detailed description of regulation of phenazine biosynthesis is outside the scope of this work.

This work concerns itself chiefly with the investigation of the enzymes PhzA, PhzB, PhzG (*P. fluorescens*) and BcepA (*B. cepacia);* and the elucidation of the 'core' phenazine biosynthesis pathway, with respect to the intermediates generated during the formation of PCA.

Objectives of this work

'Now, I give you fair warning,' shouted the Queen.
Alice in wonderland, Lewis Carroll

2.0 Objectives of this work

As discussed in the introduction, phenazines are versatile and multi-functional compounds; but relatively little information is available about the biosynthesis of these molecules in nature. Chemically modified or synthesised phenazines are being explored for various applications, however, no efficient method of chemical synthesis of phenazines has yet been found. Tapping into the natural methods of phenazine production, as employed by microorganisms like pseudomonads, could potentially provide means to generate novel phenazines for various application from pH indicators (exploiting their unique spectral properties, which vary with change in pH), and antibiotics, to DNA intercalators (as anti-tumour agents). It could also provide insights into the development of inhibitors of phenazine biosynthesis and other pharmaceutical applications and help tackle the problem of fatal infections by phenazine-producing micro-organisms in immuno-compromised individuals.

To this effect, this project intends to deepen the understanding of the functioning of the 'core' phenazine biosynthesis pathway involving enzymes PhzA-G and leading to the formation of PCA. The specific aims of this work encompasses firstly, the over-expression, crystallisation and elucidation of the three-dimensional structures of the enzymes PhzG, PhzA and similar enzymes (PhzB from *P. fluorescens* and BcepA from *Burkholderia cepacia*) to discover the role played by these enzymes in phenazine biosynthesis. Secondly, this work intends to investigate the exact mechanism of phenazine biosynthesis to establish the identity of the substrates and products of the various enzymes as well as the intermediates formed during the production of PCA by using various biochemical and mass spectroscopic methods.

Results & Discussions

'What is the use of repeating all that stuff,
if you don't explain it as you go on? It's by far
the most confusing thing I ever heard!'
- The Mock Turtle (Alice in wonderland, Lewis Carroll)

Section I

This section describes the details of cloning, over-expression and crystallisation of PhzA, PhzB, BcepA and its complex, PhzG and PhzG complexed with PCA. The results of the bioinformatics analysis undertaken for each of the proteins are also discussed here.

3.1 Sequence Analysis

3.1.1 PhzA, PhzB and BcepA

The sequences of proteins PhzA, B and A_Bcep were found to be 70% identical to each other and upto 60% identical to sequences of similar proteins from other Pseudomonads (Figure 3.1). The sequences were compared using the program BLAST (BLASTp, NCBI. Altschul et al., 1997).

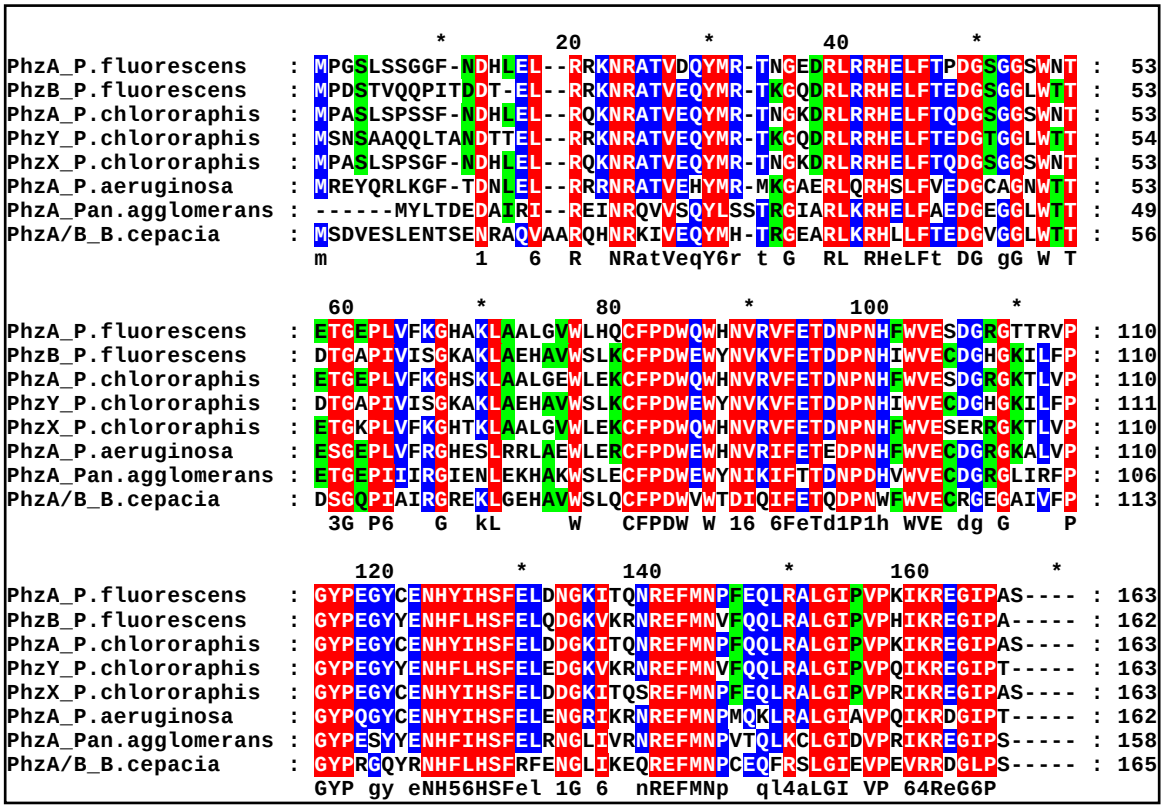

Figure 3.1: Multiple alignment of proteins similar to PhzA and B.
(Colour key: Red = 100%; blue = 80%; green = 60% similarity)

The potential folds of these proteins were identified using the structure prediction program 3DPSSM (Kelley et al., 2000), which predicts protein fold based on the sequences of proteins. 3DPSSM predicted these three proteins to be similar in fold to the members of the nuclear transport factor-2 (NTF2-like) superfamily. This superfamily includes members of the NTF2 family, Δ^5-3-ketosteroid isomerases, scytalone dehydratases, and the beta subunit of ring-hydroxylating dioxygenases. This family represents a classic example of divergent evolution where the proteins have a common fold, but diverge greatly in their sequence and function. For example, nuclear transport factor 2 (NTF2) mediates the nuclear import of RanGDP and binds to both RanGDP

and ‘FxFG’ repeat-containing nucleoporins while ketosteroid isomerases catalyze the isomerization of Δ^5-3-ketosteroid to Δ^4-3-ketosteroid, by intramolecular transfer of the C4-beta proton to the C6-beta position. While the function of the beta subunit of the ring-hydroxylating dioxygenases is not known, scytalone dehydratase catalyzes two reactions in the biosynthetic pathway producing fungal melanin. Members of the NTF2-like superfamily are widely distributed among bacteria, archaea and eukaryotes. In the sequence alignment shown in Figure 3.2, sequences of one representative each of ketosteroid isomerase (1OPY), nuclear transport factor-2 (1ASK) and scytalone dehydrates (1SJW) have been aligned to the sequences of PhzA, PhzB and BcepA. No meaningful similarity can be observed between these sequences.

Thus, although tertiary structure of the PhzA group of enzymes (PhzA, B and BcepA) could be predicted with some confidence, no conclusion as to the potential function could be drawn from the sequence alone.

```
                              *        20         *        40         *
PhzA_P.fluorescens : MPGSLSSGGFNDH---LELRRKNRATVDQYMRTNGEDRLRRHELFTPDGSGGSWNTET :  55
PhzB_P.fluorescens : MPDSTVQQPITDD---TELRRKNRATVEQYMRTKGQDRLRRHELFTEDGSGGLWTTDT :  55
PhzA/B_B.cepacia   : MSDVESLENTSENRAQVAARQHNRKIVEQYMHTRGEARLKRHLLFTEDGVGGLWTTDS :  58
1OPY               : -----MNLPTAQEVQGLMARYIELVDVGDIEAIVQMYADDATVED--------PFGQP :  45
1ASK               : ---------MGDKPIWEQIGSSFIQHYYQLFDNDRTQLGAIYIDAS------CLTWEG :  43
1SJW               : ---------MSRQTEIVRR-MVSAFNTGRTDDVDEYIHPDYLNP---------ATLEH :  39


                     60         *        80         *       100         *
PhzA_P.fluorescens : GEPLVFKGHAKLAALGVWLHQCFP-DWQWHNVRVFETDNPNHFWVESDGRGTTRVPGY : 112
PhzB_P.fluorescens : GAPIVISGKAKLAEHAVWSLKCFP-DWEWYNVKVFETDDPNHIWVECDGHGKILFPGY : 112
PhzA/B_B.cepacia   : GQPIAIRGREKLGEHAVWSLQCFP-DWVWTDIQIFETQDPNWFWVECRGEGAIVFPGY : 115
1OPY               : PIHG----REQIAAFYRQGLG-GGKVRACLTGPVRASHNGCGAMPFRVEMVWNGQP-- :  96
1ASK               : QQFQG----KAAIVEKLSSLPFQKIQASITAQDHQPIPDSCIISMVVGQLKADEDP-- :  95
1SJW               : GIHTGPKAFAQLVGWVRATFSEEARLEEVRIEERGPWVKAYLVLYGRHVGRLVGMPPT :  97
                                                                    P

                      120         *       140         *       160         *
PhzA_P.fluorescens : P--EGYCENHYTHSFELDN-GKITQNRE-FMNPFEQLRALGIPVPKIKREGIPAS-- : 163
PhzB_P.fluorescens : P--EGYYENHFLHSFELQD-GKVKRNRE-FMNVFQQLRALGIPVPHIKREGIPA--- : 162
PhzA/B_B.cepacia   : P--RGQYRNHFLHSFRFEN-GLIKEQRE-FMNPCEQFRSLGIEVPEVRRDGLPS--- : 165
1OPY               : ---CALDVIDVMRFDEHGRIQTMQAYWSEVNLSVREPQ------------------ : 131
1ASK               : --IMGFHQMFLLKNINDAWVCTNDM----FRLALHNFG------------------ : 127
1SJW               : DRRFSGEQVHLMRIVD-GKIRDHRD-WPDFQGTLRQLGDPWP--DDEGWRP------ : 144
                                 6                 f
```

Figure 3.2: Alignment of PhzA, PhzB and PhzA (*B.cepacia*) with sequences of similarly folding proteins. (Colour key: Red = 100%; blue = 80%; green = 60% similarity)

3.1.2 Analysis of genes similar to PhzA/B.

An analysis of the evolution of various genes similar to PhzA/B, including those from *B. cepacia, Erwinia carotovora* and *P. agglomerans* (Figure 3.3) indicated the possibility that the pseudomonal phzA/B genes had arisen later in the evolutionary timeline and that these genes were orthologs of BcepA and *Erwinia carotovora*-A (ErwA). BcepA and ErwA are thus the predecessors of genes of the PhzAB family in *Pseudomonas*. This leads to the conclusion that an event of gene duplication might have occurred in the genomes of *Pseudomonas*, which led to the formation of two copies of PhzA-like genes in this species. Thus the genes *phzA* and *phzB* are infact paralogs. This explains the high level of sequence similarity between phzA/B-like genes among *Pseudomonas*.

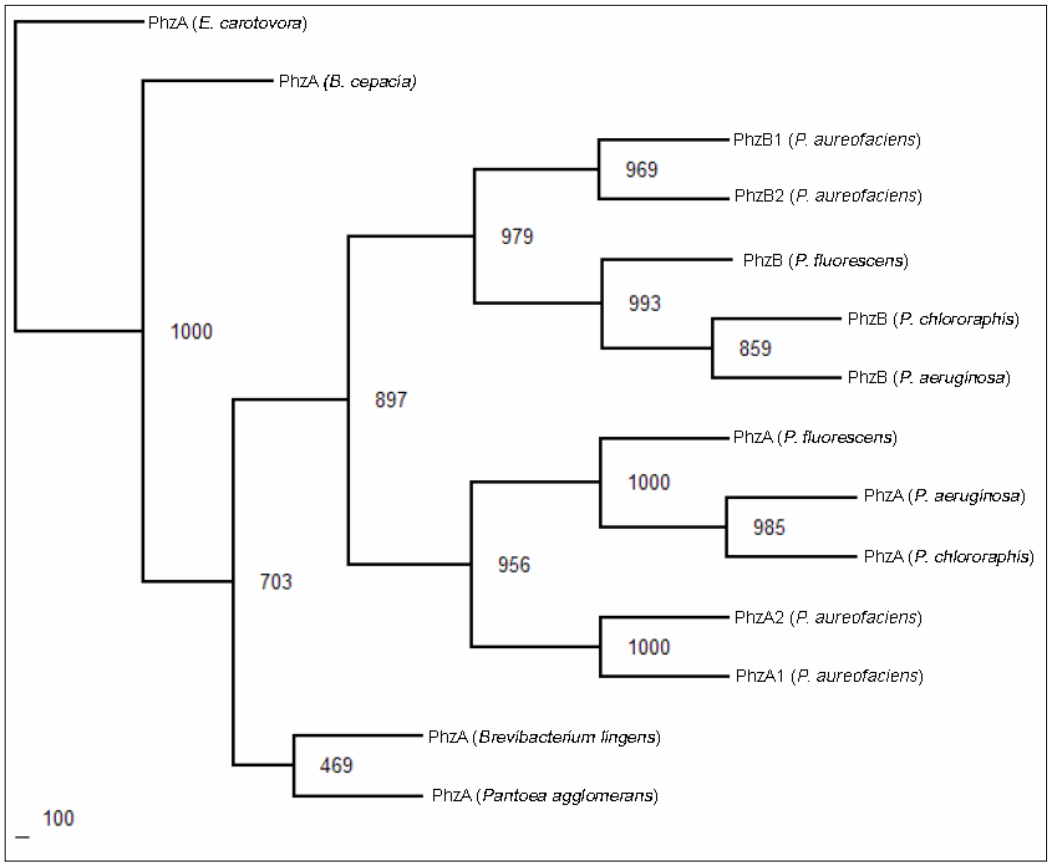

Figure 3.3: Evolutionary tree of the sequences similar of PhzA/B.

Another interesting fact highlighted by the evolutionary tree in the Figure 3.3 is that the PhzA and B of various Pseudomonads belong to different branches.

This implies that despite having a very high degree of sequence identity, these two genes belong to inherently different evolutionary clusters, which could be an indication of differing functions of PhzA and B like proteins.

3.1.3 Sequence analysis of PhzG

The protein sequence of PhzG has highest homology (70%) to pyridoxyamine 5'-phosphate oxidase (PNPOx) from *Pseudomonas chlororaphis* and upto 50% sequence homology with similar enzymes from other organisms. The PNPOx family is the smallest member of the flavin-containing oxidase class of enzymes. Figure 3.4 shows the alignment of PhzG with sequences of similar proteins.

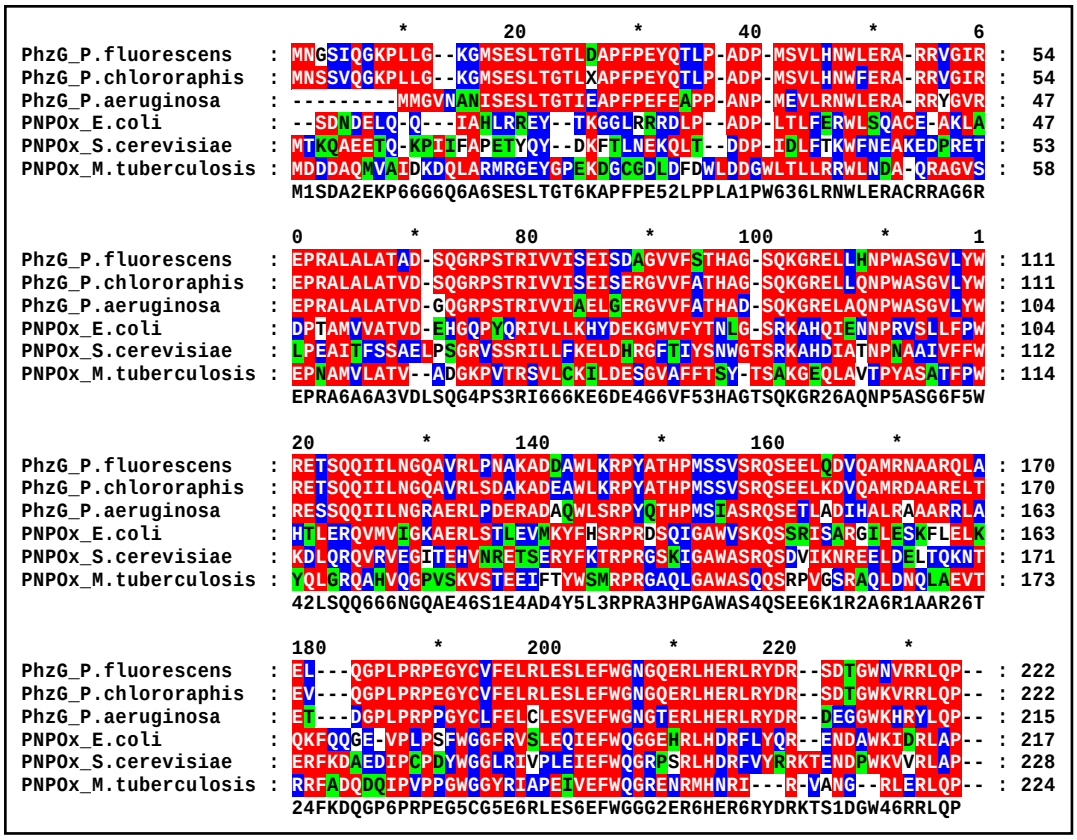

Figure 3.4: Multiple alignment of PhzG. (Colour key: Red = 100%; blue = 80%; green = 60% similarity)

Of the sequences aligned here, the ones denoted as 'PNPOx' are proteins for which structural data is available. There is approximately 25% sequence homology between the sequences of the proteins whose tertiary structure is known and PhzG. This suggests that all members of the PNPOx family and

thus PhzG have the same fold and gives a reliable estimate of the function of PhzG being a FMN-dependent oxidase.

With the results of this bioinformatical analysis, cloning, over-expression and crystallisation of these four proteins i.e PhzA, B, BcepA and PhzG was initiated.

3.2 Cloning, over-expression and purification

Genes encoding the proteins PhzA, BcepA, PhzB and PhzG investigated in this work were cloned into the plasmid pET15b (Novagen) which contains N-terminal 6×His-tag. These plasmids were then transformed into Rosetta-*pLysS* competent cells (Novagen) and initial expression tests were carried out to determine the optimal conditions for growth and expression.

All proteins were over-expressed according to the respective optimal conditions and purified as described in section II. Figure 3.5.1 depicts a typical SDS-PAGE for both steps of purification for PhzA.

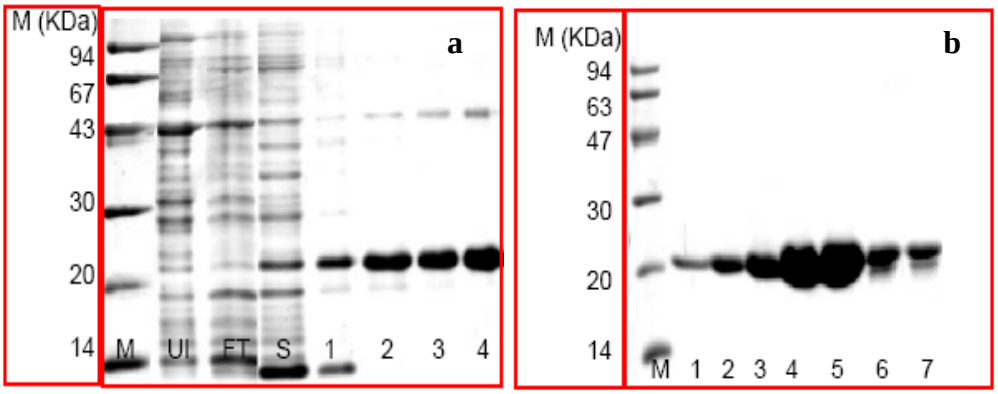

Figure 3.5.1: Purification of PhzA. (a) SDS-PAGE after Ni-chromatography. Fractions 1-4 were pooled for gel filtration chromatography (b).
(Legend M- Marker; **UI**- Un-induced; **FT**- Flow-through; **S**- Soluble cell extract)

Figure 3.5.2 (overleaf) shows the MALDI-TOF mass spectroscopy for confirmation of cleavage of the 6xHis-tag. The expression and purification protocol remained identical for seleno-L-methionine labelled proteins.

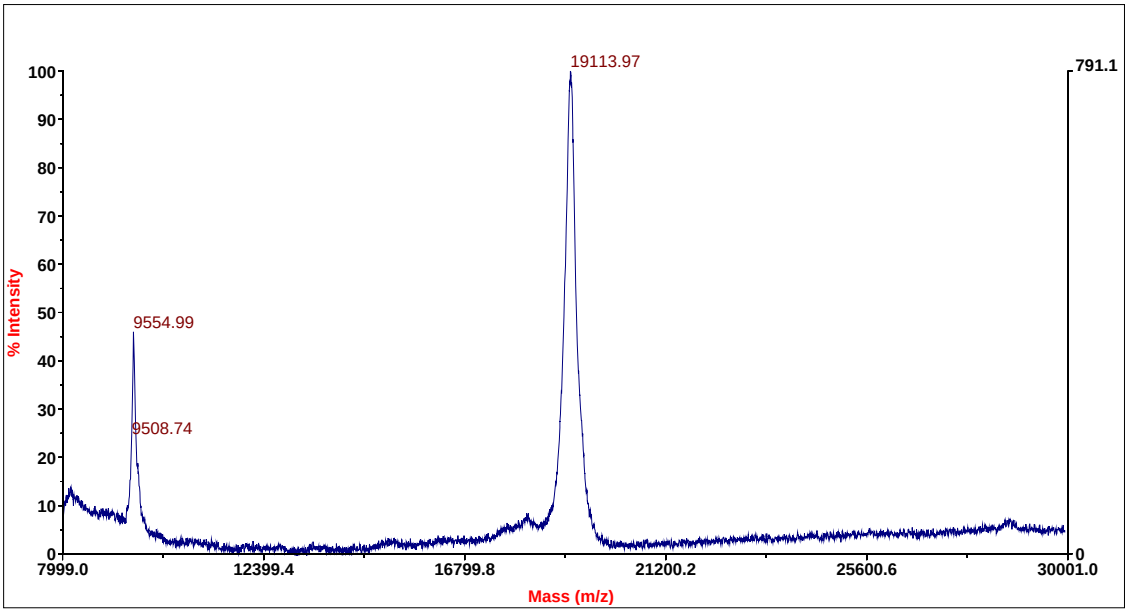

Figure 5.5.2: MALDI-TOF spectra for Seleno-L-methionine labelled PhzA.

The purified protein obtained at the end of this purification protocol was used to set-up crystallization trials.

3.3 Crystallisation

3.3.1 Crystallisation of Native Proteins

All crystallisation experiments were performed at room temperature with the hanging-drop vapour-diffusion method. Crystallisation conditions for the proteins are summarized in Table 3.1. Panel 3.6 shows photographs of crystals used for data collection and structure elucidation.

Protein (concentration of protein)	**Condition of crystallisation**
PhzA (long needles) (23-26 mg ml^{-1})	0.8 M sodium/potassium tartrate; 0.1 M sodium HEPES pH 7.5.
PhzA (used for data collection**)** (23-26 mg ml^{-1})	1.6 M magnesium sulphate; 0.1 M MES pH6.5
BcepA (10-12 mg ml^{-1})	0.2 M ammonium sulphate; 20% PEG-3350
PhzG (10-15 mg ml^{-1}**)**	0.2 M ammonium sulphate; 0.1 M Bis Tris pH 6.5; 25% PEG-3350; 10 mM FMN

Table 3.1: Crystallisation conditions of the proteins.

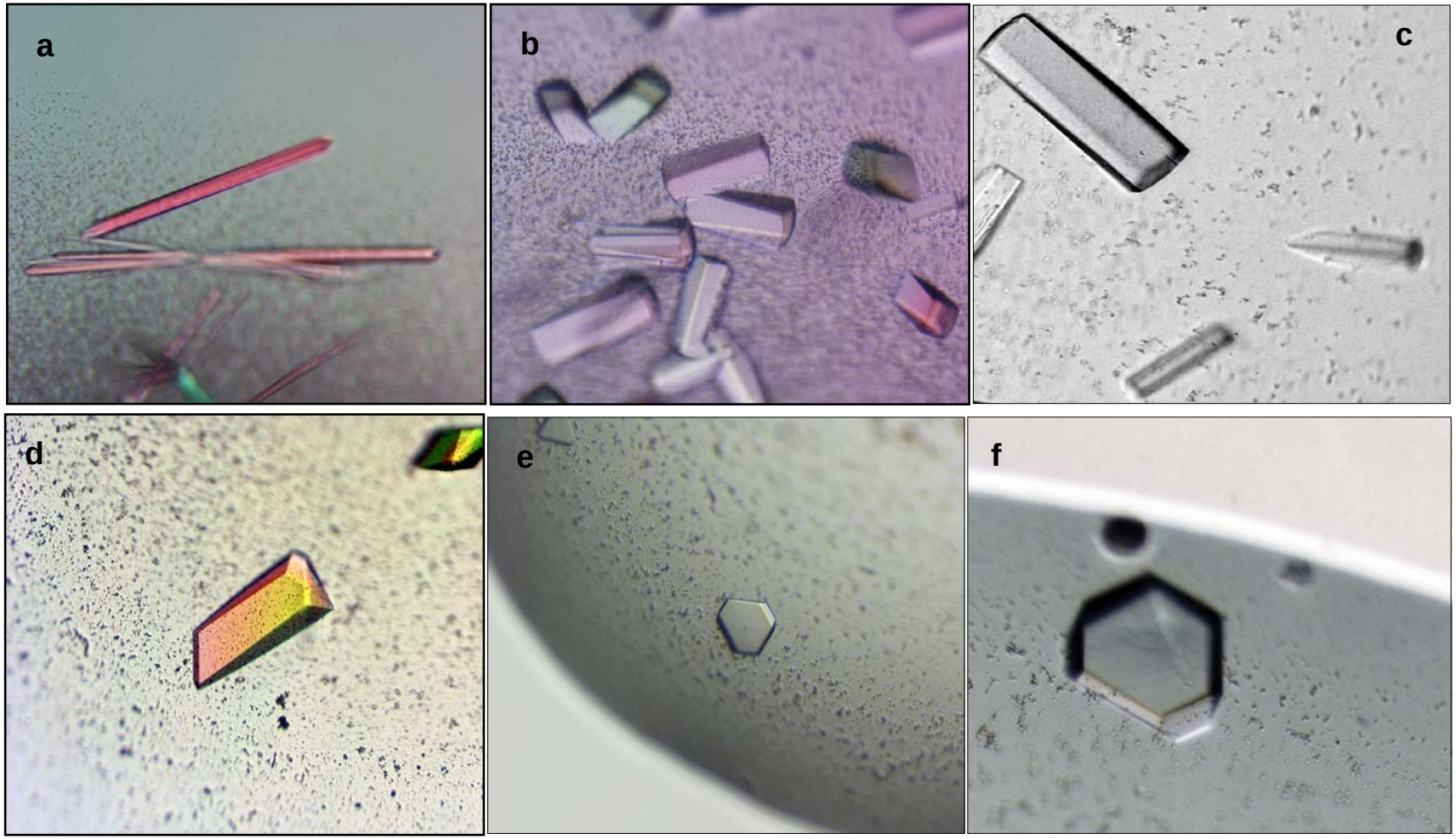

Panel 3.6: Crystals of PhzA and PhzA_Bcep. (a) long needle-shaped crystals of PhzA (b) & (c) crystals used for data collection; (d) PhzG,(e) & (f) crystals of BcepA.

For PhzA, the first condition produced long needle like crystals (Panel 3.6 ‘a’). On data collection, these crystals were found to be unsuitable for structure elucidation owing to a very long axis of the asymmetric unit. Hence more optimisation was undertaken and a second crystal form was obtained, which was used for data collection and eventual structure elucidation (Panel 3.6; ‘b’ & ‘c’).
In case of PhzB, no diffraction quality crystals could be obtained despite various optimisation trials. This, in part, led to the investigation of BcepA, to obtain the structure of a protein similar of PhzA/B and gain more structural and functional insight into this family of proteins. Diffraction quality crystals of BcepA were obtained in the initial screen (Panel 3.6; ‘e’ & ‘f’). Crystals of a good size (50-100 µm) and diffraction properties were also obtained for PhzG, which was crystallised in the presence of 10 mM FMN (Panel 3.6 ‘d’).

3.3.2 Crystallisation of protein complexes

To gain further understanding of the active site and the process of ligand-binding, co-crystallisation and crystal soaking trials were performed for PhzA, BcepA and PhzG. In case of PhzA soaking trials, native crystals were initially washed and incubated in mother liquor in which MES buffer was substituted with another buffer, while maintaining the same pH to remove this molecule from the cavity of the protein. However, this washing step led either to the complete dissolution of the crystal, or in no uptake of the ligand into which the crystals were soaked after this washing step (as determined by diffraction, data collection and structure solution of the data of soaked crystals). The reasons for this could be two fold, one, tight binding of MES within the active centre resulting in the inability of other buffers (piperidine, caodylate etc.) to displace this molecule. Or the large conformation changes necessary for displacement of MES, which disturb the crystal packing, leading to the dissolution of the crystal. Moreover, no crystals were obtained when the original conditions sans MES were used for co-crystallisation. Co-crystallisation trials of PhzA with 3OHAA, the analogue of the DHHA did produce crystals, but these did not diffract on exposure to X-rays.

Further optimisation trials did not improve the diffraction properties of these crystals.

Soaking trials of native crystals with product/proposed intermediate of phenazine biosynthesis in *Pseudomonas* - PCA and PDC, was undertaken for both PhzA and BcepA. Moreover, compounds that were synthesised based on the structural properties of PCA and PDC were also used (more details in section 3.6.4) for soaking trials. Co-crystallisation of BcepA with the compound B75 was successful and the structure of BcepA complexed with B75 was solved.

Native crystals of PhzG soaked in mother liquor containing PCA (10 mM) for 24 hrs successfully incorporated PCA and structure of the complex of PhzG with PCA was determined.

Data-sets were collected for all crystals at synchrotrons and the results obtained on data-collection, structure analysis and analysis of these structures are described in the following chapters.

Section II

The final statistics of data collection and structure elucidation with the quality of the final model are described in this section. The structural highlights, binding of substrates, cofactors etc for PhzA, BcepA, PhzG, and their complexes are also described. The results obtained on comparison of homologous structures from the Protein Data Bank (PDB) and the implications of this similarity to the potential function of the proteins are also discussed.

3.5 Data collection, Structure Determination & Quality of Model.

Crystals shown in Panel 3.6 were exposed to synchrotron radiation and data-sets were collected for structure solution. Molecular Replacement methods of structure solution being unsuccessful in all cases, the structures were solved by SAD (Single-wavelength Anomalous Diffraction) using Seleno-L-methionine labelled protein. The initial steps of data processing and phase determination for all structures were similar and are described in detail in section 9.4.5. The particulars of structure determination for each of the proteins are detailed below.

3.5.1 PhzA

The program MAPMAN (Kleywegt and Jones, 1994) in the RAVE suite (Jones, 1992) was used to generate skeletonised electron density after data processing and phase determination. The 3DPSSM program had predicted Δ^5-3-ketosteroid isomerase (PDB ID: 1OPY) from *E. coli* to be the closest structural homologue of PhzA (as previously described). A poly-alanine model of this structure was superimposed on these 'BONES' to find the correct connections between the various secondary structure features of PhzA.

NCS operators were then generated with the program LSQMAN (Kleywegt, 1996), refined using program IMP in the RAVE suite. The program MAMA (RAVE suite) was used to generate a mask of the monomer and overlay regions were removed by the program NCSMASK in the CCP4 suite. These operators and mask were used to generate averaged electron density by using the program DM. The electron density map after NCS averaging was of sufficient quality to manually build the backbone of a monomer of PhzA, by using the poly-alanine model of a monomer of 1OPY to detect the correct fold of PhzA.

Using the Se atoms as anchor points and bulky aromatic (Trp, Tyr, Phe) residues as "light houses", side chains were incorporated into this poly-alanine model and 135 of the total 163 residues (per monomer) were fitted. This model was then further refined using the program REFMAC5 (Murshudov et al., 1997).

In the final model, homo-dimeric PhzA comprises of 268 residues starting at residue Glu12 till Ala146 (per monomer). Additionally, 222 molecules of water, 2 MES molecules, 1 magnesium cation (Mg^{+2}) and 3 sulphate anions (SO_4^{-2}) make up the total residues present in the completed model of PhzA. The final structure of PhzA at 2.1 Å resolution has R-factor of 19% and R_{free} of 21%. The Ramachandran plot (Figure 3.7) obtained by the validation programme 'PROCHECK' shows 104 amino acids in the most favoured region with 10 amino acids in the additionally or generously allowed region and none in the disallowed region.

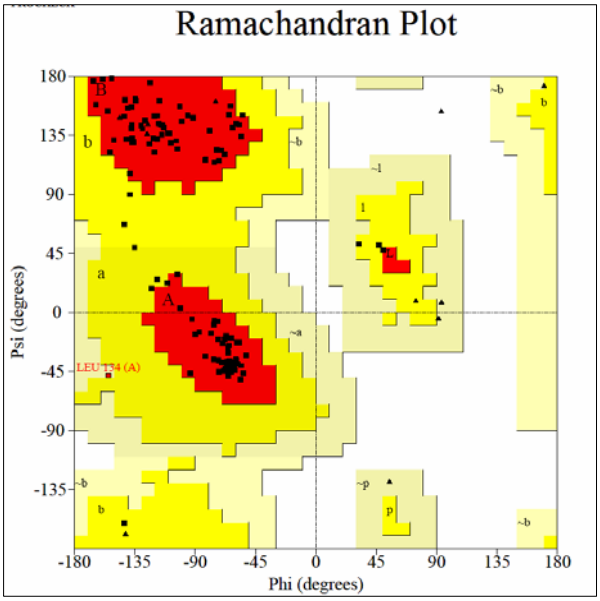

Figure: 3.7: Ramachandran plot of the final model of PhzA.

3.5.2 BcepA

BcepA was predicted to fold like PhzA, hence, the poly-alanine trace of PhzA was used as a guide for deducing the correct backbone of the dimer of BcepA using 'BONES' generated by the program COOT (Emsley et al., 2004). The residues were then fitted per hand using the electron density (also in COOT). Residues starting from Ser11 to Phe148 were built using this strategy. The second monomer was generated in the same program and the model was then further refined. During the manual refining of this structure (at 2.1 Å resolution), another crystal with better diffraction quality (1.9 Å resolution) was obtained. The native data from this crystal was hence used and the electron

density improved using the solvent flattening program 'DM'. This improved data was then submitted to the automatic model-building programme 'RESOLVE' which fitted 156 of the total 165 residues per monomer and 317 molecules of water. After two rounds of refinement (using program REFMAC), the final model of BcepA and complex of BcepA with B75 has an R-factor of 18% and R_{free} of 24%. The structure of BcepA complexed with B75 contains additionally, two molecules of B75 (2-(2-fluorophenylamino) benzoic acid). On validation (PROCHECK) 92.5% of the residues were found in the allowed region and 7.5% in the additionally allowed region of the Ramachandran plot (Figure 3.8).

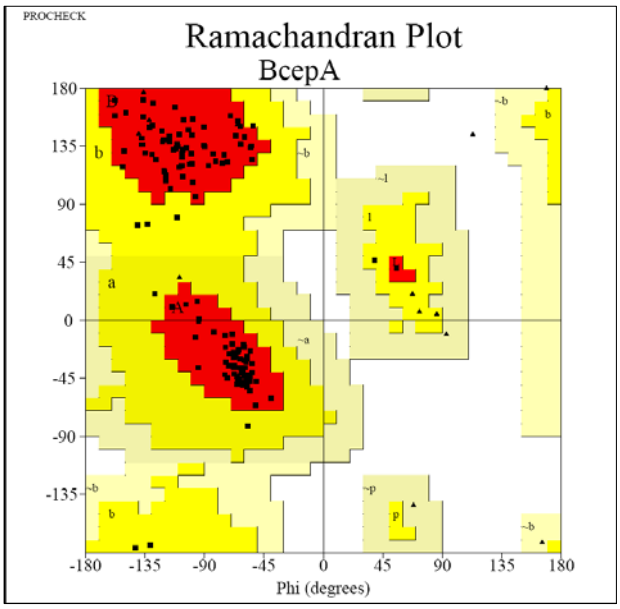

Figure 3.8: The position of various residues of the completed model of BcepA in the Ramachandran plot.

The final statistics of data collection and structure refinement for these two proteins have been tabulated overleaf (Table 3.2).

3.5.3 PhzG & complex of PhzG with PCA

PhzG crystals diffract to a resolution of 1.2 Å. Hence, it was possible to build the structural model automatically using the program ARP/Warp 6 (Perrakis et al., 1997). This program is based on an interpretation of the difference electron density of free atoms, followed iteratively, by atomic refinement and interpretation of the atomic coordinates in terms of a poly-peptide chain. PhzG was present as a dimer in the asymmetric unit and hence the unit cell contains

Data collection	PhzA Long Axis	PhzA Native	PhzA SeMet-SAD	BcepA Native	BcepA SeMet	BcepA Complexed with B75
Wavelength (Å)	0.934 (ID14-EH1)	0.934 (ID14-EH1)	0.9792 (BM14)	0.934 (ID14-EH1)	0.9792 (BM14)	0.934 (ID14-EH1)
Resolution (Highest Shell, Å)	20.0- 6.5 (6.5-6.6)	55.9 – 2.1 (2.1-2.2)	19.8-3.5 (3.5-3.6)	18-1.9 (1.9-2.0)	15-3.0 (3.0-3.1)	15-2.3 (2.3-2.4)
Space group	R32	$P2_12_12_1$	$P2_12_12_1$	$P3_221$	$P3_221$	$P3_221$
Cell constants (Å; º)	a=b=95.4, c=1955.7 α=β=90, γ=120	a=66.8 b=75.2, c=84.5 α=β=γ=90	a=67.3 b=75.4, c=84.6 α=β=γ=90	*a=b=64, c=160; α=β=90, γ=120*	*a=b=64, c=160; α=β=90, γ=120*	*a=b=64, c=160; α=β=90, γ=120*
VM (Å °/Da)	-	2.5	2.5	2.3	2.3	2.3
Unique reflections	7142 (331)	47100 (6080)	10461 (856)	31058 (4297)	14735 (1381)	9556 (954)
Average redundancy	2.8 (3.0)	2.9 (2.2)	2.9 (2.6)	5.4 (3.8)	11 (11)	4.7 (4.3)
I/(σ) I	7.1 (2.8)	10.7(2.6)	19.7 (4.8)	18.3 (3.7)	25 (7.6)	20.7 (3.8)
Completeness (%)	94.3 (100)	98.2 (97.7)	99.8 (100)	99.6 (98.2)	99.6 (98.6)	97.6 (99.4)
Anom. completeness (%)[a]	-	-	98.3 (100)	-	97.6 (97.1)	-
Wilson-B ($Å^2$)	-	44	30	37	51	73
Rsym[b]	10.5 (39.8)	4.6 (36.8)	9.3 (19.6)	5.4 (38.5)	8 (36.4)	7.2 (31.3)

Table 3.2: Data collection statistics for PhzA and BcepA.

[a]Completeness calculations treat Friedel pairs as separate observations

[b]$R_{sym} = \Sigma \mid I(h)_j - \langle I(h) \rangle \mid / \Sigma I(h)_j$ where $I(h)_j$ is the scaled observed intensity of the i-th symmetry-related observation of reflection h and $\langle I(h)_i \rangle$ is the mean value

444 amino acid residues, of which 400 were successfully built by ARP/Warp. Electron density for the cofactor FMN was exceptionally clear and these molecules were then added. The rest of the residues were built by hand using the graphics program 'O' (Jones et al., 1991). The structure of PhzG with the ligand PCA was built using the backbone of native PhzG structure. Two molecules of PCA were fitted into the density observed. The amino acid residues were checked by hand and the ones showing alternative confirmations were introduced.

Final model of PhzG contains 651 water molecules and 2 FMN molecules apart from the amino acid residues and is refined to an R-factor of 20% and R_{free} of 21%. The model of PhzG complexed with PCA has a final resolution of 1.2 Å and contains two PCA molecules per dimer in addition to the molecules present in the native structure. Of the total residues for both the native and complex structure, 91.5% lie in the most favoured region of the Ramachandran plot (PROCHECK (Laskowski et al., 1993); Figure 3.9). Most of the residues with poorer electron density are located in the additionally allo-

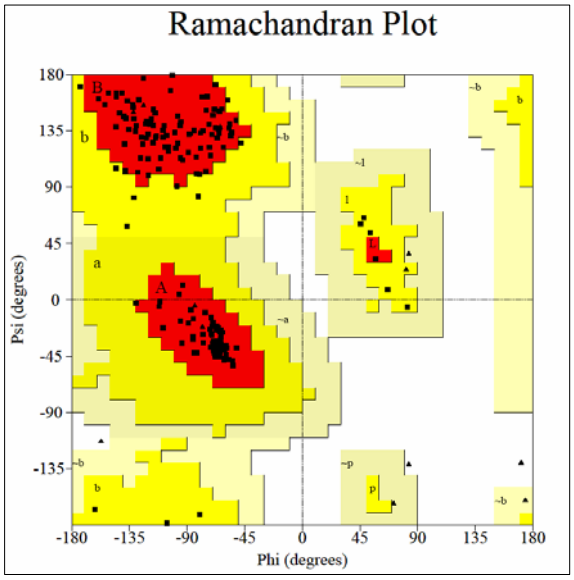

Figure 3.9: Ramachandran plot for PhzG.

-wed regions, with no residue in the disallowed region. The final data collection statistics for the structure of PhzG and its complex with PCA are tabulated overleaf.

Data collection	Native	SeMet-MAD	PhzG-PCA complex
Wavelength (Å)	0.9791 (ID29)	0.934 (BM14)	0.9791 (ID29)
Resolution (Å)	19.2-1.2 (1.2-1.3)	67.4-2.3 (2.3-2.4)	20-1.5 (1.5-1.6)
Space group	$P2_12_12_1$	$P2_12_12_1$	$P2_12_12_1$
Cell constants (Å; º)	a=57.5, b=63.2, c=132.8, α=β=γ=90	a=57.5, b=63.6, c=133.4, α=β=γ=90	*a=57.5, b=63.2, c=133.8; α=β=γ=90*
VM (A°/Da)	2.2	2.2	2.2
Unique reflections	95809 (6581)	41974 (2438)	94771(44327)
Average redundancy	3.9 (3.9)	4.3 (4.3)	10.1 (10.1)
I/σ	11.9 (4.8)	10.5 (4.8)	28.7 (19.8)
Completeness (%)	99.7 (100)	99.8 (100)	99.7 (100)
Anonymous completeness (%)[a]	-	99.8 (100)	-
Wilson-B (Å2)	18.4	32.9	13.8
R_{sym}[b]	6.4 (36.6)	9.7 (30.8)	5.2 (11.3)

Table 3.3: Statistics of data collection for native and complexed PhzG.

([a]Completeness calculations treat Friedel pairs as separate observations
[b]$R_{sym} = \Sigma \mid I(h)_j - \langle I(h) \rangle \mid / \Sigma I(h)_j$ where $I(h)_j$ is the scaled observed intensity of the i-th symmetry-related observation of reflection h and $\langle I(h)_i \rangle$ is the mean value)

The structures obtained after this segment of work were then analysed and this analysis is described in the following sections.

3.6 Structural Features of PhzA from *Pseudomonas fluorescens*

3.6.1 The monomer of PhzA

PhzA is a 36 kDa homodimer comprising of two identical single domain subunits of 163 amino acids each. The monomer of PhzA belongs to the α+β class of proteins that are made up of a combination of α-helix and β-strand motifs. It displays α-β roll architecture and belongs to a class of proteins having a topology similar to nuclear transport factors/ ketosteroid isomerase family of proteins (Bullock et al., 1996; Kim et al., 1997; Cho et al., 1998) (Figure 3.10). This confirms the result from the sequence based structure prediction by 3DPSSM.

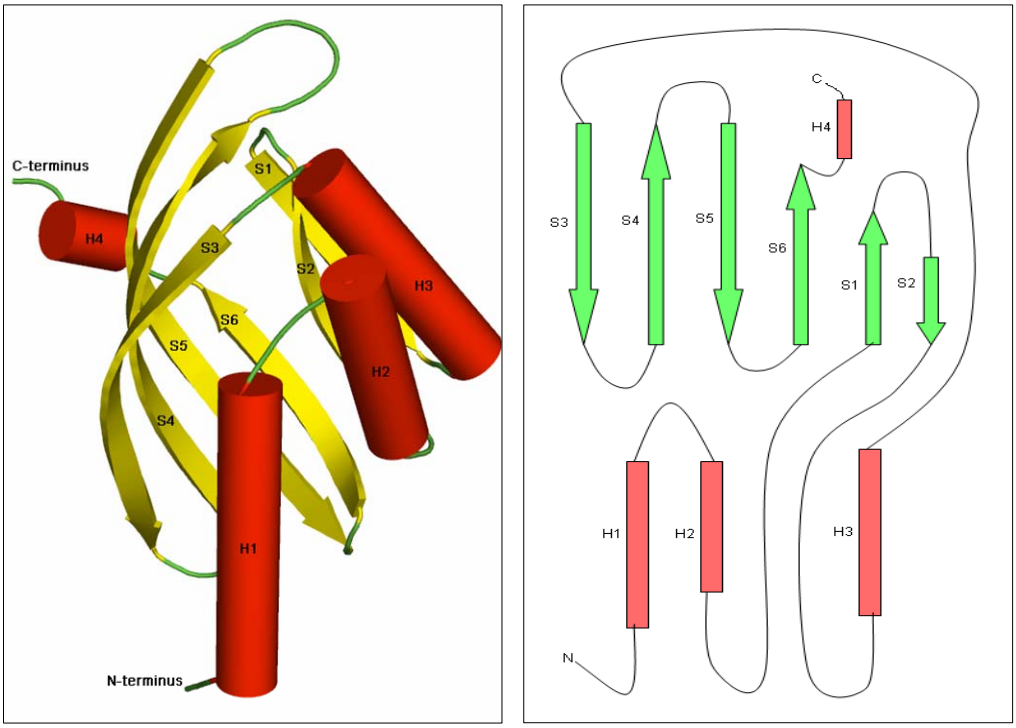

Figure 3.10: Schematic representation of a monomer of PhzA.

The structure of PhzA is broad at one and tapers at the opposite end to form a 'cone-shell' shaped structure which encloses a cavity where a molecule of MES (2-**m**orpholino**e**thane-**s**ulphonic acid monohydrate) is bound.

The largest motifs of this structure is a central six-stranded β-sheet dominated by three long anti-parallel strands S3 (Asp80-Glu90), S4 (His96-Thr107) and S5 (Gly115-Asp128) which are continuous in the sequence (Figure 3.10) and span the entire monomeric structure. The strand S3 is the longest in the structure and is made up of 11 residues. Of the three shorter strands (S6

(Lys131-Phe138), S1 (Ser47-Asp52) and S2 (Gly56-Lys62)), S6 and S1 run in parallel and S1 and S2 in anti-parallel orientation. Together, the six strands form a very curved β-sheet structure. The three helices H1 (Leu14-Arg29), H2 (Glu33-Leu41) and H3 (His64-Cys77) complement the sheet to create a mixed barrel-type structure. This 'barrel' is anchored by the third helix, H3, which links the highly curved strand S3 and stabilises the curvature of the sheet. The helices H1, H2 and H3 run anti-parallel and form the opposite side of the β-sheet motif and thus the other half of the cone. The β-strand S6 extends further as a one-turn helix H4 and then a disordered loop forming the carboxyl terminus of PhzA. The last 17 residues of this terminus do not show any density and hence are not present in the final structure of PhzA. As seen in the structures of numerous other homologous proteins, this highly flexible loop could potentially act as a 'lid', controlling the entry and exit of the ligand from the active centre of PhzA.

The mode of dimerisation of PhzA is similar to 1S5A (Hypothetical protein apc1116) and 1NU3 (limonene-1, 2-epoxide hydrolase), both members of the ketosteroid isomerase family of proteins.

3.6.2 Dimer of PhzA and the dimer interface

The narrow and long patch of β-sheets, comprising of stands S3, S4 and S5 of each monomer face each other forming the dimer interface (Fig. 3.11, below).

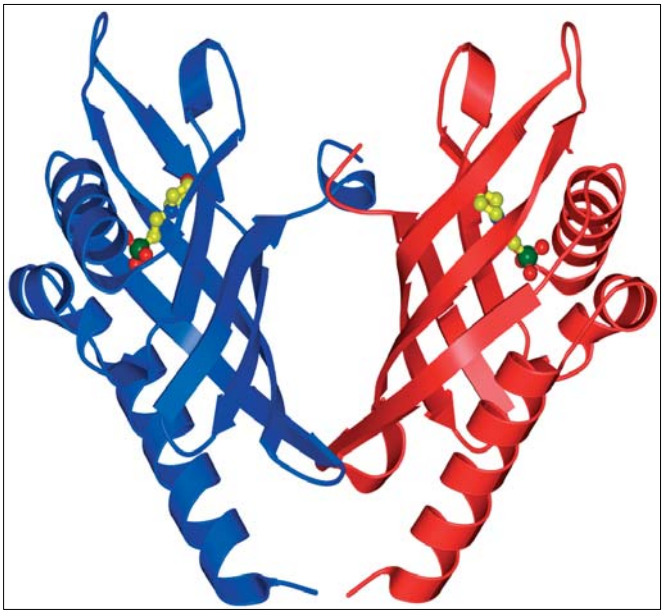

Figure 3.11: A dimer of PhzA with MES molecules.

The dimer interface covers an area of 1831 Å, calculated using the protein-protein interaction server at http://www.biochem.ucl.ac.uk/bsm/PP and corresponds to 23% of the total accessible surface area of the dimer. This is a value typical for dimer interactions (Figure 3.12).

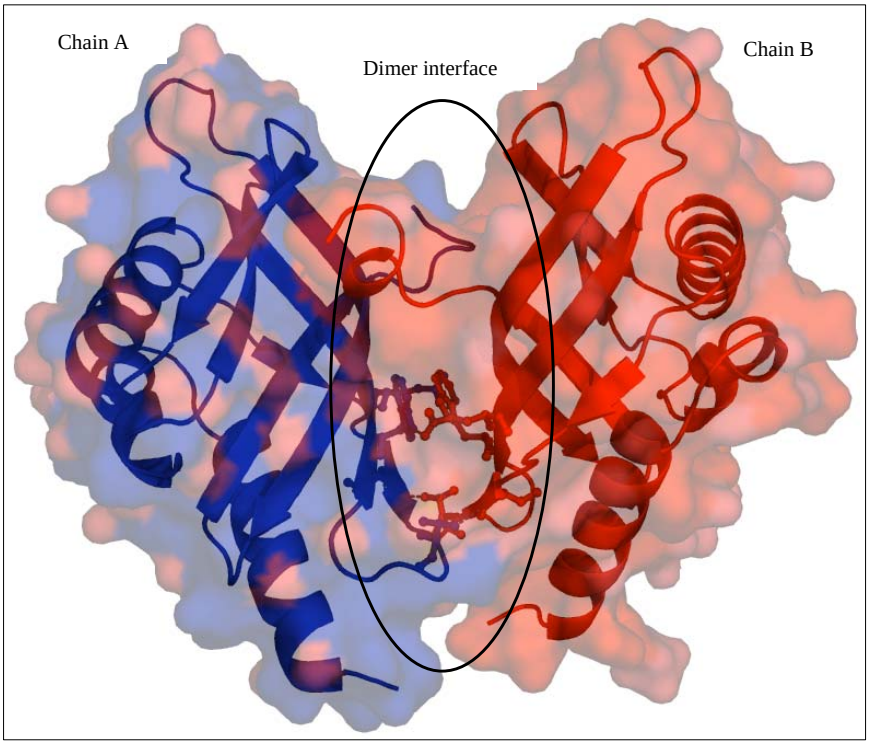

Figure 3.12: Dimer interface of PhzA (marked inside the oval) with the residues forming hydrogen bonds.

This dimer interface comprises mainly of hydrophobic interactions; with 32% polar, 62% non-polar residues and 9 water molecules participating in dimer formation. Altogether, 27 residues are within a distance of 3.8 Å from each other and these include Arg10, Ser39, Pro58, Trp51, Val60, Arg87, Phe89, His96, Phe97, Trp98, Glu100, Ile122, Arg136, Glu137, Phe138, Pro141, Phe142, and Leu145. Five hydrogen bonds involved in dimerization are tabulated here.

Residue of chain A	Atom	Residue of chain B	Atom	Distance
Glu 90	O	Glu 90	N	2.9
Glu 90	N	Glu 90	O	2.8
Thr 91	OG1	Val 88	O	2.7
Val 88	O	Thr 91	OG1	2.7
Glu 100	OE2	Trp 98	NE1	2.9

Table 3.4: Hydrogen bonds making up the dimer of PhzA.

3.6.3 Active site cavity and binding of MES

Packing of the three helices (H1, H2 & H3) into the concave face of β-sheets of each monomer of PhzA creates a pocket which extends ~ 16 Å into the protein core. This pocket is lined mainly with hydrophobic residues, with the exception of a cluster of polar and charged residues at the deepest point, which coincides with the broad end of PhzA monomer. This cavity, which corresponds to the active site cavity in proteins with structures similar to PhzA, has a volume of 498 $Å^3$ as calculated by the program 'Pocket-finder' (based on the 'Ligsite' algorithm written by Hendlich *et al.,* 1997) A molecule of the crystallisation buffer, MES is bound within this cavity (Figure 3.13).

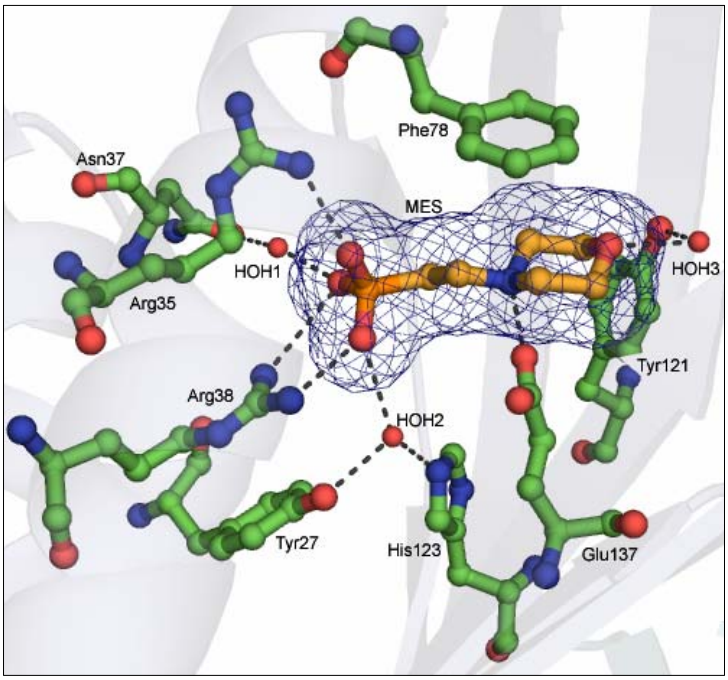

Figure 3.13: Co-ordination of a molecule of MES within the active site cavity of PhzA. (MES shown with the Omit map of its electron density.)

Three water molecules participate in the binding of MES, alongwith 8 amino acid residues which form hydrogen bond or stacking interactions and 4 residues (Thr53, Leu74, Trp81, Trp83) which are involved in hydrophobic interactions. The main interactions are between the residues Phe78, Arg35, Arg38 and Glu137. Phe78 makes stacking interactions with the ring of MES, while the nitrogen atoms (NH1 and NH2) of Arg38 form salt bridges with the oxygen atoms (O2 and O3; lengths 2.9 Å and 3.3 Å respectively) of the sulphate. The O1 atom of MES is stabilised by another salt bridge formed by the nitrogen NH1 of Arg35 (2.8 Å). The negatively charged Glu137 stabilises

the positively charged nitrogen in the ring of MES (2.5 Å).

3.6.4 Ligand docking studies

While co-crystallisation trials of PhzA were underway the program GOLD (Jones et al., 1995; Jones et al., 1997) was used to dock various intermediates, analogues of intermediates and/or known products of the phenazine biosynthesis pathway into the active site cavity of PhzA. GOLD considers the protein surface as a rigid body and does an energy minimization to find the position and orientation of the ligand which is most energetically favorable.The three-dimensional structure and docking studies provide insight into the structure and the theoretical probability of the accommodation of the docked compounds in the cavity of this protein.

For this purpose, DHHA and its analogue 3OHAA (inhibitor of PhzF), PCA and PDC were used for docking studies. These experiments were designed so as to gain an insight into the feasibility of binding of these molecules in the cavity of PhzA and hence the potential substrates of this protein. Moreover, these results would also provide an indication of the position at which PhzA acts in the pathway, i.e. before dimerisation of DHHA or after the formation of the tricyclic scaffold of PCA.

The results of this study (Figure 3.14; overleaf) clearly indicate that the active centre of PhzA is large enough to accommodate all of these molecules. However, the only other conclusion that could be derived from this set of experiments was that the residues involved in the co-ordination of MES are also important for ligand binding. This knowledge of the active-site cavity of PhzA was used to model inhibitors similar to both PCA and PDC.

The primary motivation for the modelling and synthesis of these inhibitors was to synthesise compounds which would bind PhzA more strongly than MES, thus be able to displace MES (which is not a structural analogue of any of the intermediates/products of phenazine biosynthesis pathway and thus provides no information about the binding of substrates in the active site cavity of PhzA) from the active cavity and provide as to the catalytically important residues. Hence, these experiments were designed to provide an approximation of the function of PhzA.

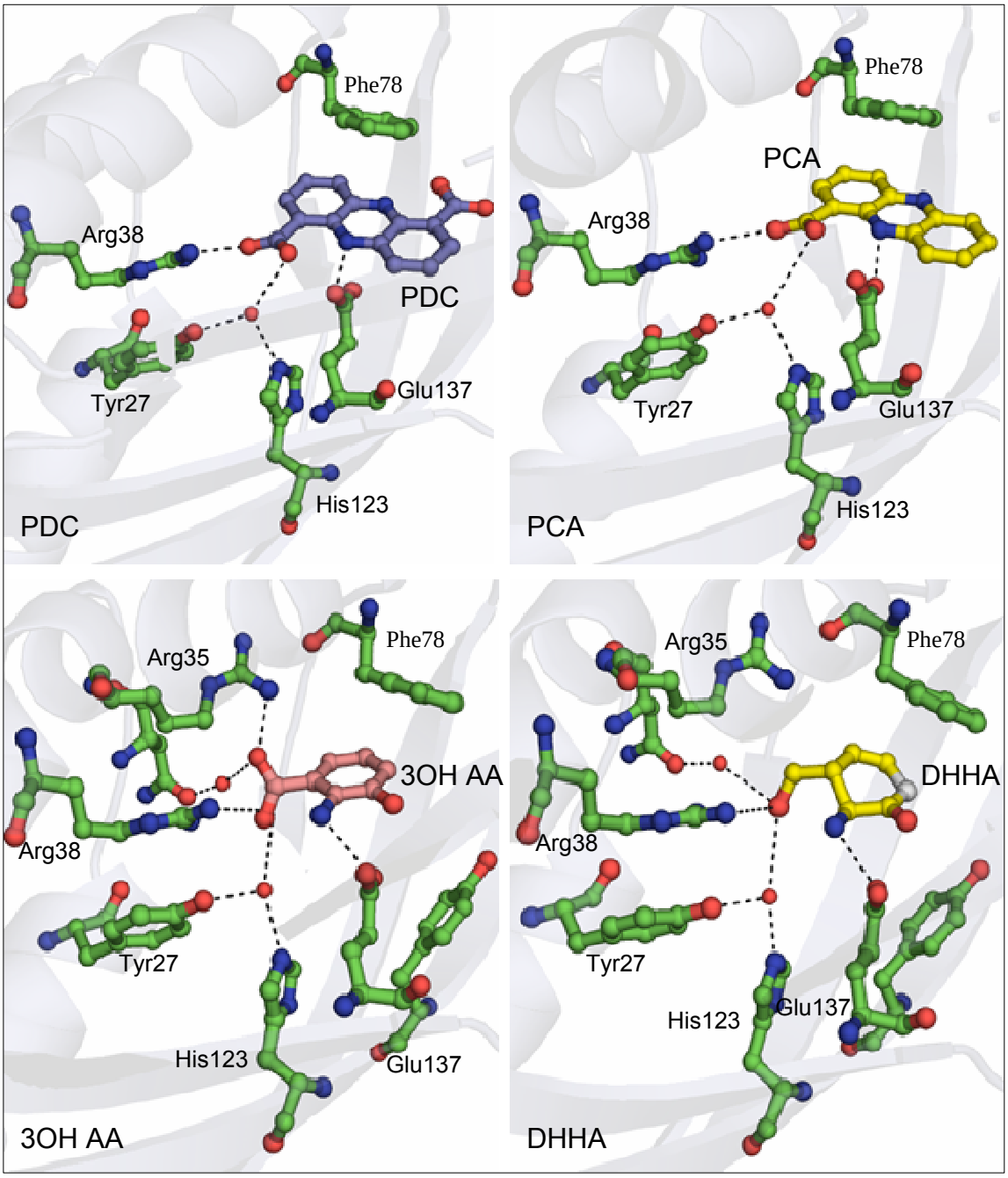

Figure 3.14: Output of the programme GOLD displaying the binding of ligands DHHA, 3OHAA, PCA and PDC. The common residues involved in binding of MES, which also bind these ligands, have been shown.

The structures of the six compounds synthesised by A. Graebsch (Graebsch A, Diplomarbeit-2005) are shown in the Figure 3.15 overleaf.

These compounds were then used for co-crystallisation and soaking trials with both PhzA and BcepA (described in section 3.3.2). The co-crystallisation trials were unsuccessful, or failed to yield diffraction quality crystals for PhzA.

However, since no information was available for BcepA, the protein homologous to PhzA, from *B. cepacia*, these compounds were also used for co-crystallisation and soaking trials with BcepA. These soaking/co-crystallisation trials would thus help provide an insight into the binding properties of the active site of BcepA with respect to the kind of substrate used by this enzyme for the biosynthesis of phenazine synthesised by *B. cepacia*. Soaking trials with the compound B75, which is a 2-(2-fluorophenyl-

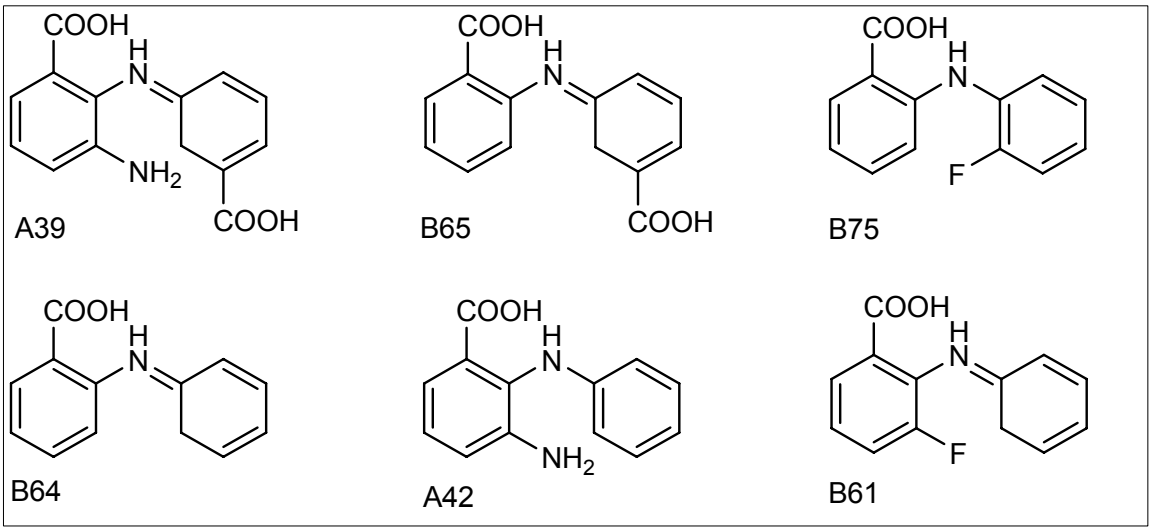

Figure 3.15: Structures of the inhibitors designed for investigating functional properties of PhzA and BcepA.

-amino) benzoic acid were successful. The diffraction data for the complex of BcepA with the compound B75 (2-(2-fluorophenylamino) benzoic acid) was obtained and the structure of native BcepA and BcepA complexed with B75 are described in the following sections.

3.7 Structural analysis of BcepA from *Burkholderia cepacia*

The structure of BcepA belongs to the same class of α+β family as PhzA, which was expected, given the high degree of sequence similarity between the two proteins.

3.7.1 The monomer of BcepA

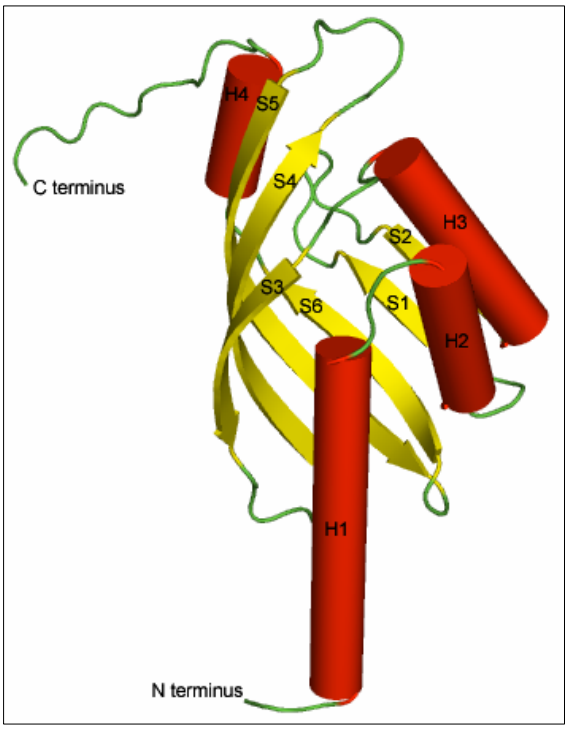

Figure 3.16: Schematic representation of a monomer of BcepA. (α-helices shown in red and β-strands in yellow, with loop regions in green.)

The monomer of BcepA is shown above (Figure 3.16). The highlight of this structure is that only 7 residues (11 in PhzA) of the N-termini and 2 residues (17 in PhzA) of the C-termini are un-fitted due to unclear or missing density. BcepA is thus more complete of the two structures.

All secondary structure features of PhzA are also conserved in BcepA. The only differences lay in the lengths of the α-helix H1 which is longer for BcepA, comprising of 21 residues instead of 15; the helix H4 which is twice the length of H4 in PhzA and the much longer flexible region at the C-terminus. Moreover, BcepA is also a homodimer, its mode of dimerisation and other details are described henceforth.

3.7.2 Dimer of BcepA and dimer interface.

The dimer interface of BcepA, like PhzA is also formed at the interface of the strands S3, S4 and S5. Figure 3.17 shows the dimer of BcepA, with the monomers highlighted in different colours. From the available structures of both proteins and keeping in context the absence of the density of last 17 C-terminus residues of PhzA, the mode of dimerisation differs in one essential aspect between PhzA and BcepA.

Figure 3.17: A dimer of BcepA. (monomers depicted in yellow and magenta)**.**

The very long C-terminus region that plays a vital role in the dimerisation of BcepA. As shown in the figure 3.18, this region consists of the last 14 residues of one monomer of BcepA which 'flip-over' to the second monomer and form a lid-like structure, covering the broad-end of the cavity of the opposite monomer. This is an 'arm-exchange' mode of dimerisation, described in detail by Bergdoll and co-workers (1997). The monomer of BcepA is shaped like a 'question-mark' (Figure 3.18 'a' overleaf) with the C-terminus forming the hook region of this question-mark. This hook region ends at the broad-end of the cavity of the second monomer. The Figure 3.17 ('b'; overleaf) shows a top-down view of a dimer of BcepA to further clarify this observation of 'arm-exchange'.

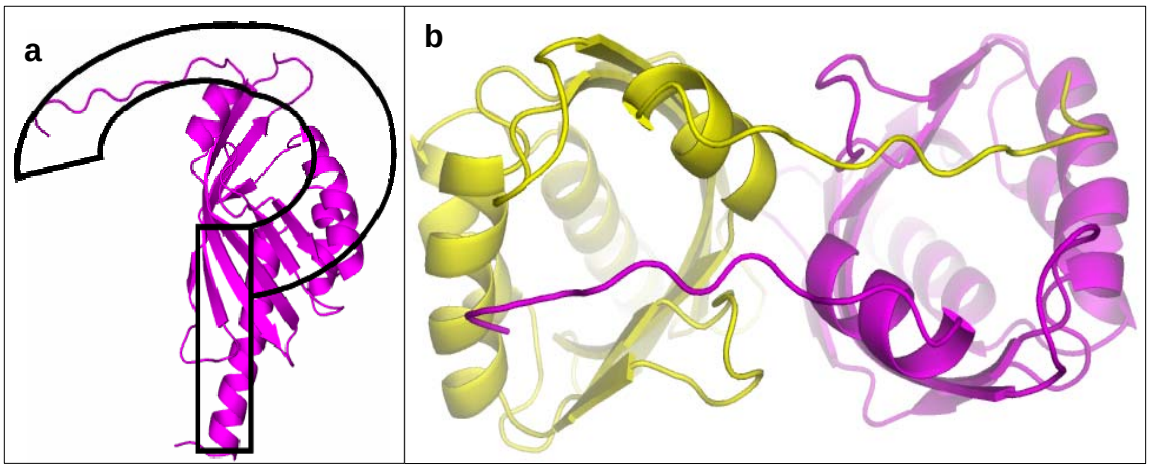

Figure 3.18: (a) The 'question-mark' like arrangement of a monomer of BcepA. (b) A top-down view of BcepA displaying the 'arm-exchange' mode of dimerisation, involving the C-terminal regions of the two monomers (coloured yellow and magenta).

The dimer interface of BcepA comprises of an area of 2011 Å and constitutes 22% of the total accessible surface area of the dimer, a normally observed value for dimers. Of the residues participating in the dimer interactions, 39% are polar, 61% non-polar residues and 16 water molecules. There are 20 hydrogen bonds participating in this dimerisation, with one salt-bridge, between residues Arg 149 of one monomer and Asp 57 of the second monomer. Most of the hydrogen bonds forming the dimer are located in the above-mentioned C-terminal loop region, the residues of which form 14 of the 20 hydrogen bonds (Figure 3.19, overleaf). All calculations for dimerisation were performed using the protein-protein interaction server at http://www.biochem.ucl.ac.uk/bsm/PP and the program LIGPLOT (Wallace et al., 1995). Other polar and non-polar residues participating in dimerisation are tabulated below.

Polar Residues	Asn9,143,149; Arg24,139,159,160; Thr55,56; Asp57; Ser58; His73; Gln90,147; Glu93; Thr94; Gln95; Glu103, 146, 154, 157; Pro113, 144, 156; His123; Cys145
Non-Polar Residues	Leu53, Trp54, 76, 99, 100; Gly59, 162; Ile62, 91, 153; Leu80, 125, 151, 163; Phe92, 112, 141, 148; Tyr115; Met142; Val155,156; Ala164

Table 3.4: The residues participating in dimerisation of homodimeric BcepA.

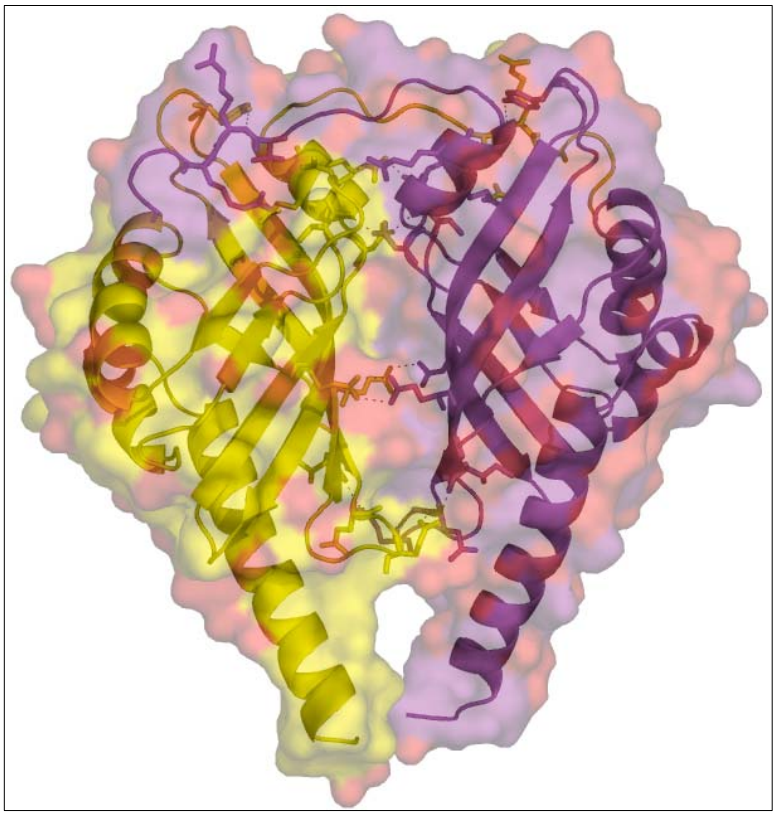

Figure 3.19: The dimer of BcepA, with the monomers (different coloured cartoon representation) and the residues (shown in stick representation) forming hydrogen bonds.

The mode of dimerisation is one of the several differences observed between the structures of PhzA and BcepA. Another difference observed is in the size of the active site cavity of BcepA, described in the following paragraphs.

3.7.3 The active site cavity of BcepA and binding of B75.

As observed for PhzA, the packing of three helices (H1, H2 & H3) into the concave face of β-sheets creates a pocket in each monomer of BcepA. This is also the active site cavity of BcepA, which extends ~ 19 Å into the protein core and is thus larger than the cavity of PhzA. It has a volume of 697 $Å^3$ as compared to 498 $Å^3$ of PhzA (calculated by the program 'Pocket-finder' based on the 'Ligsite' algorithm written by Hendlich et al., 1997, using a probe radius of 1.4 Å).

This difference is largely due to the shifting to the outside of the sheet-loop-sheet motif (discussed in detail in section 3.8.2) and the overlapping C-terminus of the opposite monomer.

Successful soaking trials of native BcepA crystals led to the elucidation of the structure of a complex of BcepA with the compound B75 (2-(2-fluorophenylamino) benzoic acid). Figure 3.20, shows the representation of a homodimer of BcepA complexed with B75.

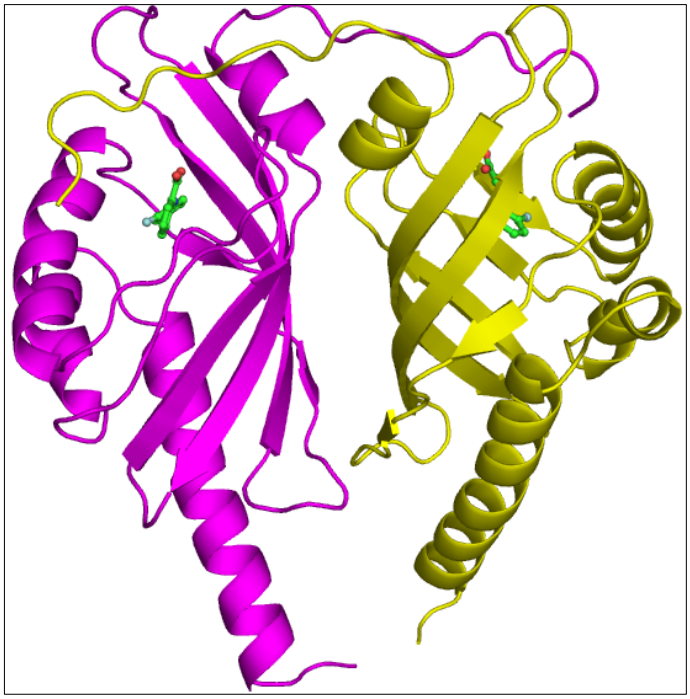

Figure 3.20: Two molecules of B75 bound within the active site cavity of BcepA.

As can be seen from the figure above, binding of B75 does not result in any conformational changes or in an altering of the positions of the residues of BcepA. The structure of complex, however, provides more credence to the hypothesis that the C-terminus region does play an important mechanistic role, by acting as a 'lid' to the ligand-bound state of the protein.

This is particularly clear by the observation that Arg160 of the C-terminus of one monomer forms a hydrogen-bond with the carboxyl moiety of B75 in the second monomer (Figure 3.21; overleaf). This argenine residue and the Gln147, which is located on the helix H4 of BcepA and participates in the binding of B75 do not exist in PhzA. The other two residues, Phe81 which forms stacking interaction with the aromatic ring of B75 and Glu137 which stabilises the fluorine atom through two water molecules, are not only conserved in PhzA, but also participate in the binding of MES. A comparison of ligand-binding within the active sites of these proteins is detailed in section

3.8 and Figure 3-23.

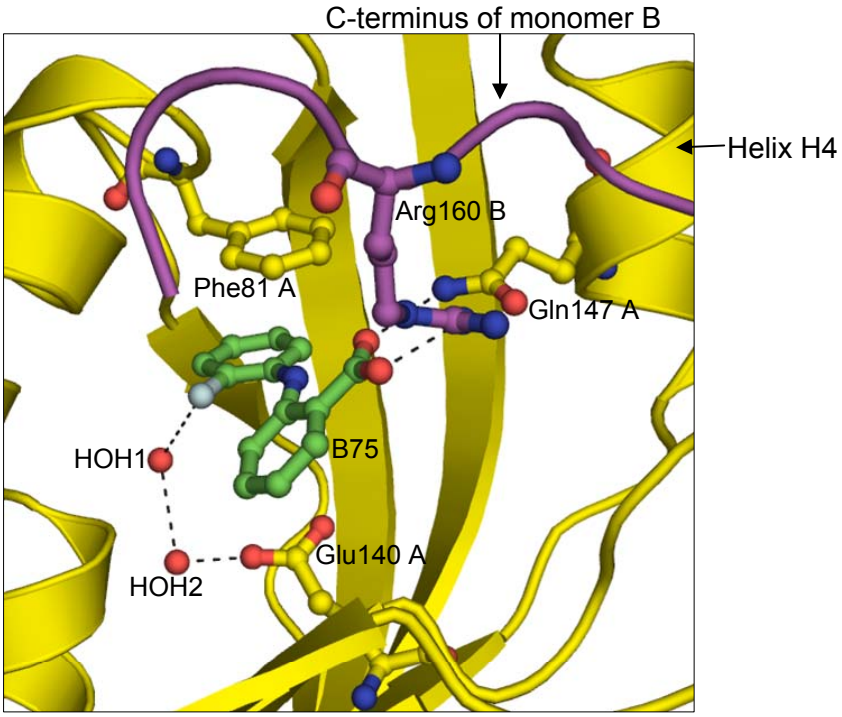

Figure 3.21: The binding of B75 within the active site cavity of BcepA showing the Arg160 from monomer 'B' and other residues interacting with the compound.

This concludes the structural analysis of BcepA. With the structures of PhzA and BcepA elucidated and analysed, a systematic comparison of the structures of these two proteins is described next, to understand the differences between these two homologous proteins and to gain some insight into their potential roles in phenazine biosynthesis.

3.8 Comparison of the structures of PhzA and BcepA.

The monomers of PhzA and BcepA were superimposed using the program COOT and the result is shown in the figure below:

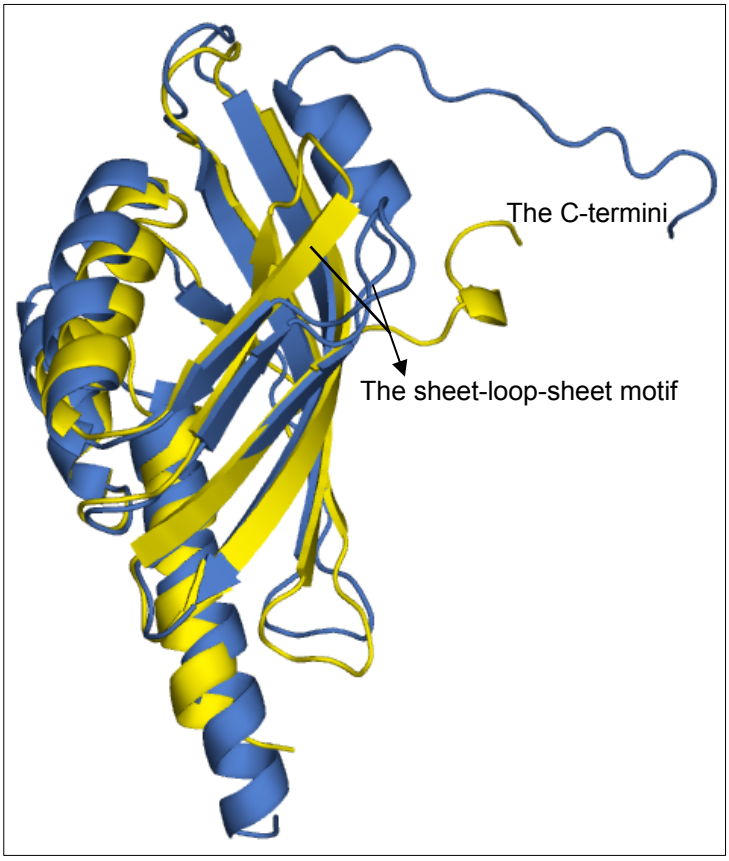

Figure 3.22: Superimposed monomers of PhzA (yellow) and BcepA (blue) with the two major differences labelled.

As mentioned before, PhzA and BcepA have a high degree (69%) of sequence similarity and as previously seen, structural similarity. The two structures superimpose with an rmsd of 1.6 Å and as stated before, all secondary structure elements of PhzA are conserved in BcepA, with differences of lengths. However, there are two very important regions where these structures differ (Figure 3.22; overleaf).

The residues of the C-termini are the first and the most interesting difference between two structures. In case of PhzA, although this region has the tendency of forming a helix (a one-turn α-helix - H4), no estimate of the behaviour of the loop can be made due to the absence of last 17 residues. In BcepA, this region participates not only in the dimerisation, but as discussed in further in this section, also plays an important role in substrate-binding.

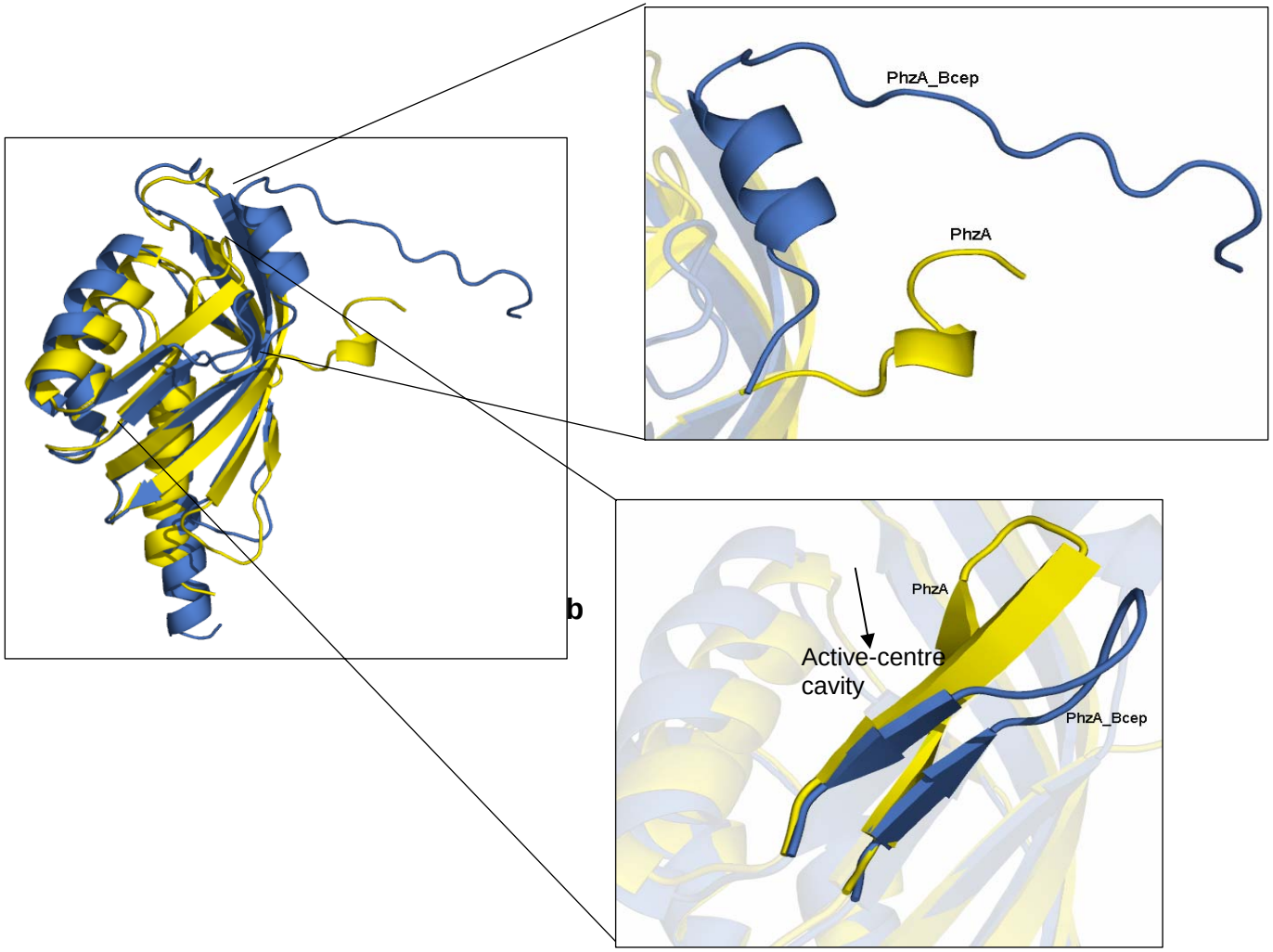

Figure 3.23: The superimposition of the structures of PhzA and PhzA_Bcep, highlighting the main areas of differences between the two structures.

The second difference between the two structures is the sheet-loop-sheet region composed of residues 50-65 (47-62 in PhzA) which appears to be shifted to the outside by approximately 6 Å in BcepA as compared to PhzA. This shifting leads to a more 'open' cavity of BcepA (Figure 3.22) and thus its roomier active centre.

It is tempting to hypothesise that these differences might have also arisen due to the ligand-bound state (closed conformation) of PhzA leading to the inward motion of the sheet-loop-sheet motif, which in an un-bound state (apo conformation) might be similar to that shown by the BcepA structure. Moreover, the interpretable density of the C-terminus residues could also be considered an indication of this region getting disordered on the entry and binding of the ligand into the active-site cavity of PhzA. Alternatively, this could also hint at different routes of entry and exit of ligands, where the ligand enters the protein from the top of the cavity in case of PhzA but from the more 'open' side in case of BcepA. However, these questions will only be resolved on the elucidation of the structure of PhzA in a form where the last 17 residues are clearly visible.

The second difference between these structures is the outward shifting of the sheet-loop-sheet motif which leads to a bigger cavity of BcepA, as compared to PhzA, despite the same sizes of both proteins. *B. cepacia* is known to synthesises compounds like PDC, PDC-dimethyl ester etc (Introduction, Figure 1.4) which are indeed larger than PCA. Hence, it is plausible to hypothesise that this difference in the volume of the active site is to accommodate substrates with larger space requirements as those of PhzA. Figure 3.24 shows the residues involved in the binding of MES in PhzA overlaid with those involved in the binding of B75 in BcepA. As mentioned earlier, the argenine (Arg160), a part of the C-terminus of second monomer of homodimeric BcepA forms hydrogen bonds with the carboxyl moiety of B75. Moreover, the residue Gln137 of the helix H4 also interacts with B75. These observations hence point towards the importance of the C-terminus to the catalytic functions of BcepA. Moreover, the highly ordered C-terminus and its participation in substrate-binding lends further weight to previously stated argument, that perhaps ligand-entry occurs from the side in BcepA, as opposed to from the top in PhzA.

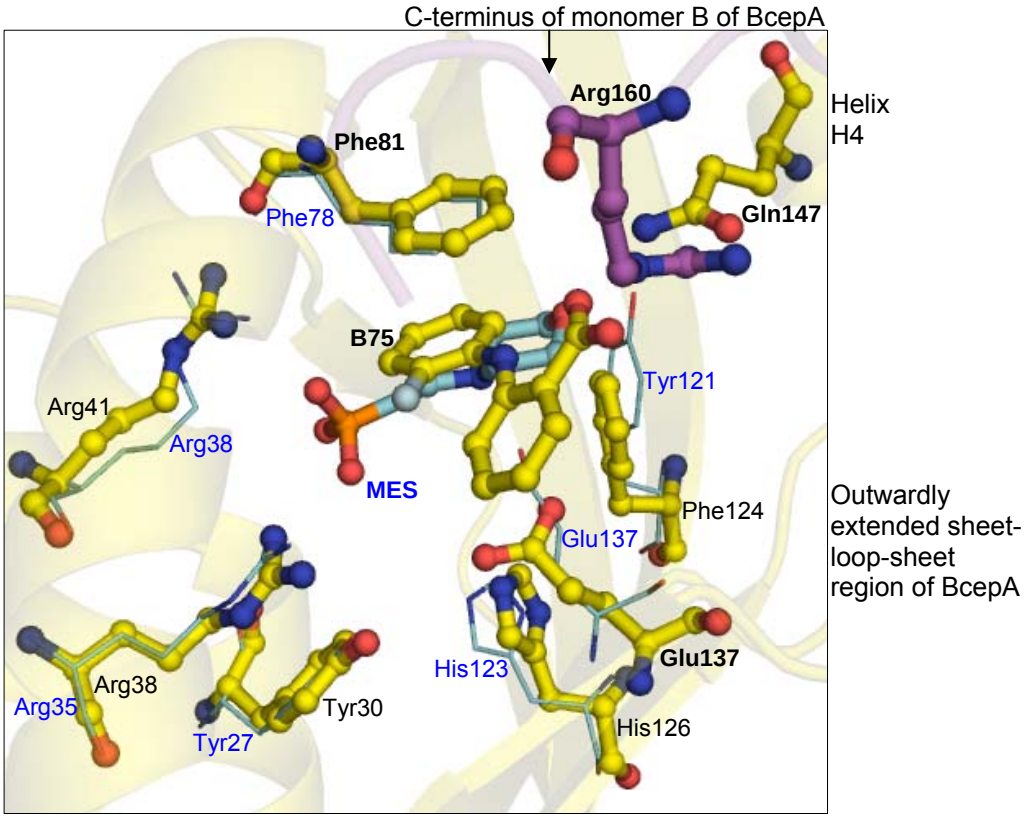

Figure 3.24: Comparison of residues involved in binding of MES (blue) and B75 (yellow) in PhzA and BcepA respectively.

As can been seen from the figure above, all residues involved in the binding of MES in PhzA are conserved in BcepA (except Tyr121, (Phe124 in BcepA)) and two of these, Phe81 and Glu137 are involved in stacking and hydrogen bond formation respectively, with B75. Another interesting observation in this figure is the location of positively charged Arg38 of BcepA, which can be envisioned to interact with the carboxyl moiety of a molecule of/similar to PDC, which, when present would lie in approximately the same position as the sulphate moiety of MES (Figure 3.24).

This comparison of the structures of PhzA and BcepA thus highlights the adaptation of proteins of similar fold and sizes to the metabolic requirements of their respective organisms. To further understand these differences, a comparison of the structures of PhzA and BcepA with homologous proteins was carried out, the results of which are described in the next section.

3.9 PhzA, BcepA and homologous structures

The structural homologues of PhzA and BcepA belong to the α+β barrel fold superfamily (CATH 2.20.25.70; Orengo et al., 1997) the members of which, though displaying a similar fold, are highly diverse in sequence and vary in functionality from enzymes to transport proteins. Like PhzA & BcepA, many proteins displaying similar α+β roll architecture are dimeric, with the β-sheet forming the dimer interface.

The two most closely related structures to both PhzA & BcepA are those of Δ^5-3-ketosteroid isomerase (KSI) from *Pseudomonas putida* (PDB id-1OHO) and limonene-1,2-epoxide hydrolase (PDB id-1NU3) from *Rhodococcus erythropolis*. Structures with rmsd value <3 Å on superimposition to PhzA and BcepA are tabulated below:

Homologous structures (PDB name)	Rmsd on super-imposition (Å)		Name	Ascribed function
	PhzA	BcepA		
1OHO	2.4	2.3	Δ^5-3-ketosteroid isomerase	Binds Δ^5-3-ketosteroids, cleaves C–H bond adjacent to carbonyl, enol formation
1NU3	2.2	2.1	limonene-1,2-epoxide hydrolase	Binds limonene-1,2-epoxide, cleaves C–O epoxide bond
1OUN	2.6	2.7	nuclear transport protein (NTF-2)	Binds RanGDP and FxFG nucleoporins transport
1S5A	2.4	2.3	Hypothetical protein apc1116	unknown
1TUH	2.6	2.2	Hypothetical protein Bal32a	unknown

Table 3.6: Structures similar to PhzA and BcepA, with rmsd value <3Å.

A superimposition of these structures (Panel 3.24, overleaf) highlights the strong conservation across the family of the β-strand elements with most variations at the top of the 'cone'.

All the structures contain a solvent accessible ligand-binding cavity lined with hydrophobic residues at the broad-end of the cone. The catalytic residues (when present) reside in a pocket that does not span the entire depth of the cavity, but is truncated by the presence of a bulky/aromatic residue (except 1S5A). In Δ^5-3-ketosteroid isomerase (1OHO), PhzA and BcepA, this is a

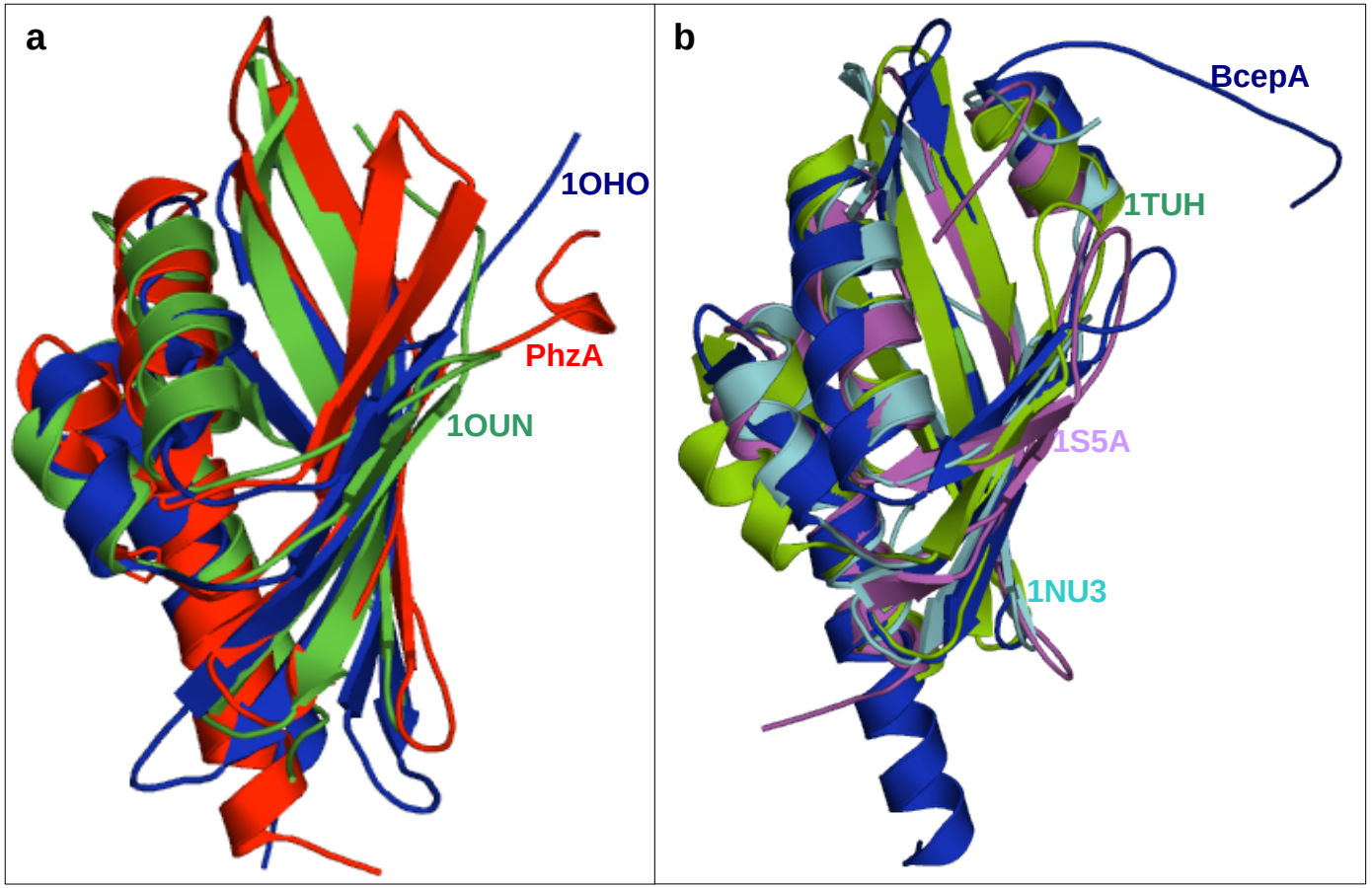

Panel 3.25: Comparison of structures similar to PhzA ‘a’ and BcepA ‘b’

tyrosine residue.

As discussed in the previous section, there are two significant differences between PhzA and BcepA, namely the C-terminal residues and the sheet-loop-sheet motif, these are also observed in the homologous structures.

3.9.1 The C-terminal region

The length of the C-terminal region is indeed a varying factor in all members of this α+β roll family. However, a distinct trend can be observed, which divides the structures into two discreet groups. The first comprises of PhzA, 1OHO and 1OUN (Figure 3.25 & 3.26 'a'), where the C-terminal is rather short and disordered. However, this statement only holds true due to the absence of electron-density for the last 17 residues of PhzA, whose behaviour cannot be predicted with confidence. Both 1OHO and 1OUN are short proteins of 126 and 127 amino acids respectively.

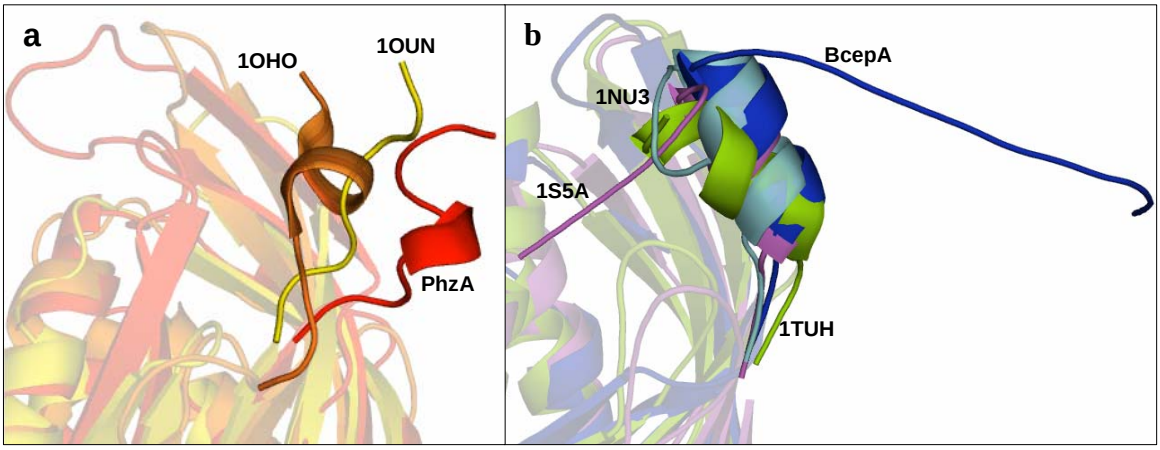

Figure 3.26: The differences between the C-termini of the two groups of homologous structures.

In the second group, comprising BcepA, 1NU3, 1S5A and 1TUH, (Figure 3.24 & 3.25 'b') this region is longer and highly ordered with a 2-turn α-helix and forms a 'lid'-like structure, either on the same monomer (1S5A, 1NU3 and 1TUH), or the second monomer of the homodimer (BcepA).

BcepA, like PhzA, is a new addition to the α+β barrel family, and the only member which displays this 'arm-exchange' mode of dimerisation.

3.9.2 The 'sheet-loop-sheet' motif

The figure 3.25 shows this motif for all the superimposed structures. The most significant observation is the highly ordered β-sheet region in PhzA, which is a disordered loop region in all the other structures. Moreover, this motif is most in-facing for PhzA (coloured red in Figure 3.27), while that of BcepA (blue) is indeed the most 'relaxed'. It is difficult to arrive to any significant conclusion from the fold of this motif, since all the structures except 1OHO are in ligand-free state; and this motif is as flexible for 1OHO as for the other structures.

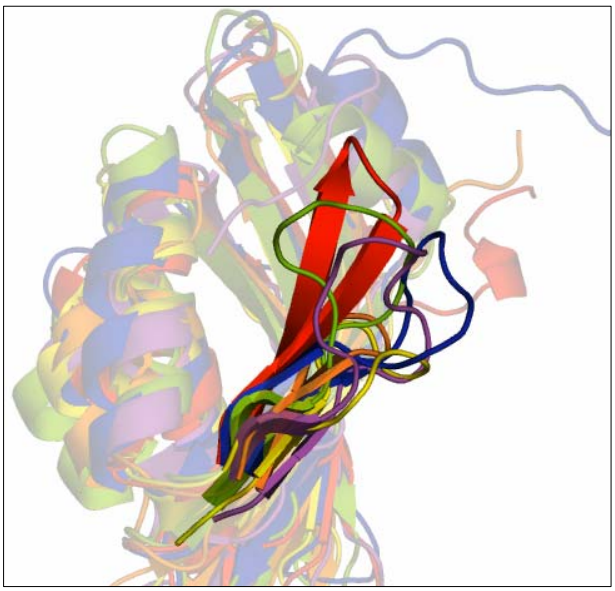

Figure 3.27: A close-up of the sheet-loop-sheet regions of the superimposed structures. (The colour scheme is identical to the previous figures.)

The aim of structural comparison is to understand the structural similarities/differences between homologous structures and the implications these have on the function of the protein/s being investigated. Only two of the structures homologous to PhzA/BcepA (superimposable with rmsd <3 Å) have been functionally characterised.

First of these is a ketosteroid isomerase (KSI; PDB id 1OHO), which catalyses the isomerization of a wide variety of 3-oxo-Δ^5-steroids to their Δ^4-conjugated isomers. 1NU3 is the PDB id of a limonene epoxide (LEH) which catalyses the hydrolysis of epoxides to corresponding diols. The following paragraph analyses the reactions catalysed by these enzymes, their catalytically important residues and the comparison of these to derive the potential function of PhzA/BcepA in phenazine biosynthesis.

3.9.3 Function of homologous structures & implications for PhzA/BcepA.

The reactions mechanisms of both enzymes KSI and LEH alongwith catalytically important residues are depicted in Figure 3.28.

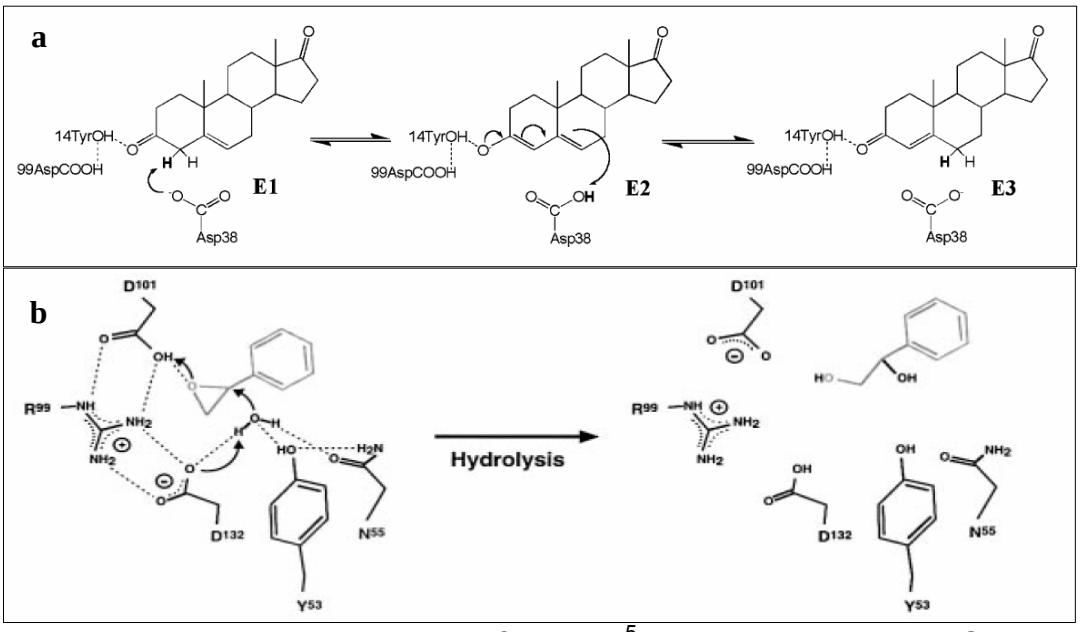

Figure 3.28: (a) The isomerization of 3-oxo-Δ^5-steroid catalysed by KSI (From Pollock et al., 2004). (b) Hydrolysis of epoxide to diol catalysed by LEH (From Arand et al., 2003).

The table below summarises the catalytically active residues of these two enzymes and the residues in equivalent positions in PhzA and BcepA.

Equivalent residues in	**Key active site residues of KSI (1OHO)**				
	Tyr14	**Tyr30**	**Tyr55**	**Asp38**	**Asp99**
PhzA	Tyr27	Phe42	Gly71	Ser50	His123
BcepA	Tyr30	Phe45	Ala74	Leu53	His126

	Key active site residues in LEH (1NU3)				
	Tyr53	**Asn55**	**Arg99**	**Asp101**	**Asp132**
PhzA	Gly48	Ser50	Ser101	Gly103	Glu137
BcepA	Gly51	Leu53	Cys104	Arg105 (faces outward)	Glu140

Table 3.7: Comparison of catalytically important residues.

Tyrosine residue (Tyr14) is the only one of the five catalytically important residues of 1OHO conserved in PhzA and BcepA. Moreover, this table also highlights the fact that the Asp99 of 1OHO is substituted by a histidine residue

(His123 and 126 for PhzA and BcepA respectively) and the Tyr30 by a phenylalanine residue (Phe42 and 45), in both PhzA and BcepA. The Histidine and the conserved Tyrosine residues do play a role in the binding of the MES molecule in the cavity of PhzA (section 3,8; Figure3.23).

In case of the key active site residues of 1NU3, none of the residues are conserved. Also, the charges in case of Asp132 are similar; but reversed for Arg99. A potential catalytic site thus can been identified within the α+β roll scaffold which is in an equivalent position to the active sites of LEH and KSI and coincides with the MES-binding site in case of PhzA and B75 in case of BcepA. However, the only thing that can be said about PhzA and BcepA at this time is that both these proteins show yet another arrangement of putative catalytic residues within the preserved cone-like cavity characteristic of the α+β roll family of proteins.

As a summary of this section of structural analysis of PhzA and BcepA, it can be said that the α+β roll artitecture provides a robust scaffold whose function can be tuned by altering the properties of the residues lining the interior cavity. This correlates with the observed functional diversity, but, in turn, makes it difficult to predict the precise function of either PhzA or BcepA from their structure only. Moreover, the observations from superimposition of homologous structures further re-iterate the conclusions drawn from the evolutionary analysis of PhzA-like proteins (section 3.1.2) that these enzymes share a common evolutionary ancestry, not only with proteins of similar sequences, but also with proteins belonging to the α+β roll superfamily, in which the position of the active site remains preserved whereas specific catalytic groups alter to meet particular demands.

This comparison of the structure of PhzA and BcepA wraps up the discussion about these proteins and the following sections describe and discuss the structure of PhzG and its complex with PCA.

3.10 PhzG & complex of PhzG with PCA.

PhzG is a 48 KDa functional homodimer where the two monomers interact extensively along three regions on one-half of each monomer. There are two clefts at opposite ends of the dimer which extend from top to bottom of the dimer. These clefts contain the flavin mono nucleotide (FMN) binding sites (Figure 3.29). PhzG displays an α+β fold, typical of the pyridoxyamine-5'-phosphate (PNPOx) family of enzymes. The structure of PhzG shows highest similarity to PNPOx from *E.coli* (PDB id 1G79), with identical overall fold and secondary structure elements.

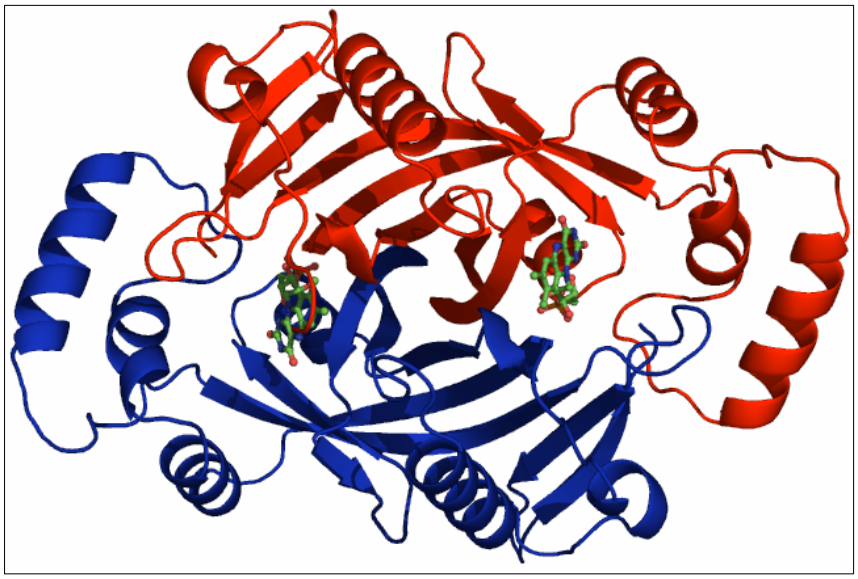

Figure 3.29: Biological subunit (homo-dimer) of PhzG

3.10.1 Monomeric structure description

The structure of each of the monomers of PhzG comprises of six α-helices and eight β-strands and can be divided into two domains (Figure 3.30, overleaf). The larger domain (domain 1) is composed of the β-sheets (S1-S8) and three of the helices (H1-3). These include the residues 57-64 (S1), 67-79 (S2), 84-89 (S3), 103-110 (S4), 114-125 (S5), 181-195 (S6), 203-209 (S7), 214-219 (S8), 27-31 (H1), 36-50 (H2) and 93-100 (H3). The strands S1-S6 are highly curved and are extended by S7&8 into an eight stranded anti-parallel β-sheet.

The smaller of the two domains (domain 2) is made up of the three α-helices H4 (128-137), H5 (140-148) and H6 (158-171). One-turn helix H1 and helix H2 alongwith N-terminal residues 1-26 (of which only the residues 18-26 are

visible in the structure) flank this β-sheet structure from one side. With the helices H3-H6 (domain 2), which are located between β-strands S3 and S4. Thus, this whole protein subunit comprises of compact eight stranded β-sheet core surrounded by six α-helical structures. Figure 3.28 depicts a schematic representation of a monomer of PhzG. There are three salt bridges which connect the secondary structure elements of the two monomers. These include Glu78-Lys130 connecting β-strand S2 with helix H3, Glu192-Arg204 and Asp208-Arg217 between β-strands S6-S7 and S7-S8 respectively. Of these three bonds, only the salt bridge between β-strand S6-S7 is conserved between PhzG and *E.coli* PNPOx.

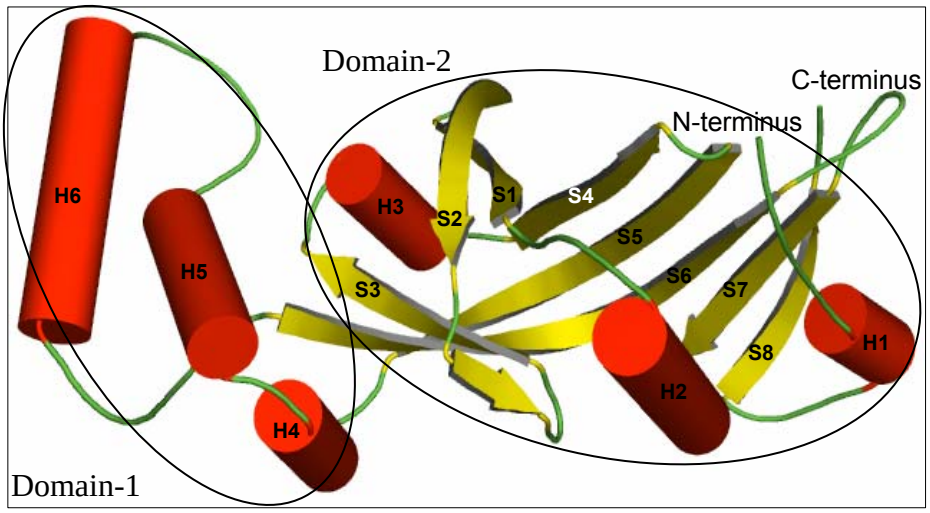

Figure 3.30: Schematic representation of a monomer of PhzG with the two domains.

There are two main hydrophobic patches in the core of the structure. The first and the larger of the two hydrophobic patches is found between the β-sheet and the α-helices H1-3. There are 53 hydrophobic residues with 15 aromatic residues. The outer rim of strands S3 and S6, the helices H4 to H6 and the isoalloxine ring of FMN contain the second hydrophobic patch, composed of 29 hydrophobic residues and forming the active site cavity between the two monomers.

3.10.2 The functional dimer of PhzG

As mentioned earlier, the monomers of PhzG interact extensively along one half of each monomer. The total buried surface area between the dimers is

approximately 2850 Å, which points towards very tightly interacting monomers. Participating in this interaction are the 31 hydrogen bonds and salt bridges and 60 van der Waals contacts (residues at <4 Å distance from each other). Water molecules and FMN also contribute to numerous hydrogen bonds linking the two monomers. These interactions can be divided into three main regions which have been annotated here as the α-helical interface-1, the β-sheet interface and the α-helical interface-2 (Figure 3.31).

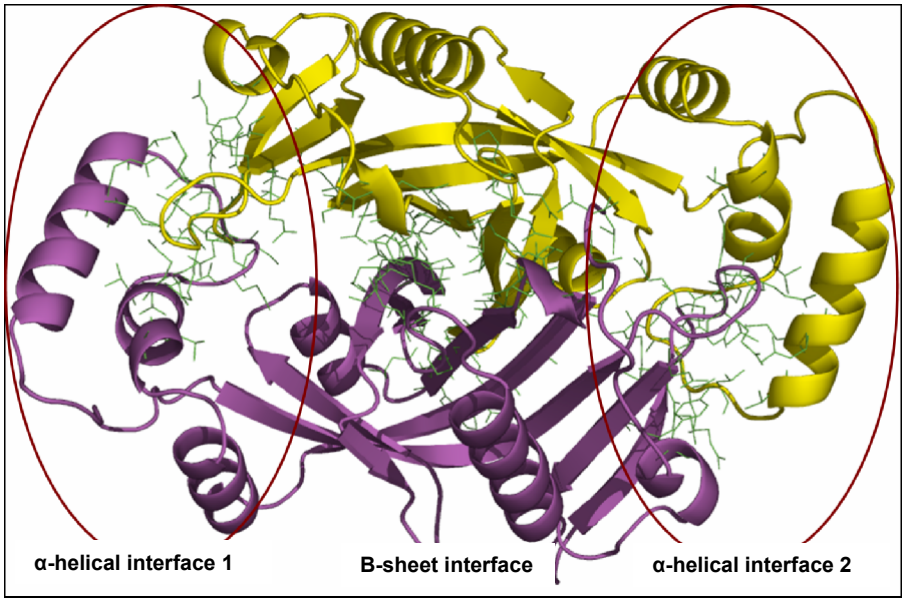

Figure 3.31: The figure shows the dimer of PhzG (cartoon) with the residues participating in dimer-interactions depicted in green.

The α-helical interface-1 and 2 are identical and lie at the two ends of the dimer. They comprise of contacts between the domain-1 of one monomer and the domain-2 of the second monomer. This interface is made-up of both hydrophilic and hydrophobic contacts, with most of the contacts in the loop regions between the helices H4 and H5. These interactions thus also stabilise the loops regions and help maintain the integrity of the edges of the dimer. This is of some consequence not only structurally but also for function, as this region binds the co-factor FMN and contains the active centre of PhzG.

The β-sheet interface coincides with the central dimer interface and includes β-sheets S1, and N-terminal residues of S2 and S4, which extend from top to bottom in the structure and form a narrow channel in the middle of the dimer. This channel is elliptical in shape, with a diameter between 6-9 Å and length of approximately 40 Å. The top and bottom parts of the channel are

predominantly hydrophilic and interact with several water molecules, while the deeper, slightly narrower bottom-end is mainly hydrophobic and inaccessible to solvent. The residues in this part of the channel mainly have small side chains and are either similar or conserved among the PNPOx family of enzymes.

The most important hydrogen bonds between the residues of the two monomers have been tabulated below:

α-helical interface-1				
Residue of chain A	**Atom**	**Residue of chain B**	**Atom**	**Distance**
Arg204	NH1	Ser152	OG	3.1
Leu155	N	Arg218	O	2.8
Gln220	O	Ser152	N	3.0
	NE2	Glu154	O	2.9
	N	Glu153	O	2.8
β-sheet interface				
Thr71	N	Ser105	OG	3.1
	OG	Ser105	OG	2.8
Gly67	O	Asn101	OD2	2.9
Tyr109	OH	Glu54	OE1	2.5
Arg111	NH2	Glu54	O	2.9
	NE1	Arg53	O	2.8
Gln198	O	Arg162	N	3.1
Gln152	NE2	Pro122	O	3.1
Arg218	O	Leu155	N	2.8
Glu199	OE1	Pro221	NE1	3.2
Glu54	OE2	Thr19	N	2.9
	OE2	Thr19	OG1	2.6
Ser105	OG	Thr71	OG1	2.7
Arg158	N	Gln220	OE1	2.8
Glu154	O	Gln220	NE2	2.9
Arg53	O	Arg111	NE	2.8
	NE2	Thr19	OG1	2.8
Glu153	O	Gln220	N	2.8
Arg166	NE	Glu199	OE1	2.9
α-helical interface-2				
Arg162	NH1	Gln198	O	3.0
Pro221	O	Gln151	NE2	3.0
Ser152	OG	Arg204	NH1	3.0
	N	Gln220	O	2.9
ILE73	N	Glu116	OE1	2.9
Asn101	ND2	Gly67	O	2.9
Glu116	OE1	Ile73	N	3.0

Table 3.8: Hydrogen bonds between the residues of the monomers of PhzG.

3.10.3 Active site cavity and the binding of FMN.

As mentioned earlier, the dimer of PhzG creates two clefts which contain the active site cavity and FMN binding site. These two clefts are separated by a distance of approximately 20 Å and are formed by the N-terminal residues of β-sheets S4-S8 of one monomer and the α-helices H3-6 and β-sheets S2 and S3 of the second monomer. These clefts are funnel shaped, binding the isoalloxazine ring of FMN at the wider end and the phosphate containing ribityl hydroxyl moiety at the narrower end (Figure 3.32).

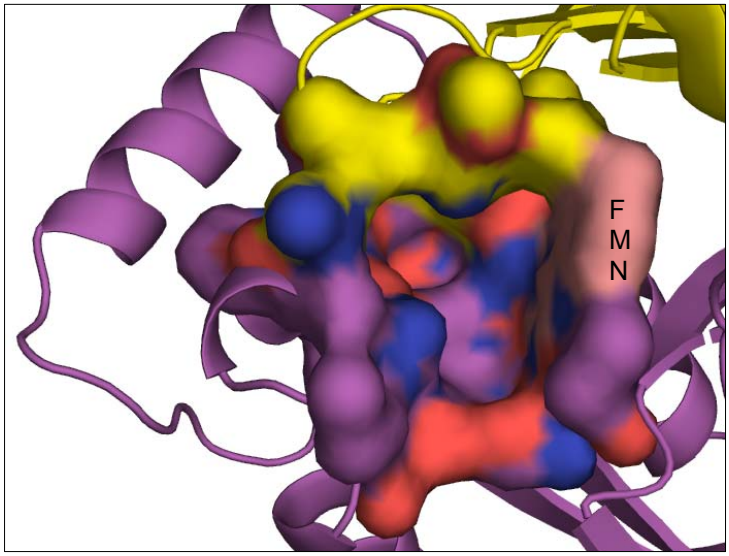

Figure 3.32: The active site cavity of PhzG with the contributions of each monomer shown in different colours (yellow and purple).

The FMN molecules are involved in extensive interactions with the residues of the dimer; the most important of these are shown in the Figure 3.33. Of the residues making hydrophobic contact with FMN namely, Tyr109A, Trp194A, Gln151B, and Val74 only two (Trp194 and Val72) are conserved in *E.coli* PNPOx. In each of the active centre and FMN binding site, more residues (10) of the α-helical domain (domain-2) interact with FMN than the residues of the β-sheet domain-1 (4 residues).

Of these interactions, residues Glu116, Ile73, Val75 and a molecule of water interact with the isoalloxazine ring of FMN. All the other residues, including two water molecules interact with the highly charged ribityl hydroxyl moiety of FMN (Figure 3.33). The residues Tyr109, Trp194, Gln151 and Val74 make hydrophobic contacts with FMN. PhzG shares 60% identity to the five main motifs of residues which are essential for the binding of FMN and are

conserved the various PNPOx. These conserved motifs and their counterpart in PhzG are tabulated in Table 3.9.

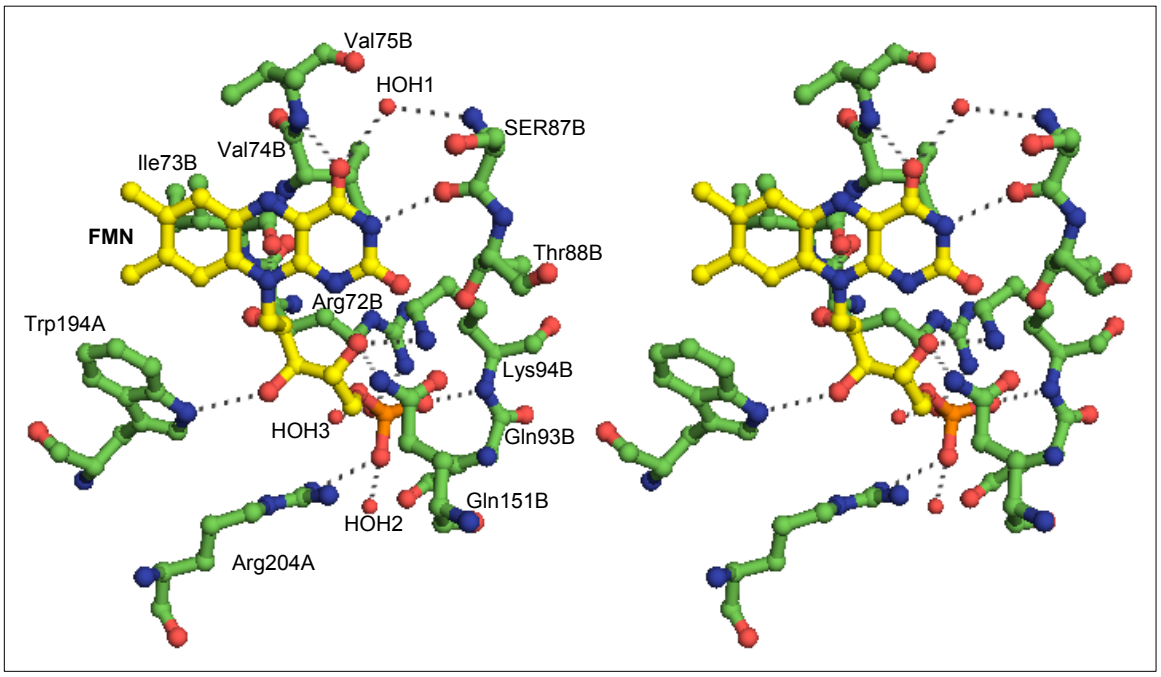

Figure 3.33: Stereo view of the co-ordination of FMN in PhzG. The residues forming hydrogen bonds with FMN are labelled with the name of the monomer they belong to (A/B).

Residues	Motif in E.coli PNPOx	Motif in PhzG
67-72	RIVLLK	RIVVIS
80-84	VFYTN	VFSTH
87-90	SRKA	SQKG
189-193	EFWQG	EFWGN
197-201	RLHDR	RLHER

Table 3.9: The conserved FMN binding motifs in PNPOx and their counterparts in PhzG.

Another notable observation in the native structure of PhzG was the presence of extra density besides the density for the FMN molecule. This extra density is shown in the figure 3.34, overleaf.

The crystallisation conditions of PhzG contained a high excess of FMN (10 mM), and this extra density corresponded to a second FMN molecule. Hence,

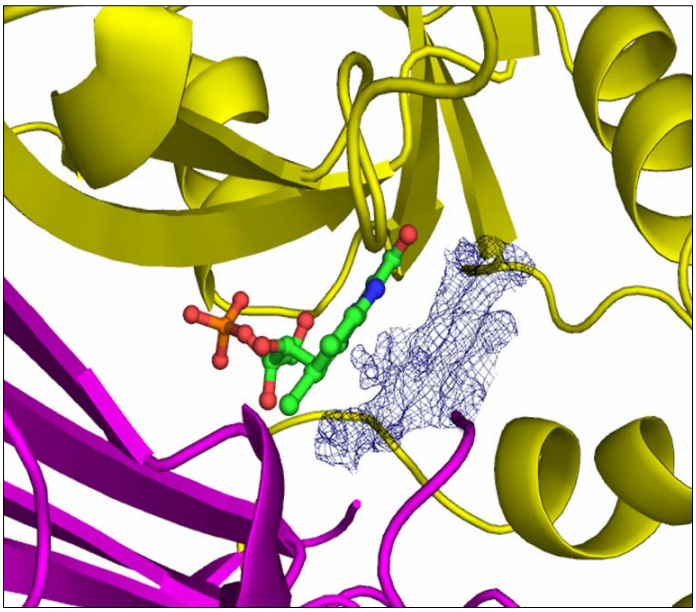

Figure 3.34: Fo-Fc map (3σ) of extra density observed in the native structure of PhzG.

a molecule of FMN was modelled into this density. This molecule however, did not completely fit the density. The density accommodated the flavin ring of FMN, however, the density for the ribityl hydroxyl moiety was unclear (Figure 3.35). This was an encouraging sign, owing to the fact that the structure of PCA and the isoalloxazine ring of FMN are 'isosters' i.e. have similar space requirements. This was thus an indication that the cavity of PhzG was capable of accommodating a structure similar to the isoalloxazine ring of FMN and

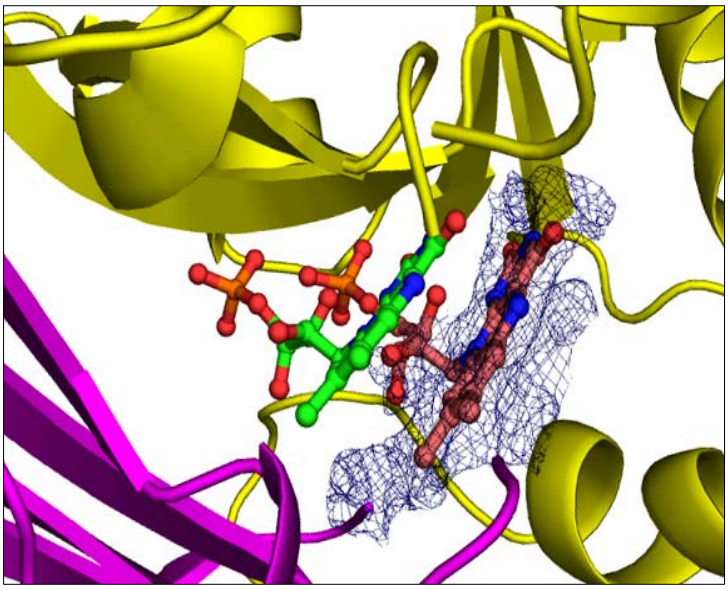

Figure 3.35: A molecule of FMN modelled into the extra density observed in native PhzG.

hence PCA. This observation led to the trials of crystallisation of PhzG with lesser FMN and of forming a complex of PhzG in the presence of PCA.

3.10.4 PhzG in complex with PCA

The soaking of native crystals of PhzG in PCA was indeed successful, leading to the elucidation of the structure of PhzG complexed with PCA.

The active site cavity of PhzG, as mentioned earlier, is formed by the helices H4-6 of one monomer; β-strands S1-4 of the second monomer and the FMN molecule and is composed mainly of hydrophobic, aromatic residues. The binding of PCA does not show any major structural changes of these residues as compared to those of the native PhzG. The most important changes are observed in the conformations of amino acids Arg138, His89 and Val75 in the active centre (Figure 3.36).

This figure also shows a molecule of PCA bound within the active site. The carboxyl moiety of PCA is facing the same direction as the negatively charged ribityl hydroxyl moiety of FMN. The main interactions between FMN and PCA include stacking interactions between the aromatic rings, hydrogen bonds between N5 of FMN and the carboxyl carbon C1 of PCA and oxygen O4 (FMN) with the nitrogen N2 of PCA.

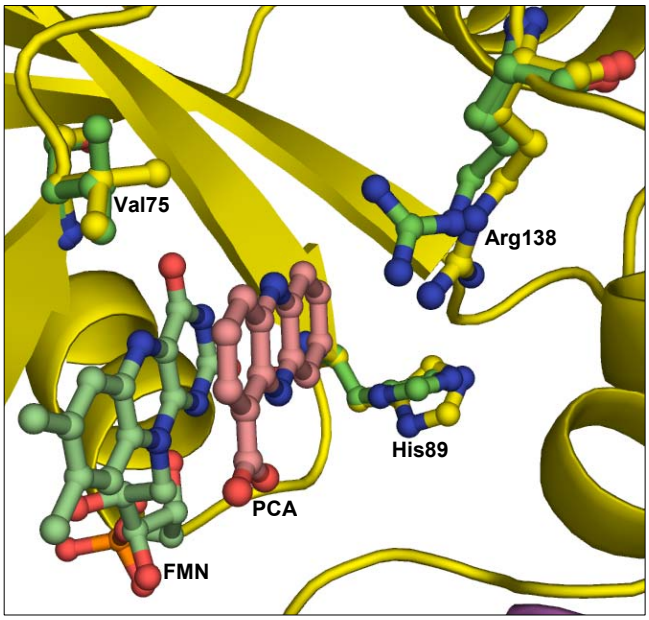

Figure 3.36: Alternative conformations of the amino acids in the active centre, on binding of PCA. (Original conformations are shown in yellow and those on binding of PCA are shown in green.)

Moreover, the residues His202, Leu18 and Arg138 are involved in hydrophobic interactions with PCA. These interactions are depicted in the Figure 3.37 below:

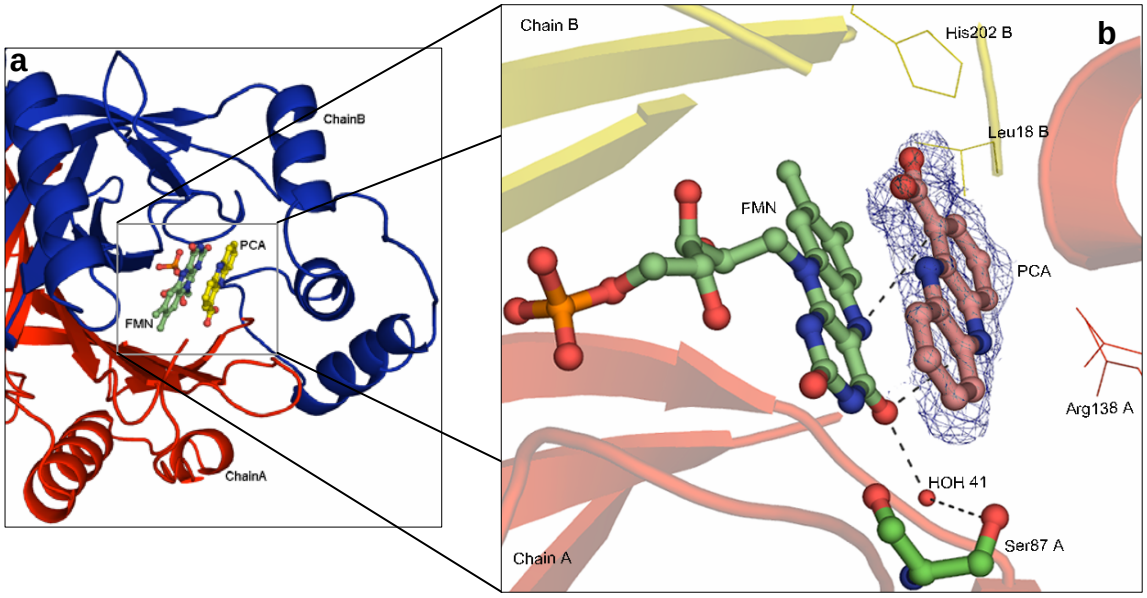

Figure 3.37: (a) PCA bound in the dimer of PhzG. **(b)** Interactions of PCA with FMN (PCA shown here with the 3σ Fo-Fc map of its density).

Though the exact mechanism of catalysis in PNPOx has not yet been confirmed, multiple structural and mechanistic studies indicated towards the catalysis occurring in this class of enzymes by the transfer of a hydride ion from the substrate (PLP, in case of *E.coli* PNPOx) to the nitrogen N5 of the flavin ring of FMN (Safo et al., 2000) (Figure 3.38).

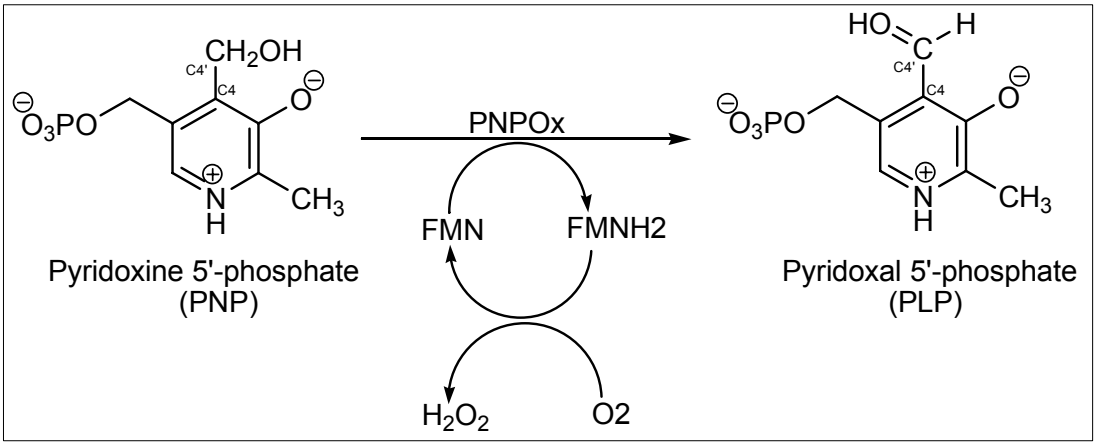

Figure 3.38: The reaction catalysed by *E.coli* PNPOx showing also the regeneration of the reduced FMN .

From the binding of PCA observed in PhzG-PCA complex and described above, it is plausible to hypothesise that this mechanism holds true in case of

PhzG as well. Interaction between FMN and the precursor of PCA (unstable, partially aromatised PCA; details in section 5.3) between N5 of FMN and the carboxyl group bearing carbon (in this case, C1) seems plausible. This scenario is also compatible with the proposed activity of PhzG as observed in mass spectroscopic studies described later in this work.

3.10.5 Comparison of PhzG and *E.coli*-PNPOx

As mentioned earlier, the structure of PhzG shows closest homology to the structure of pyridoxyamine 5'phosphate-oxidase (PNPOx) from *E.coli* with which it shares 31% sequence identity. The Figure 3.39 shows the superimposition of these two structures, the backbones of which superimpose with an r.m.s.d of 1.7 Å.

As is clear from this figure, the FMN molecules bind in the same niches for both structures and as previously mentioned with similar residues involved in the co-ordination of FMN. Two conformations of *E.coli*-PNPOx have been

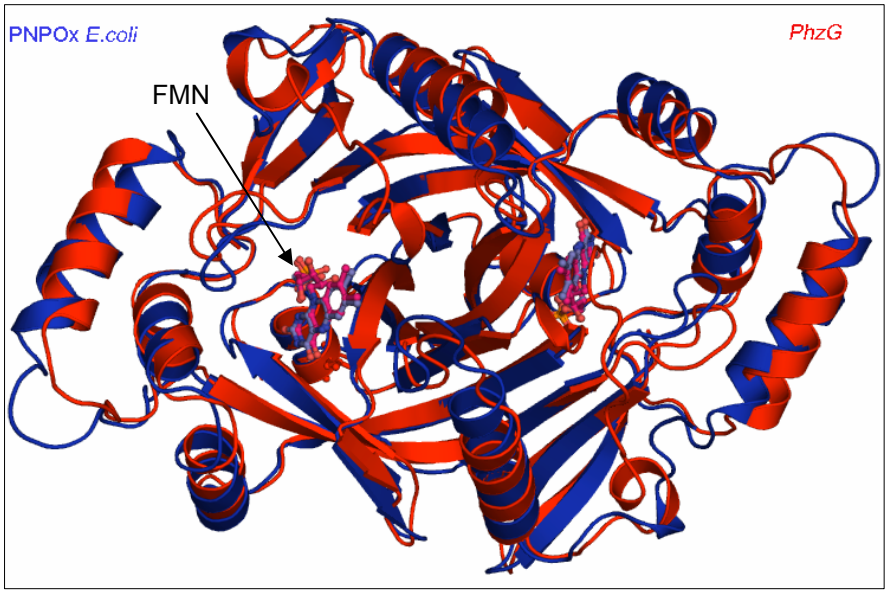

Figure 3.39: Superimposed structures of PhzG (red) and *E.coli* PNPOx (blue).

reported in literature – the 'closed' confirmation, where the N-terminal residues form a flap covering the isoalloxazine ring of FMN, whereas in the 'open conformation, this region of FMN is exposed to solvent. In case of PhzG, it is difficult to draw a conclusion about the conformation, which, from the structure, points towards being closer to the 'closed' conformation than

open, with the flavin part of FMN only partially exposed to the surrounding solvent. This is primarily due to the fact that the first 17 residues to the N-terminal do not have an interpretable density and could not be fitted into the model.

Both the PhzG-PCA complex and *E.coli*-PNPOx bind substrates at identical locations in the structure (Figure 3.40) such that the substrate stacks against the flavin ring of FMN. However, while the negatively charged phosphate group of PLP (pyridoxal 5'-phosphate) faces opposite to the negatively charged tail of FMN and is thus exposed to the solvent; PCA binds in the opposite confirmation, with the negatively charged carboxylic group pointing towards the interior of the structure.

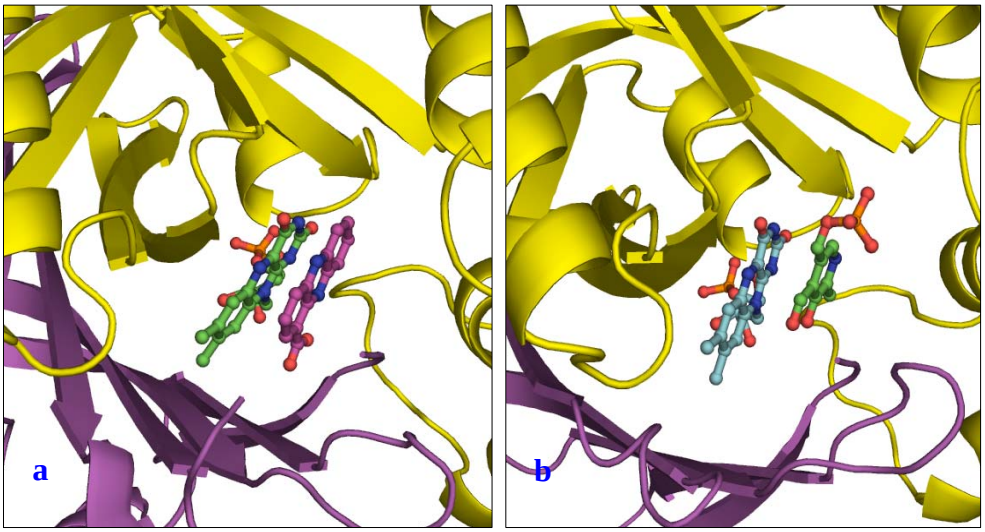

Figure 3.40: (a) Binding of PCA in PhzG. (b) PLP in *E.coli*-PNPOx.

Another distinguishing feature of *E.coli* PNPOx is that in addition to the active site, *E.coli* PNPOx contains a non-catalytic site that binds its ligand (PLP) tightly. Even repeated chromatography on size-exclusion columns does not separate the non-catalytic bound PLP from PNPOx (Yang & Schirch, 2000; Musayev et al., 2003). The Figure 3.41 ('a'; grey arrow) overleaf, shows this non-catalytic site and the putative tunnel through which the ligand is thought to travel to ultimately reach the active site.

The structure of PhzG complexed with PCA was examined for a similar non-catalytic binding site but no electron density for another bound PCA was observed. However, on examining the surface of PhzG, at the equivalent

position, a tunnel-like structure could be seen, where a molecule of PCA has been modelled (Figure 3.41 'c') and can well be envisioned to bind.
The existence of this tunnel in PhzG, which is the feature of most of PNPOx, fits very well with the hypothesised phenazine biosynthesis pathway

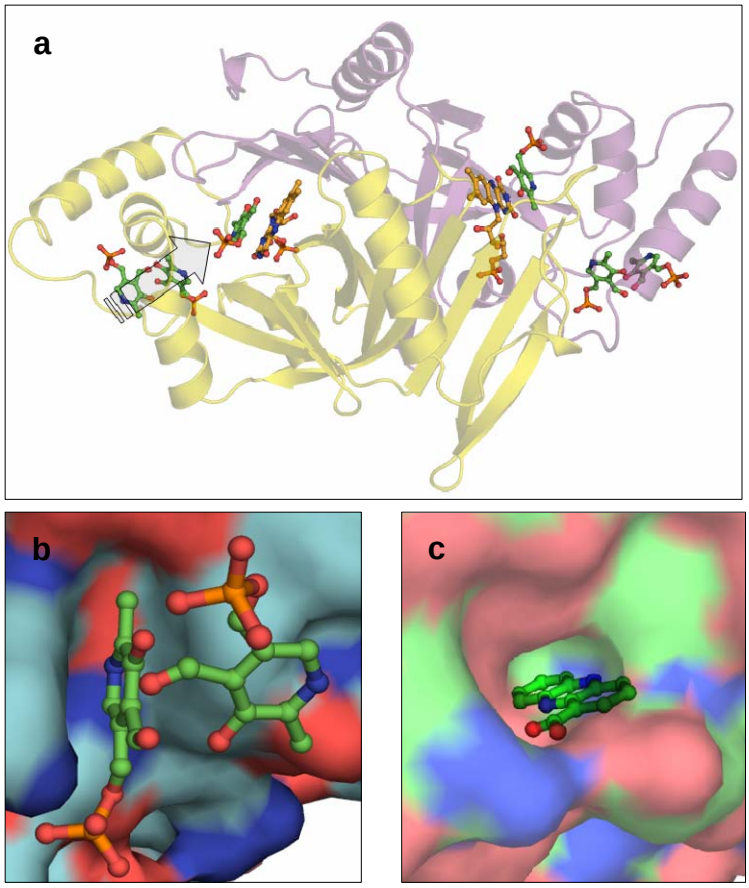

Figure 3.41: (a) *E.coli* PNPOx showing the non-catalytic binding site and the putative tunnel. (b) a close-up of the surface of PNPOx showing two molecules of the ligand PNP. (c) Equivalent position on the surface of PhzG with a molecule of PCA. (all surfaces coloured by electrostatic potential)

(section 5.2), where the unstable intermediate (partially aromatised PCA) and the substrate of PhzG could be shielded until its catalysis to PCA by PhzG. However, this observation is yet to be experimentally confirmed.

The analysis of FMN-dependent oxidase – PhzG, PhzG complexed with PCA, PhzA, its homologous enzyme BcepA and BcepA complexed with the inhibitor B75, from *B.cepacia*, conclude the structural investigations carried out during the course of this work.

The following sections describe the biochemical measurements carried out using the two-hybrid assay, HPLC, mass-spectrometry and oxygen electrode. These measurements were aimed at the elucidation the possibility of interaction between the enzymes of the phenazine biosynthesis pathway in pseudomonads, the exact mechanism of phenazine biosynthesis, identification of the intermediates produced, and the sequence in which the enzymes PhzA, B and G act in this pathway.

Section III

The investigations undertaken to analyse the intermediates formed during the biosynthesis of PCA, the effect of various enzymes and other factors are described in this section.

4.0 Intermediates formed during the biosynthesis of PCA.

The most common methods employed to investigate reactions catalysed by enzymes include enzyme assays and kinetic studies. However, very little starting information was available for the enzymes being studied in this case and this is the first study to undertake detailed analysis of the enzymes PhzA, PhzB and PhzG.

The elucidation of the structure of PhzA provided the first hint of PhzA/B probably acting as isomerases. The third enzyme, PhzG, was thought to be FMN-dependent oxidase, a conclusion reiterated on the solution of its structure, as described in the previous sections. Also, the substrates of these three enzymes, though speculated in previous studies (MacDonald et al., 2000; Blankenfeldt et al., 2004) were not well characterised and in all cases and would be undetectable by conventional kinetic methods. Moreover, none of these three enzymes could act on DHHA, the last stable intermediate of this pathway and substrate of the enzyme PhzF (Blankenfeldt et al., 2004; Parsons et al., 2004) Thus, for any study, PhzF would have to be present to initiate the reaction, the product of which is thought to be the substrate of PhzA, B and G. This would not only make kinetic studies complicated, but also, not provide any idea of the nature of intermediates formed, and hence be unable to identify of the substrates of the enzymes being studied.

Keeping all these considerations in mind, biochemical studies into the effect of these enzymes and intermediates formed during phenazine biosynthesis were initiated using High Pressure Liquid Chromatography (HPLC) based experiments. If the intermediates formed were UV-active, they could be detected by a *UV*-detector coupled to the HPLC.

4.1 HPLC experiments.

For HPLC studies (methodology described in section 9.3.7), all reactions were carried out in the presence of PhzF, with the enzymes PhzA, B and G added in varying combinations. Results from this set of experiments are depicted as graphs in the Figure 3.42, overleaf.

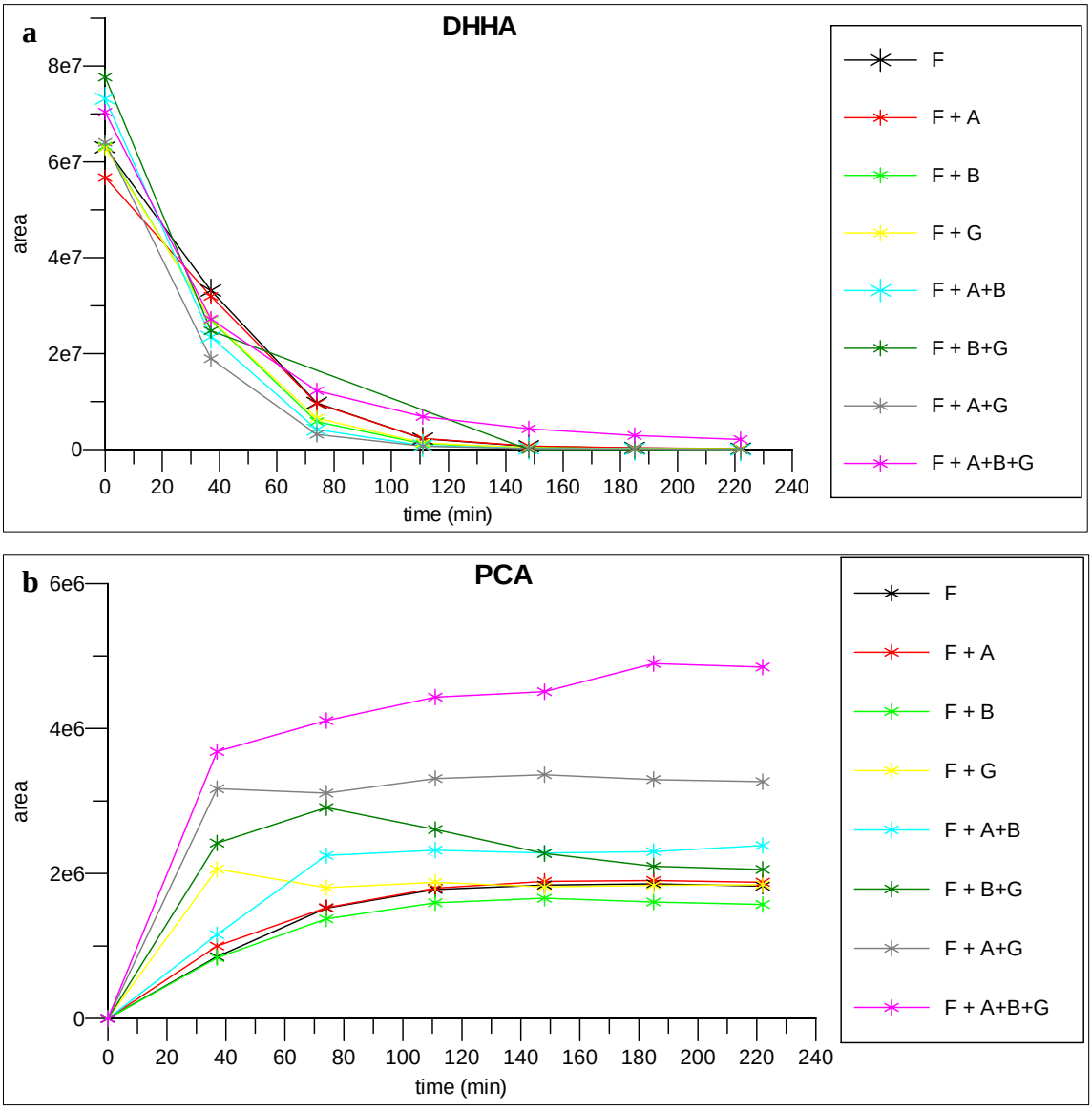

Figure 3.42: Graphs depicting the peak areas at various points during the reaction followed in the presence/absence of various enzymes.

The utilisation of DHHA, as seen in the Graph (a), does not show an appreciable variation with the presence/absence of the enzymes A, B or G. This clearly reiterates that PhzF is the only enzyme capable of using DHHA as substrate. Moreover, all DHHA was depleted within 150 minutes. The only exception was the reaction containing all the enzymes i.e. PhzFABG, where a weak signal indicating the presence of DHHA in the reaction mixture was observed right upto the end of the experiment at 220 minutes.

In contrast, the presence of the enzymes PhzA, B or G, results in an increase in the amount of PCA formed, as compared to reactions containing PhzF alone (Figure 3.42 ‘b’). The combination of PhzFABG forms the highest

amount of PCA, with PhzFAG, the second highest. In the rest of the enzyme combinations, the amount of PCA formed is still almost double that in the presence of PhzF alone; Thus reiterating the observations of both McDonald and co-workers (2000) and Blankenfeldt et al (Blankenfeldt et al, 2004) that these three enzymes work past the formation of 1,2,4-dihydro-3-oxo-anthranilic acid, catalysed by PhzF, using the substrate DHHA.

An inverse correlation between the amounts of PCA formed and utilisation of DHHA can also be seen from these graphs. After approximately 80 mins, the amount of DHHA in the reaction is at its lowest while the amount of PCA formed at its maximum, after which a plateau-like state of PCA formation is observed until the end of measurements at 220 mins.

Although these measurements confirmed the fact that all three enzymes affect PCA formation, the need for a different type of detector was felt, to be able to identify intermediates, which were not detectable in this set of experiments.

4.2 Mass Spectroscopic measurements – ESI-MS

Mass spectroscopy was the next method tried for this investigation. The underlying motivation was the detection of the molecular weight of various intermediates formed, by measuring the mass-to-charge ratio (m/z), provided, the UV-inactive intermediates were MS-active. The structures of the compounds could then be predicted based on the Mw and prior knowledge about the nature of the substrate and final product of this pathway. These experiments were performed using the same reaction set-up as in HPLC experiments.

The results of electrospray ionisation mass spectroscopy (ESI-MS) described here have two main differences to the HPLC measurements. Firstly, no HPLC was used prior to ESI-MS; thus, the reaction mixture introduced into the instrument was not separated. Secondly, of course, was the mode of detection. The Figure 3.43 (overleaf) shows the results obtained at the end of these measurements. All enzymes were used at a molar ratio of 1:1.

The ESI-MS measurements were successful in identifying two new intermediates with a molecular weight of 274 Da (m/z 275) and 228 Da (m/z 229)

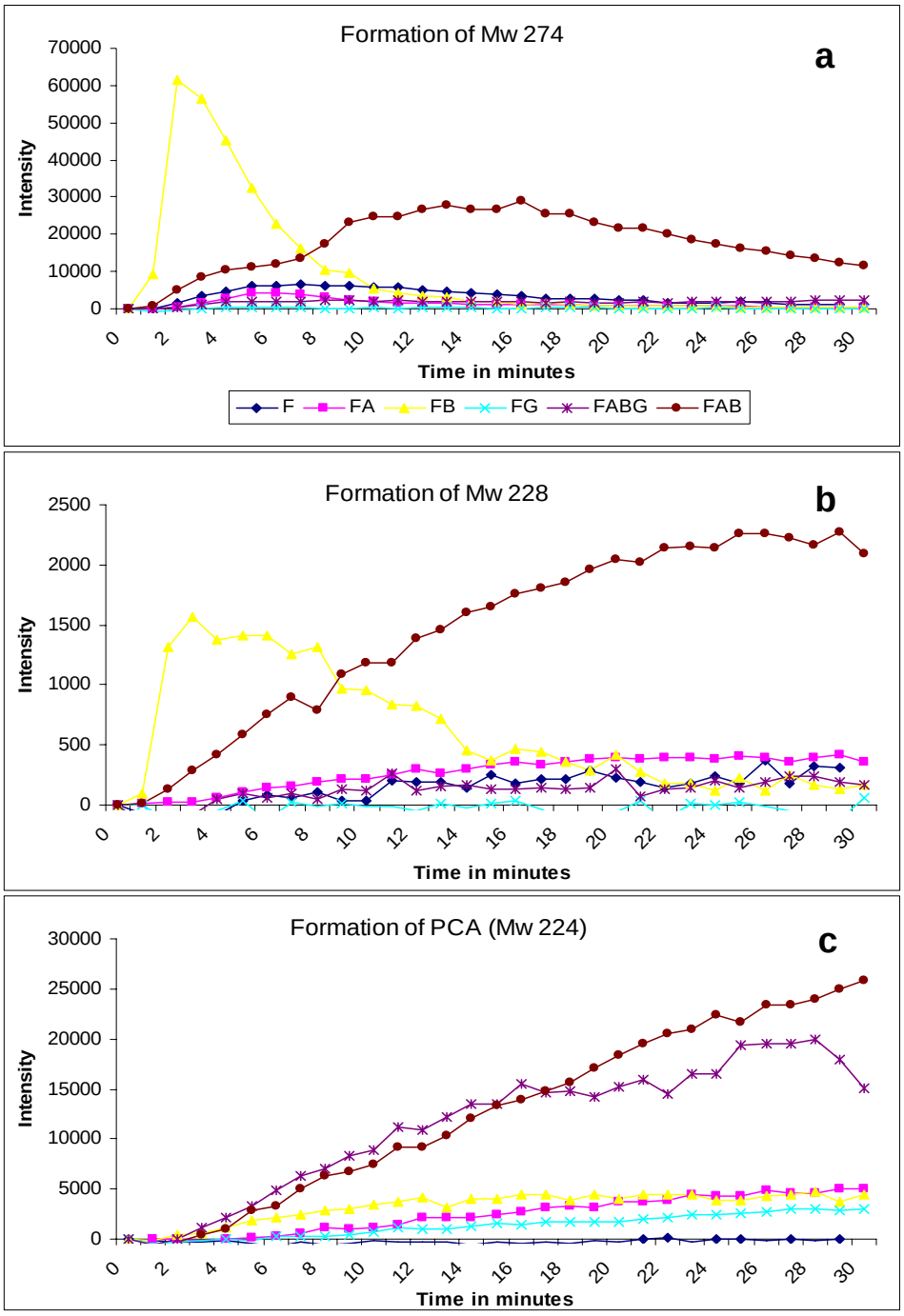

Figure 3.43: Graphs of intensities of the two intermediates (Mw 228 Da and 274 Da) and PCA from the various reactions followed by ESI-MS.

These intermediates were found to be present for all reactions, however, in the presence of enzymes PhzA and B much higher signal intensity was observed.

This observation restates the observation of McDonald et al. (2000) that PhzA and B are indeed involved in steps following PhzF. Additionally, these results

show that both PhzA and B are involved in the formation of the above-mentioned intermediates.

Though the graphs have been grouped on the basis of signal intensity of intermediates and PCA generated during the course of different reactions, the various spectra are not directly comparable. Also, these experiments are not indicative of the quantities formed. Moreover, no intensity for DHHA could be observed, making it difficult to compare the effect of enzymes on DHHA utilization and thus the effect of various combinations of enzymes on the efficiency of PCA produced. These are inherent drawbacks of ESI-MS. Hence, these results only indicate the presence or absence of the particular compound in presence/absence of various enzymes in a set of reactions, but give no comparable or quantifiable results.

The structures of the intermediates were hypothesised on the basis of their mass and are depicted in Figure 3.44. The suitably modified scheme of phenazine biosynthesis pathway including these two new species of intermediates and is shown overleaf (Figure 3.45).

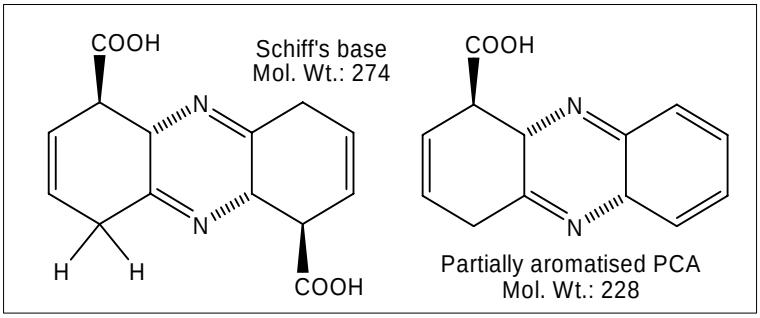

Figure 3.44: The hypothesised structures of the two intermediates identified by ESI-MS measurements, during the biosynthesis of PCA.

An interesting observation in this scheme, is the higher intensity observed for the intermediate with Mw 274 Da, when the enzymes PhzA and PhzB are present in the reaction mixtures. This is a modification of the scheme proposed by Blankenfeldt et al. (2004) where this intermediate (Mw 274 Da) was thought to be the product of the enzyme PhzF and the enzymes PhzA, B and G were shown to act after its formation. Thus, although this scheme (Figure 3.43) takes into account the intermediates formed, the ESI-MS results do not clarify the role of PhzA, B or G. Hence, these observations and the results obtained at the end of ESI-MS needed to be repeated, to obtain

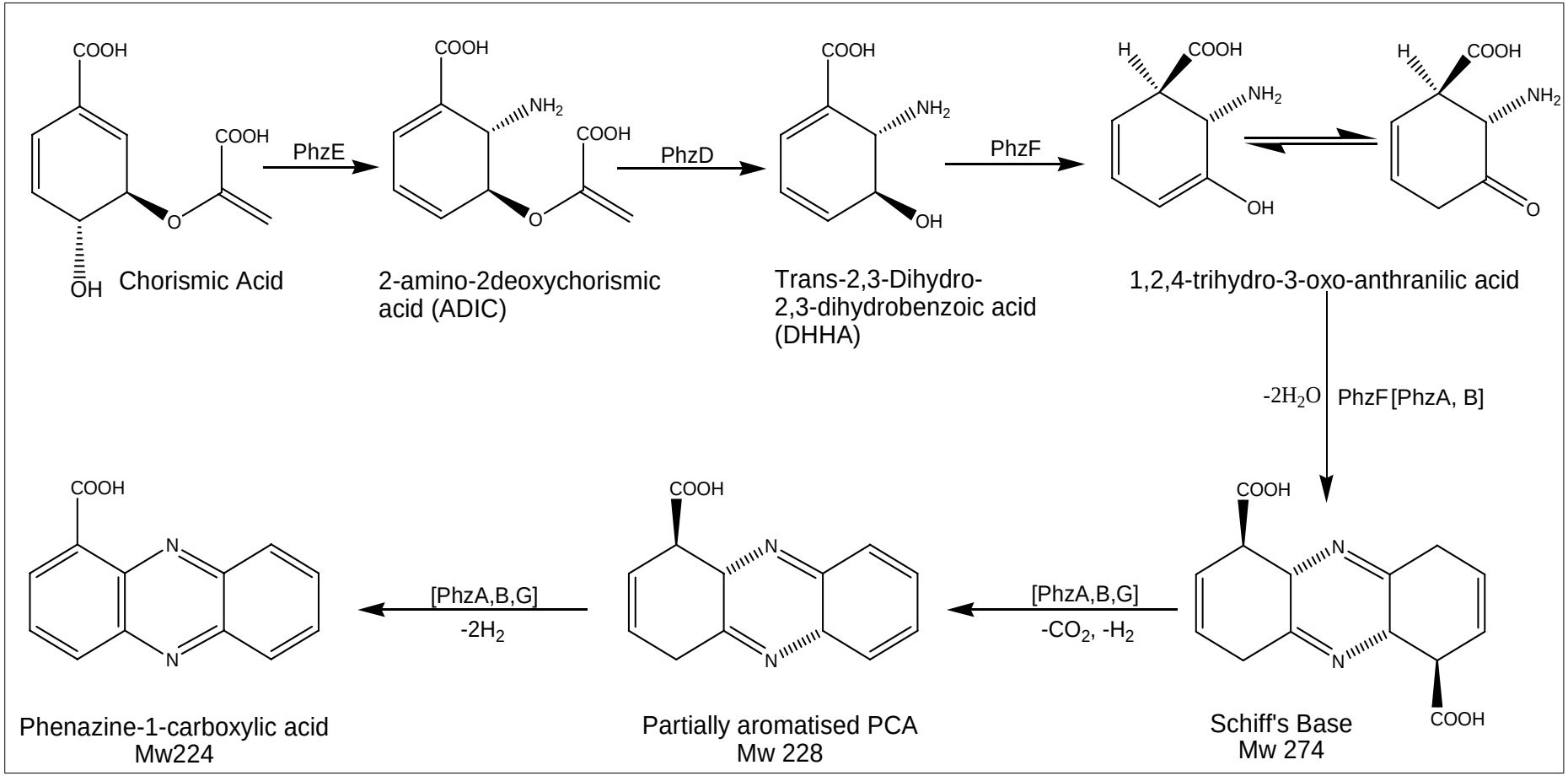

Figure 3.45: The modified scheme of phenazine biosynthesis (Blankenfeldt et al. 2004).

quantative and comparable information about the intermediates formed and the correct sequence of enzymes. Towards these aims, another MS-based method, Atmospheric pressure based ionisation (APCI-MS) was then carried out.

4.3 APCI-MS measurements

The primary intention of APCI-MS measurements was that of obtaining quantifiable and comparable data of the intermediates formed during phenazine biosynthesis by using an instrument i.e. APCI-mass spectrometer, with a higher sensitivity than that of ESI-MS. Towards this end, these measurements were performed in the presence of constant concentration (1 mM) of the molecule caffeine, for which the mass and spectral properties were already known. Moreover, caffeine was found to be inert and non-interfering to the reactions. Thus, all calculations were now comparable and quantifiable, by using the ratio of the peak area of compound produced and that of caffeine. Moreover, to have a better separation and detection, an HPLC was coupled to APCI and each experiment lasting 330 mins, consisted of 30 measurements each, with injection interval of 11 minutes. (details in section 7.3.8.3). The results obtained are described here, grouped according to the compounds formed during the course of PCA biosynthesis.

4.3.1 Effects of various enzymes on DHHA

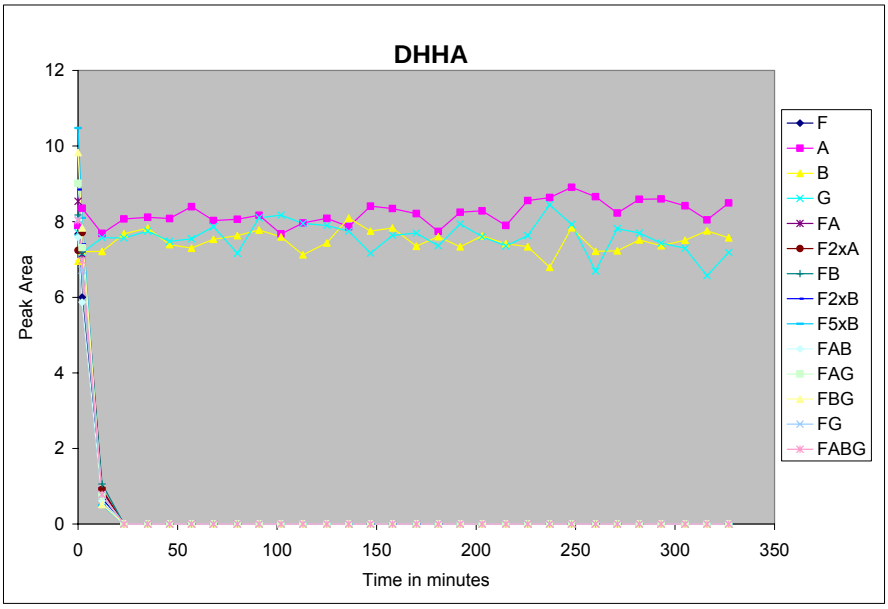

Figure 3.46: Utilisation of DHHA followed over a period of 330 minutes in the presence of different enzymes.

The graph of utilisation of DHHA with time (Figure 3.46) in presence/absence of various enzymes clearly shows that utilisation of DHHA is unaffected by the presence/absence PhzA, B or G; Thus, reiterating that DHHA is the substrate of PhzF. Moreover, the conversion of DHHA to its product 1,2,4-trihydro-3-oxo-anthranilic acid is fast, with most of the DHHA depleted within 10 minutes of addition of PhzF.

4.3.2 Formation of 1,2,4-trihydro-3-oxo-anthranilic acid

PhzF converts DHHA to 1,2,4-trihydro-3-oxo-anthranilic acid (Figure 3.45; pg 77) by abstraction of a proton from C3 carbon, rearranging the double bond system and reprotonating at the C1 position (Blankenfeldt et al., 2004). 1,2,4-trihydro-3-oxo-anthranilic acid has a molecular weight of 155 and displays keto-enol tautomerism (Figure 3.47) (Blankenfeldt et al., 2004). Both DHHA and its product have the same molecular weight of 155. Hence these compounds were distinguished in APCI-MS measurements by two main

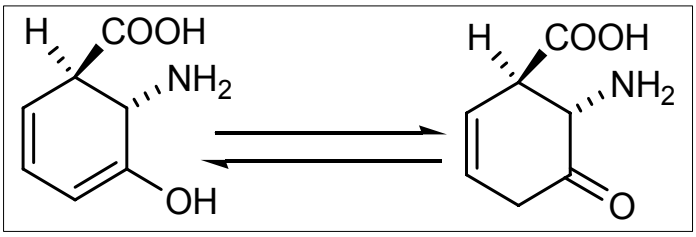

Figure 3.47: The two tautomers of 1,2,4-trihydro-3-oxo-anthranilic acid.

factors. Firstly, the DHHA peak shows the highest amounts at reaction time zero (i.e. before the addition of PhzF), depleting rapidly thereafter (Figure 3.48). Secondly, the peak for 1,2,4-trihydro-3-oxo-anthranilic acid appears after the addition of PhzF and a delay of approximately 2 mins. The graphs in Figure 3.48 show the formation of 1,2,4-trihydro-3-oxo-anthranilic acid.

The graphs can be divided into two clear subdivisions, based on the absence/presence of the enzyme PhzB. The first, consists of reactions carried out in the in the absence of PhzB (top 5 curves in the graph). Here, 1.5 times more 1,2,4-trihydro-3-oxo-anthranilic acid is observed. Moreover, at the end of these measurement, at 330 minutes, there is still an appreciable amount (also 1.5 times more) of this compound still present in the reaction mixture. Another interesting fact is that the amounts of 1,2,4-trihydro-3-oxo-anthranilic acid

formed in this group is not affected by the presence/absence of either PhzA or G. This is a clear indication, that neither PhzA nor PhzG are capable of utilising 1,2,4-trihydro-3-oxo-anthranilic acid as their substrate.

The second sub-division of reactions, which are all performed in the presence of PhzB, show a different profile. In these reactions, the sharp peak of 1,2,4-trihydro-3-oxo-anthranilic acid formation is still observed, but the amount is

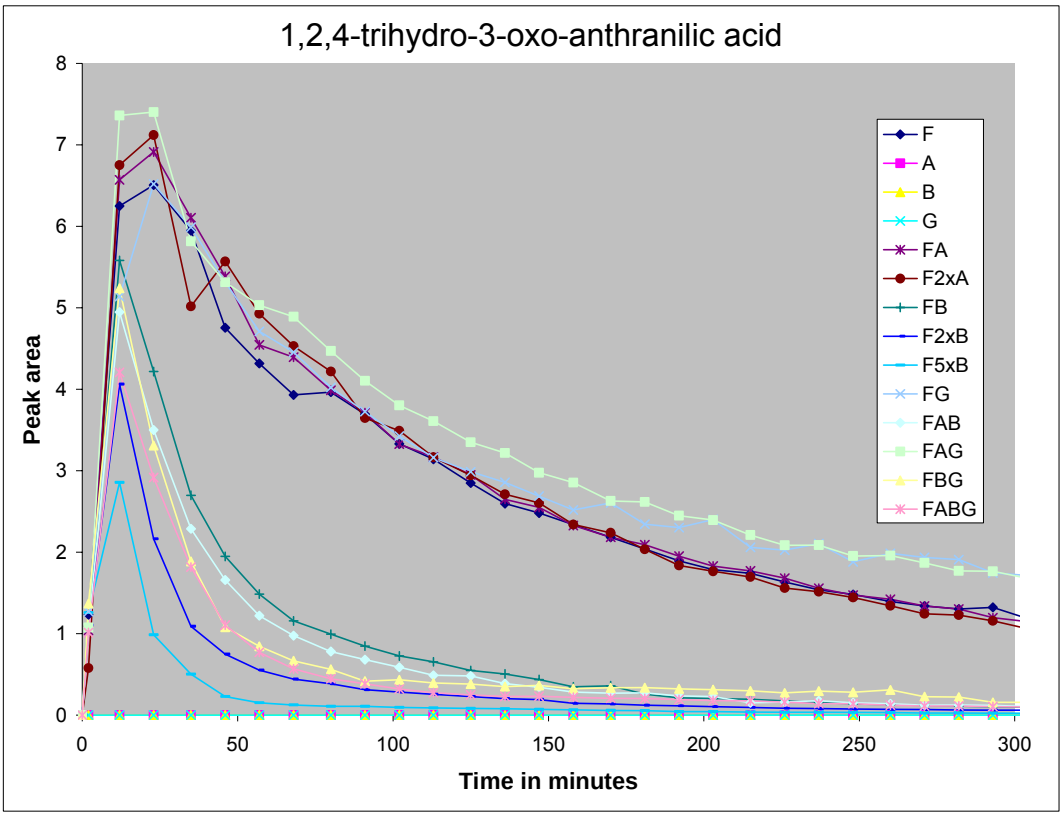

Figure 3.48: Formation of 1,2,4-trihydro-3-oxo anthranilic acid.

reduced. Moreover, the depletion of 1,2,4-trihydro-3-oxo-anthranilic acid is quick, and reaches near zero values by 180 minutes.

Taken together, this graphs shows that 1,2,4-trihydro-3-oxo-anthranilic acid is formed by PhzF and is utilised by PhzB as substrate. Neither PhzA nor PhzG plays any role in this step of the pathway.

4.3.3 Formation of intermediate with Mw 274 Da

The peak for m/z 275 (Mw 274 Da) is observed immediately on the addition of the enzyme PhzF into the reaction mixture as shown in Figure 3.49 overleaf.

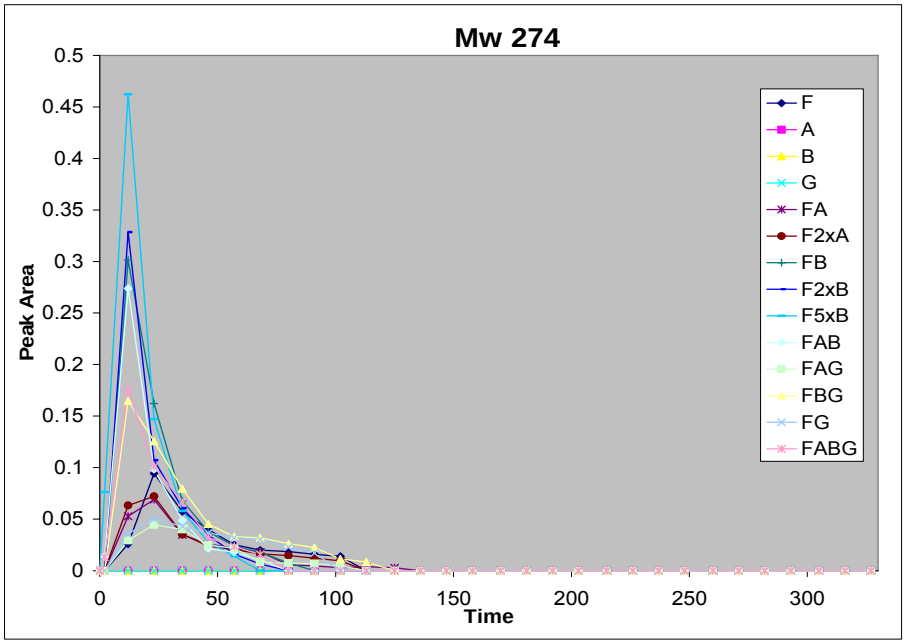

Figure 3.49: Graph showing formation of Mw274 Da.

For better visualisation, the graph below shows the first 120 minutes of the experiments:

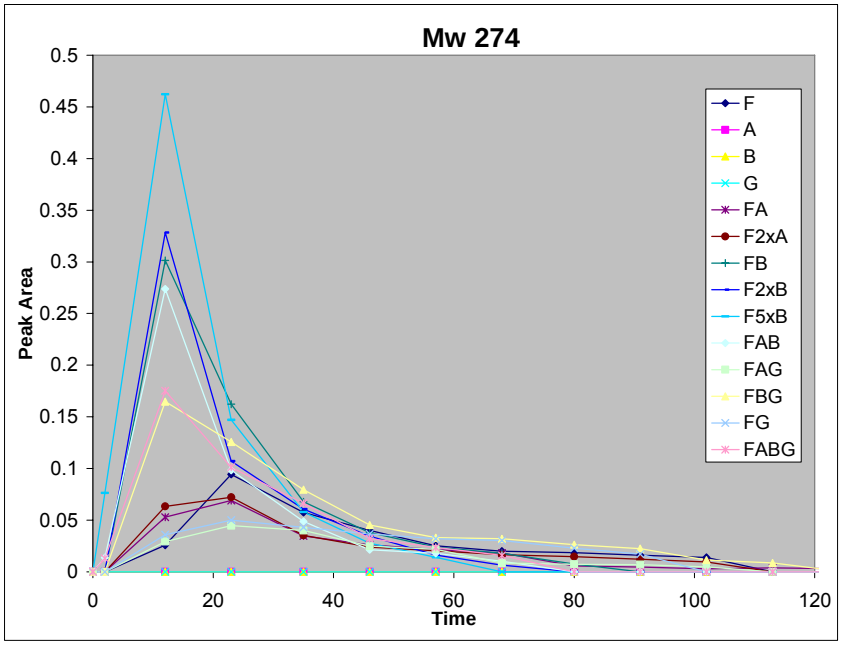

Figure 3.50: Formation of Mw 274 Da in the first 120 minutes.

The maximum amount of this species is formed at approximately 12 minutes which coincides with the minimum levels of DHHA (Figure 3.46) in the reaction mixture. The highest amount of this intermediate is formed in experiments performed in the presence of PhzB. The interesting observation in this graph is that PhzA, which is 70% identical to PhzB, seems not to have

the same effect on the production of this peak as PhzB. Where a five-fold increase in amounts of PhzB (F5xB) results in a 5-fold increase in the formation of this intermediate (as compared to FB), no effect is observed on varying the amounts of PhzA. Also, no significant difference is observed in the amounts of Mw 274 Da produced by PhzF in the presence/absence of PhzG; thus implying that neither PhzA nor PhzG participates in the formation of this intermediate.

The results pertaining to the formation of 1,2,4-trihydro-3-oxo-anthranilic acid and the Mw 274 Da thus indicate that PhzB is involved in the reactions catalysing the conversion of 1,2,4-trihydro-3-oxo-anthranilic acid to the compound with Mw 274 Da.

4.3.4 Formation of intermediate with Mw 228 Da

PhzB affects the formation of the compound with Mw 228 Da (m/z 229) in a fashion similar to that of Mw 274 Da formation (Figure 3.49 & 3.50). The graph

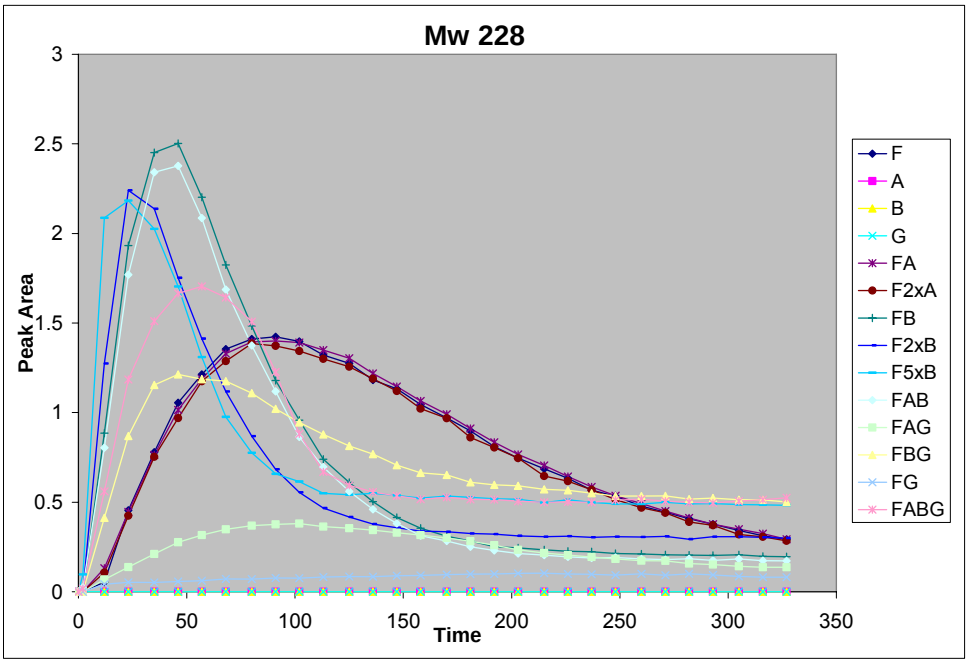

Figure 3.51: Graph depicting the formation of the intermediate with Mw 228 Da.

above also clearly shows that the enzyme PhzB speeds up the formation of Mw 228 Da, with the peak maxima reached in half the time required for reactions containing PhzF with PhzA and/or G and PhzA only (Figure 3.51). This can be partially explained by the higher Mw 274 Da formed in presence

of PhzB, which being a highly unstable intermediate, would spontaneously yield higher amounts of Mw 228 Da, which is a more aromatised and hence more stable of the two intermediates.

At the same time, in the presence of PhzB, Mw 228 Da also depletes much faster as compared to the other reactions. Another interesting observation from these graphs is a dramatic reduction in the amount of this intermediated when PhzG is present alongwith PhzF.

4.3.5 Formation of PCA

The highest amount of PCA formed is during the reaction where all the four enzymes are present i.e. PhzFABG (Figure 3.52). Moreover, the presence of the enzyme PhzG is indeed the deciding factor for the amount of PCA formed, in the presence/absence of either PhzA or B.

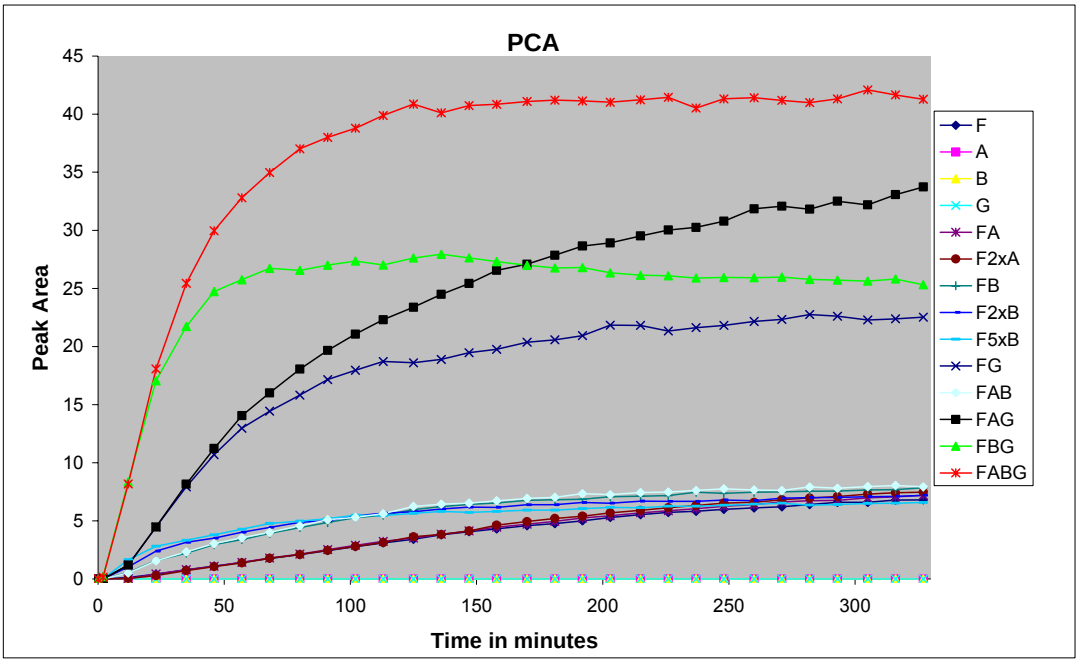

Figure 3.52: The graphs of PCA formed in the presence of various enzymes.

No significant difference observed in PCA formation where only PhzA and/or PhzB were present alongwith PhzF. Thus higher amounts of the intermediates with Mw 228 Da and 274 Da formed in the presence of excess PhzB do not translate to a higher yield of PCA, in the absence of PhzG. Moreover, the combination of enzymes PhzF and PhzG which showed very low quantities of intermediates with Mw 274 Da and 228 Da shows a proportionally much

higher yield of the product PCA. Another interesting observation from the graphs 3.50 & 52 is that the amounts of Mw 228 Da formed in the presence of PhzF and A does not translate into higher yields of PCA.

4.3.6 Implications of the results of APCI on phenazine biosynthesis.

It was proposed by Blankenfeldt et al., (2004) that phenazine biosynthesis involves the formation of a highly unstable double Schiff's base with Mw 274 Da. This compound was also proposed to be formed within the cavity of dimeric PhzF, from two molecules of the product of this enzyme, i.e. 1,2,4-trihydro-3-oxo-anthranilic acid.

This molecular weight (274 Da) was indeed observed during APCI measurements (Figure 3.49 and 3.50). The structure of this compound was hypothesised as shown in Figure 3.53 below. The enzyme PhzB leads to a much higher synthesis of this intermediate.

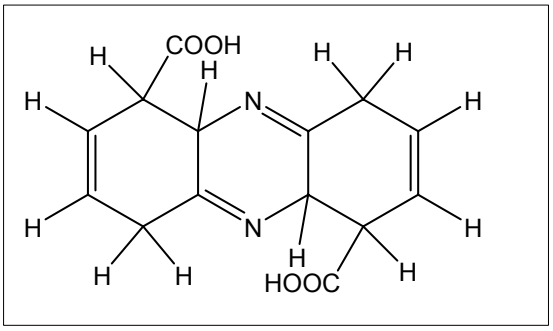

Figure 3.53: The structure of the intermediate with molecular weight of 274 Da.

As can be seen from the figure above, this intermediate is highly unstable, oxidation (as oxidative decarboxylation) or hydrolysis in the presence of oxygen/water would be sufficient to yield the intermediate with Mw 228 Da (partially aromatised PCA). This inference is backed by the amounts of this partially aromatised PCA observed in reactions not containing PhzB, where the formation of this compound is not influenced by the presence/absence of any other enzyme (Figures 3.46 and 3.48). Moreover, this also explains the higher yield of partially aromatised PCA (intermediate with Mw 228 Da) in all reactions containing PhzB, since, more Mw 274 Da formed due to the presence of PhzB would lead to a proportionally higher yield of Mw 228 Da.

This partially aromatised PCA needs oxidation for the formation of PCA, a reaction that can be catalysed by the FMN-dependent oxidase, PhzG. This is indeed the case and in all reactions containing PhzF, G and B, where the yield of PCA is at least two-fold higher than reactions in which either PhzB or PhzG is absent (Figure 3.52).

In all these measurements, however, the only effect of PhzA is observed in the final yield of PCA, when present in reactions containing PhzG (Figure 3.52). The reactions containing PhzA alongwith PhzB and G yield the highest amounts of PCA (Figure 3.52). Thus, although PhzA and B are more than 70% identical, the effect displayed by PhzB is not mirrored by PhzA. One explanation, (detailed in Section 5.1, Two-hybrid assay) could be the role of PhzA as a sort of 'shuttle' shielding and conveying the highly unstable intermediates from one protein to the next. Another possibility mentioned earlier in the introduction, is the occurrence of an event of gene-duplication in the past. A third hypothesis could be the formation of active hetero-dimers by PhzA and B, which could be envisioned as simultaneously shielding and catalysing the unstable intermediates. However, these hypotheses though under investigation, have not been experimentally ratified yet.

Another interesting observation is the relatively high amounts of both intermediates with Mw 274 Da and 228 Da formed, in the absence of PhzB or PhzG, which do not yield the same high quantities of the product PCA. This phenomenon can be explained in terms of the inherent instability of the intermediate with Mw 274 Da. The most stable structure for this intermediate would be an aromatic, three-ring phenazine scaffold, which could be arrived at only through some chemical transformations. This intermediate is actually a Schiff's base; which are inherently unstable and highly sensitive. Thus, oxidation by oxygen or hydrolysis by water would be sufficient to transform Mw 274 Da to the partially aromatised PCA with a molecular weight of 228 Da.

Moreover, there are other ways in which this intermediate could undergo spontaneous oxidation in absence of enzymes PhzA, B and G and the presence of oxygen forming the compounds shown in the Figure 3.54. The driving force would thus be the search for higher stability by this unstable intermediate, through re-arrangement of double-bond system spontaneously

and in the presence of oxygen, towards a stable π-electron system, one of which is that of PCA. This explains the low efficiency of PCA formation (less then 20%; Figure 3.52) observed in reaction containing only PhzF or PhzF

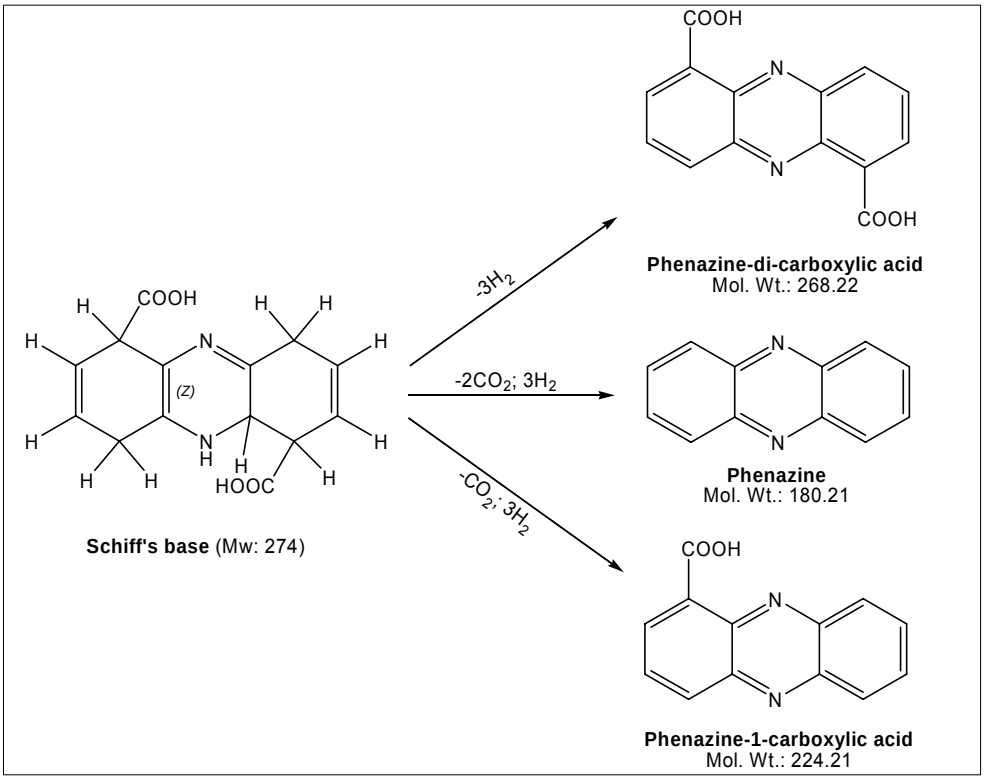

Figure3.54: Some of the stable aromatic configuration that can be adapted by the Schiff's base (Mw 274 Da).

with either PhzA or B. This is despite the fact that the presence of PhzB leads to the formation of, comparatively, the highest amount of partially aromatised PCA (Mw 228 Da). Only in the presence of the FMN-dependent oxidase PhzG, the partially aromatised PCA yields optimal quantities of PCA.

To detect the presence of stable aromatic systems arising spontaneously and thus to further validate the inferences from the previous paragraph, APCI-MS measurements were re-analysed and a small signal (peak ratio < 2 units) is indeed observed for the compound phenazine (Mw 180; m/z 181) (Figure 3.55, overleaf). In some cases, PDC (Mw 268; m/z 269), was also formed, however, its presence was too erratic for quantifiable graphs.

The graph in Figure 3.55 (overleaf) clearly shows that phenazine formed in the presence of all the four enzymes, i.e. PhzFABG is three times lower than that formed in the absence of one or the other enzymes. This observation confirms the above-mentioned hypothesis that PCA biosynthesis is better

controlled in the presence of all the enzymes. The absence of one or more of the enzymes leads to the spontaneous/un-catalysed formation of various three-ring aromatic products, including PCA, through oxidation by oxygen.

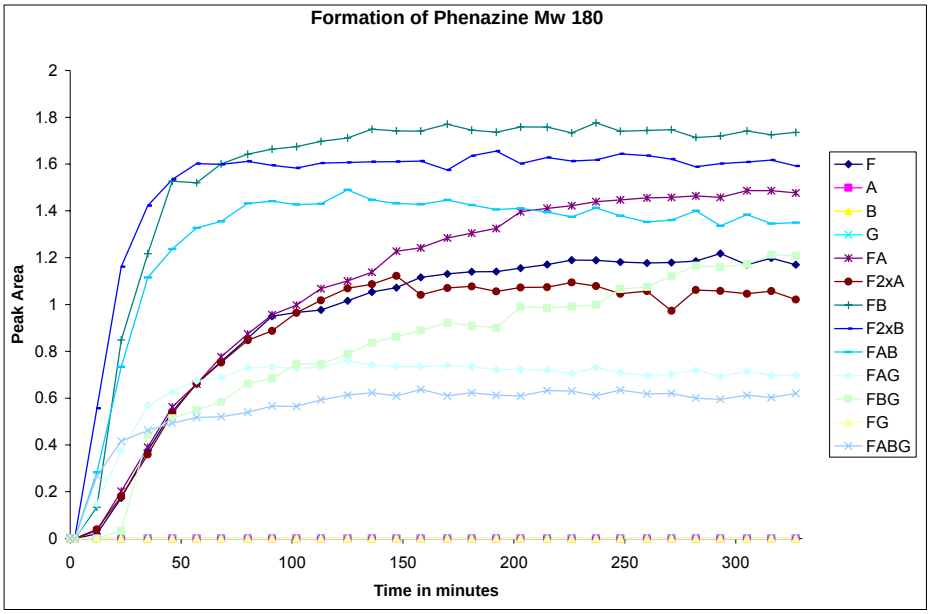

Figure 3.55: Formation of phenazine (Mw 180) for various reactions in APCI-MS measurements.

As a conclusion to this section and to further clarify the results obtained, a scheme representing the current hypothesis of phenazine biosynthesis pathway leading to the formation of PCA in *P. fluorescens* is depicted overleaf.

The effect of oxygen on the formation of aromatic systems shown in Figure 3.54, is also supported by the observation that a darker colouration can be seen at the air/buffer interface in an NMR reaction tube containing only DHHA and PhzF (Figure 3.56). On NMR, this reaction mixture gives an indecipherable spectrum of different aromatic compounds.

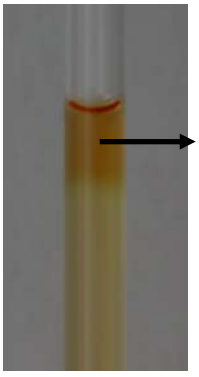

Figure 3.56: The dark colour at the interface between air and buffer solution in an NMR tube containing DHHA and PhzF. (From Blankenfeldt et al 2004)

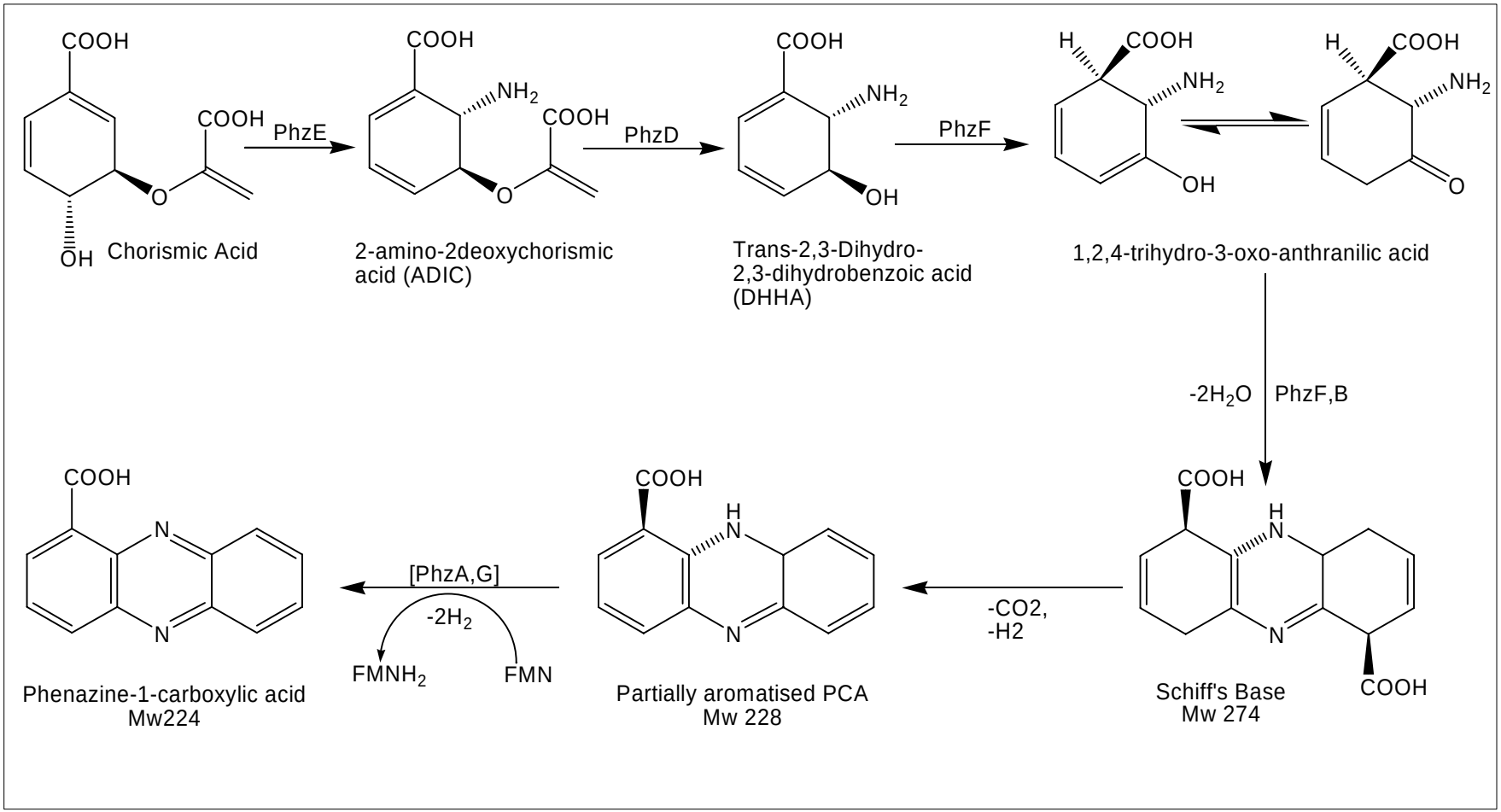

Figure 3.57: The scheme of phenazine biosynthesis pathway of *P. fluorescens* based on the results obtained from this work.

Taken together, these observations thus highlight the important role played by oxygen as an electron acceptor in PCA biosynthesis. Hence, the role of oxygen and its uptake by various enzymes of this pathway was investigated using an oxygen electrode and the results of these measurements have been described in section 6.

Also, considering the highly unstable nature of the intermediates, it was plausible to hypothesise the existence of a multi-enzyme complex by the enzymes of the phenazine biosynthesis pathway. This possibility was investigated by employing bacterial two-hybrid system and the results obtained are described in the following chapter.

Section IV

This section contains the results obtained while investigating the interactions between the seven enzymes of the phenazine biosynthesis operon.

5.0 Interactions between the enzymes of ‚phz' operon

APCI-MS measurements led to the discovery of two new intermediates in the biosynthesis of PCA. These intermediates with Mw 274 and 228 are unstable and thus, it would be advantageous if the enzymes formed a multi-enzyme complex, which, by shielding the unstable intermediates would make the process of phenazine biosynthesis more efficient.

For investigating this possibility, trials for detecting the formation of a multi-enzyme complex between the enzymes of the phenazine biosynthetic operon were initiated. Gel filtration chromatography was initially employed for this purpose; however, no conclusive results were obtained from this technique. Hence, other methods like the bacterial two hybrid system were used in order to detect the interactions between these enzymes. The bacterial two-hybrid assay is a relatively new method developed by Karimova and co-workers in 1998 (Karimove et al., 1998). This system is based on interaction-mediated reconstitution of the adenylate cyclase activity in *E.coli* observed on indicator agar (details in section 9.3.8). This was followed by quantitative assessment of the interaction using Liquid-β-Galactosidase activity assay (see also 9.3.9).

5.1 Bacterial Two Hybrid Assays on Indicator Agar

This assay was performed as described in section 9.3.8. Plating of the *E.coli* cells DHM1 containing the various two plasmid combinations on MacConkey agar at 28°C showed the outcome depicted in Figure 3.58 (overleaf).

To offset the possibility of steric hindrances due to the location of the genes on the two plasmids (pKT25 and pUT18) and thus, the steric constraints imposed by the three-dimensional structure of the hybrid protein complex, which could affect the adenylate cyclase enzymatic activity of the reconstituted complex; the interactions between the genes A-G in both orientations, i.e. one of the genes cloned in plasmid pKT25 and the second in plasmid pUT18 and *visa-versa* was performed. The names of the genes are denoted as alphabets and 'C+/-' denotes the positive/negative controls, which were performed using the plasmids supplied by the two hybrid kit.

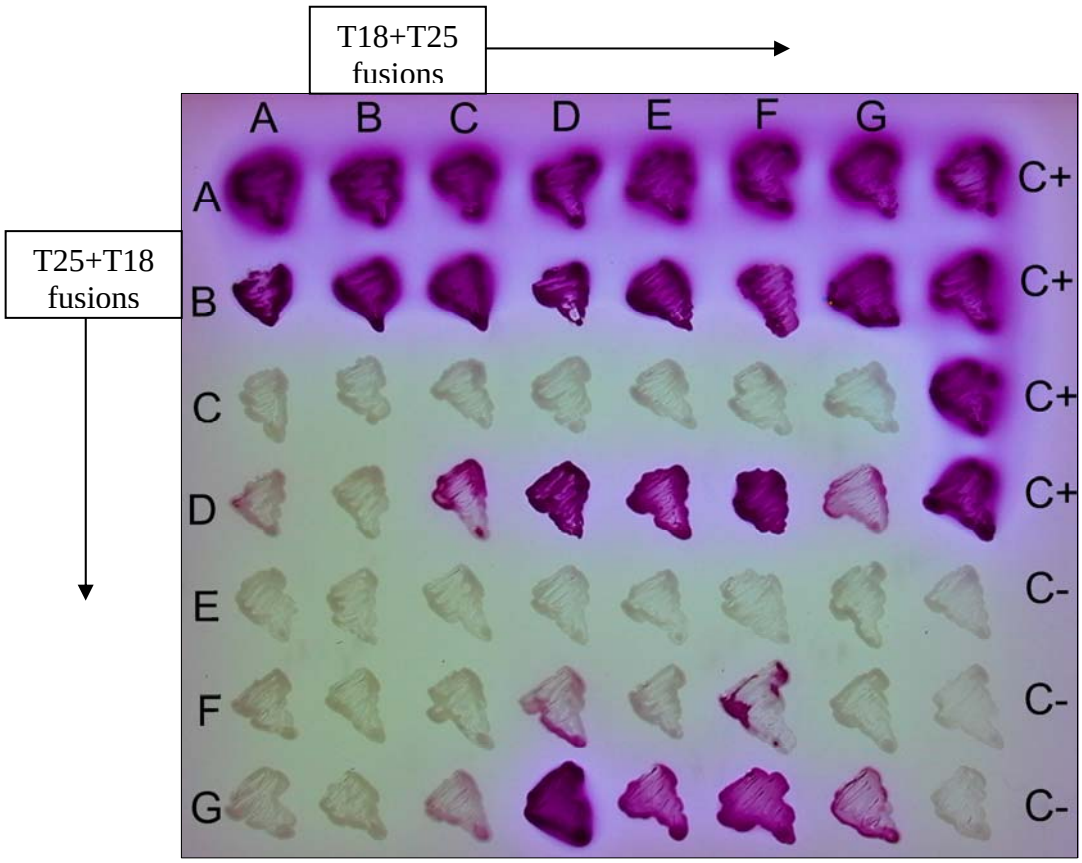

Figure 3.58: The photograph of the bacterial two hybrid assay on indicator agar. (The positive results seen as magents-pink and the negative as white colonies. A-G are the seven phenazine biosynthetic genes.)

From this figure it can be clearly seen that the genes phzA and B seem to interact with all the other genes of the phenazine biosynthesis pathway. Other interactions include those of phzD with phzC, E, F and G; phzG with phzD, E and F.

Interestingly, the precautions undertaken for negating the steric hindrance were justified, since the interactions between phzA-B and other genes are observed only in the case where these genes are cloned in the plasmid T18 (horizontal orientation in Figure 3.58). In the reverse case, where the genes are cloned in the reverse orientation (T25+T18 in Figure 3.58), the interactions are visible only between these two genes and not the other genes of the pathway.

This result seems to second not only the possibility of the formation of a multi-enzymes but also the hypothesis put forward by MacDonald and co-workers, that PhzA and B are proteins that help form the multi-enzyme complex

between the 'phz' enzymes. However, a need was felt to further clarify the results obtained on the indicator agar. Thus, the Liquid-β-Galactosidase activity assay was then performed to help both clarify and quantify the various interactions.

5.2 Liquid-β-Galactosidase activity assay

This assay was performed using the plasmids where the genes were cloned in T18 and T25 respectively. The results of this assay are depicted in Figure below.

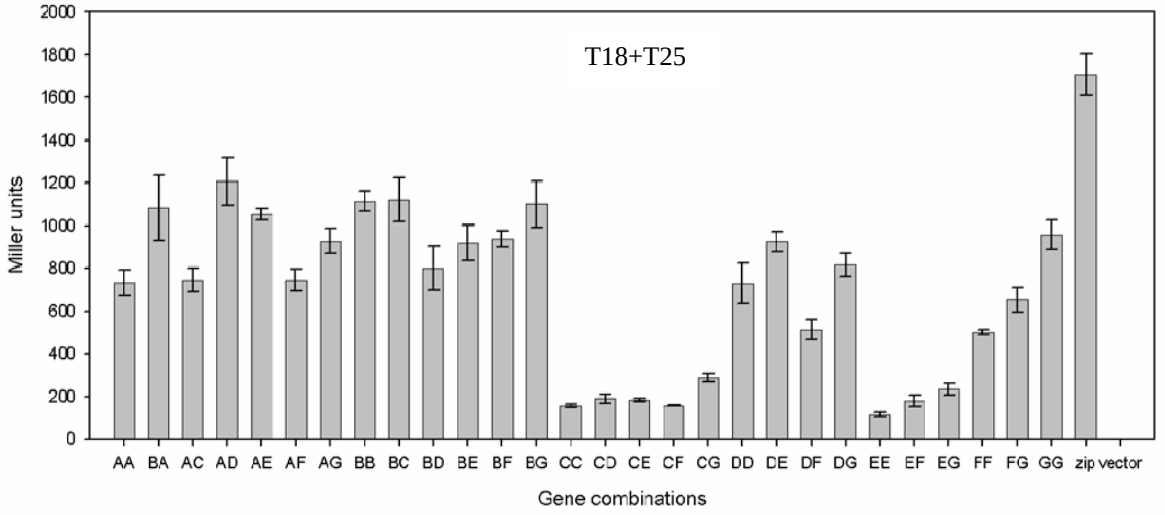

Figure 3.59: The results of the β-galactosidase assays depicted as graphs.

This figure clearly shows that the β-galactosidase assays confirm the findings of the MacConkey indicator agar (Figure 3.58).

As a further confirmation of these interactions and specially the contribution of PhzA and B to the formation of a multi-enzyme complex, pull-down assays using Nickel beads were carried out. However, the protein PhzA even after the removal of the 6xHis tag showed high levels of non-specific binding to the nickel beads. This resulted in a level of background due to which it was difficult to draw any conclusions about the interactions. Future experiments using different pull-down strategies will hence have to be undertaken, which could not be performed due to time constraints.

At the end of these two sets of experiments, it can be said that the enzymes PhzA and B interact with all other enzymes, while the other major interactions

occur between the enzymes PhzD, F and G. The conclusions drawn from these experiments are depicted in Figure 3.60 below.

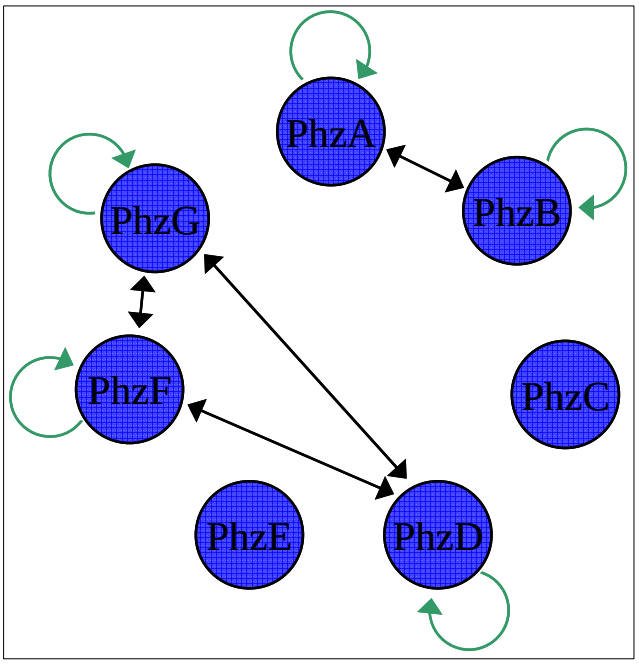

Figure 3.60: Summary of the interactions observed between the proteins of the 'phz' operon of *P.fluorescens*.(The curved arrows denote dimeric interactions of the proteins; the straight black arrows denote other interacting proteins. Interactions of PhzA, B with all enzymes not depicted for the sake of clarity.)

The next section describes the experiments performed for the detection of oxygen consumption during the biosynthesis of PCA.

Section V

This section describes results of the experiments carried out to study the effect of the presence of oxygen on yields of the PCA and the other intermediates formed during the phenazine biosynthesis pathway.

6.0 Measurements using Clarke's electrode

As mentioned in the section 4, oxygen seems to play an important role in the process of phenazine biosynthesis. In order to further investigate the effect of oxygen on PCA biosynthesis, experiments were initiated to test the efficiency of the enzymes to uptake oxygen. These experiments were undertaken using an oxygen electrode (Clark's electrode). The set-up and method has been described in section 9.1.

For these measurements, the reaction mixture was sealed in an air-tight chamber, to which PhzF, dissolved in buffer was added to initiate the reaction and the time required for each set of reaction to completely use the dissolved oxygen was measured. Varying amounts of both PhzA and B were also used to observe the effect of these enzymes on oxygen consumption. The results obtained from this set of experiments are depicted below.

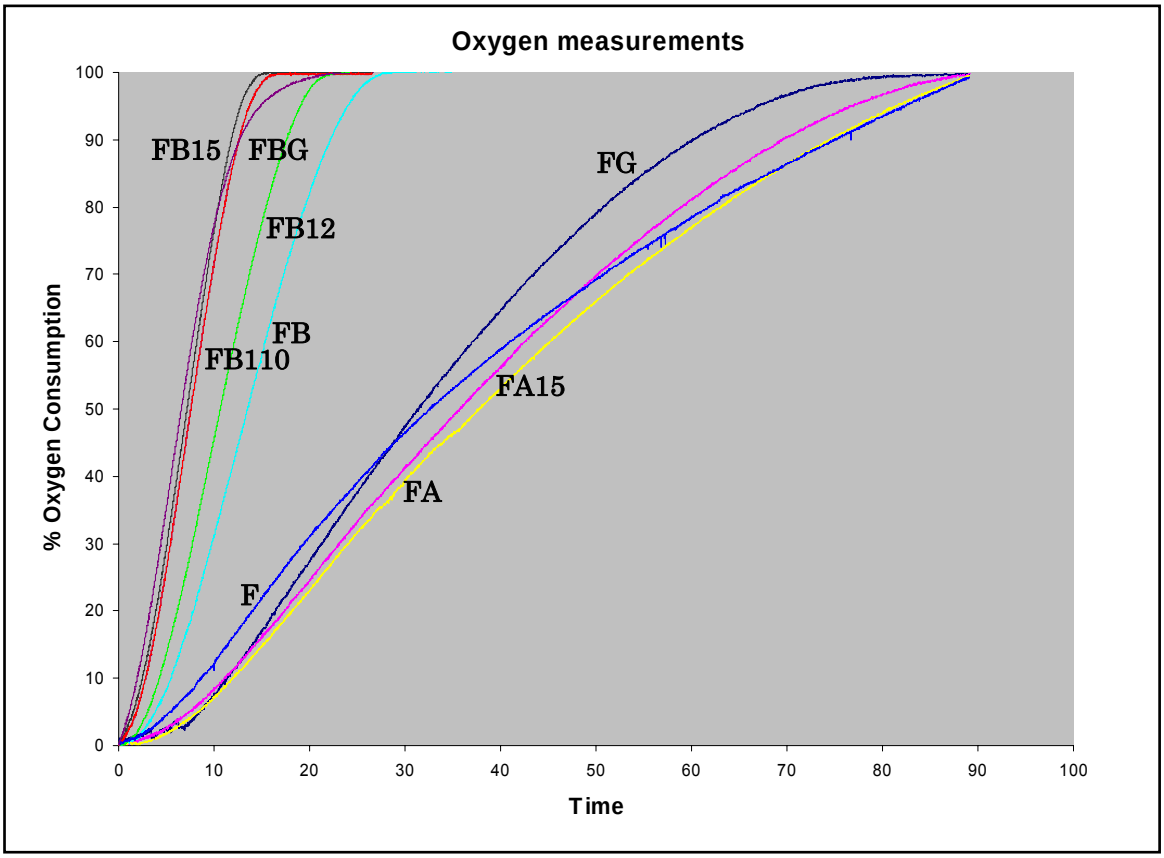

Figure 3.61: The graph of oxygen consumption versus time for various combinations of enzymes. (The digits denote the ratio of enzymes added, thus, 15 is enzymes in the ratio of 1:5.)

These measurements clearly show that the presence of PhzB with PhzF increases the efficiency of oxygen consumption while PhzA shows no effect at

all. Moreover increasing the amounts of PhzB by 5-fold, further increases the rate of oxygen consumption. But any further increase in the amount of PhzB shows no corresponding change.

The rate of oxygen consumption in the presence of 5/10-fold PhzB is comparable to that observed in the presence of PhzFBG but not when only PhzF and/or PhzG are present in the reaction.

These phenomena can be explained firstly by the fact that the amounts of the partially aromatised PCA formed are unaffected by the presence of PhzF alone or with PhzA/G (as observed from APCI-MS measurements). Since the availability of this intermediate, the substrate of PhzG, remains similar in these cases, no change is observed in the graph of oxygen consumption in reactions containing either PhzF alone or PhzF with PhzG. Secondly, there is higher amount of the partially aromatised PCA in reactions containing PhzB, hence, higher substrate availability for PhzG. PhzG is FMN-dependent oxidase, which, for catalysis, converts FMN to $FMNH_2$. The $FMNH_2$ is regenerated to FMN ($FMNH_2 + O_2 \rightarrow FMN + H_2O_2$), a step which requires oxygen; thus higher oxygen consumption observed in the reaction containing PhzFBG. These observation further reiterate the inference (together with results of APCI measurements) that PhzG catalyses the oxidation of partially aromatic PCA (Mw 228) to PCA. Also, in absence of PhzB, where lower amounts of Mw 274 and thus the substrate of PhzG - Mw 228 are present in the reaction mixture, the rate of oxygen consumption does not differ greatly to those when only PhzF is present.

At this point, it was interesting to investigate the behaviour of BcepA, with regards to its activity and to compare its behaviour to that of PhzA and B. No information is available as to the possible substrate of this enzyme or the process of phenazine biosynthesis in *B. cepacia*. However, it is assumed that this process is similar if not identical to that in pseudomonads and hence, oxygen consumption was measured for BcepA, in the presence of the enzyme PhzF from *P.fluorescens*.

The graph depicting the oxygen consumption by BcepA is shown overleaf (Figure 3.62). This graph clearly shows that BcepA is indeed active and consumes oxygen in a manner similar to PhzB. This is an interesting observation in light of the fact that PhzA, its close structural homolog is not.

However, this is only a preliminary result and the phenazine biosynthesis process of *B. cepacia* need further and more thorough investigation to be able to say more about the exact role of BcepA.

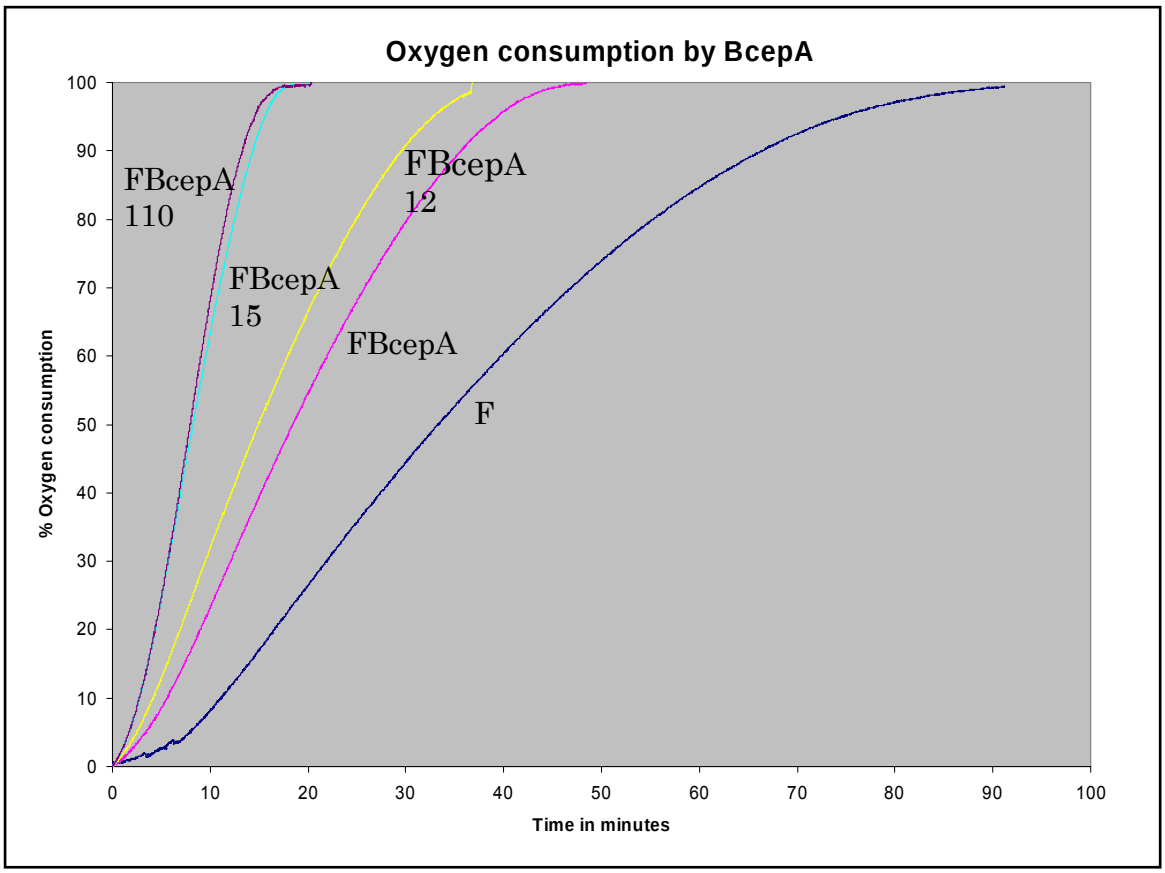

Figure 3.62: Oxygen consumption by BcepA.

Thus in this section the effect of the enzymes of the PCA biosynthesis pathway of *P.fluorescens* on oxygen uptake were analysed. The enzyme PhzB which catalyses the formation of the unstable Schiff's base with Mw 274, which through oxidative decarboxylation by dissolved oxygen forms partially aromatised PCA (Mw228) accelerates oxygen consumption dramatically. The enzyme PhzG an FMN-dependent oxidase, which requires oxygen for catalysis, also shows an acceleration of oxygen consumption, however only in the presence of PhzB, the presence of which creates a higher concentration of the substrate of PhzG – partially aromatised PCA (Mw 228). This study thus underlines the importance of oxygen in phenazine biosynthesis.

Conclusions & Future Directions

'Tut, tut, child!' said the Duchess.
'Everything's got a moral, if only you can find it.'
- (Alice in wonderland, Lewis Carroll)

7.0 Conclusions

Phenazines and phenazine biosynthesis, though a topic of research for various studies was still not completely understood, since the structure and function of the enzymes involved in this process had not been previously investigated. The objective of this study was to elucidate the structure of the enzymes PhzA, B and G of the phenazine biosynthesis pathway of *Pseudomonas fluorescens 2-79* and to gain an insight into their functions as well as the intermediates formed during biosynthesis of Phenazine - 1-carboxylic acid (PCA).

Towards this end, the structures of enzymes PhzA, PhzG and its complex with PCA were elucidated and analysed. Moreover, the structure of a homologue of PhzA/B from *Burkholderia cepacia*, BcepA and its complex with an inhibitor were also solved during the course of this work.

Structural investigation of PhzA and BcepA highlighted interesting and thus far unknown aspects of these enzymes. Structurally, both these enzymes were found to belong to the ketosteroid isomerase (KSI) family of proteins, displaying an α+β fold characteristic to this family. PhzA and BcepA are the most recently recognised members of this family, with BcepA being the first member displaying an 'arm-exchange' mode of dimerisation. The study of these two structures reiterated the conclusion by other works, that the fold of KSI-family of proteins provides a robust scaffold, whose function can be tuned by altering the properties of the residues lining the interior cavity. However, since this family contains functionally very diverse proteins (e.g. transport factors, isomerases, hydrolases, oxidases) no function can as yet be ascribed to either PhzA or BcepA from structural knowledge alone.

The enzyme PhzG, which shows sequence similarity to pyridoxamine 5'-phosphate-oxidase from *E.coli,* was found to be a FMN-dependent oxidase on the elucidation of its structure. Moreover, the structure of PhzG complexed with PCA was also solved, which helped to further clarify its role as an oxidase in the phenazine biosynthesis pathway.

Functional studies were carried out during the course of this study by using a bacterial two-hybrid system, APCI mass spectroscopy, and the oxygen electrode. A new methodology using APCI-MS was established in this work, for detection of the activity of various enzymes and the intermediates formed during the biosynthesis of PCA.

Using this method, two new, key intermediates, a proposed Schiff's base with molecular weight 274Da as well as a partially aromatised PCA with Mw 228 Da were discovered. Moreover, this work also led to the resolution of the sequential order of enzymes acting in this pathway, which is PhzE, D, F, B, G and A.

The APCI-MS studies, although hinting at some effect of the presence of PhzA did not point towards a special role for this protein in phenazine biosynthesis. Surprisingly, the enzyme PhzB, which has a 70% sequence identity with PhzA, is, in the light of this work (by APCI-MS and oxygen measurements using Clarke electrode), thought to act as a synthase. The enzyme PhzG is indeed an oxidase and catalyses the conversion of partially aromatised PCA (Mw 228) to the product of this pathway, PCA.

This is the first study to investigate the enzyme BcepA from the phenazine biosynthesis pathway of *B. cepacia*. BcepA, like PhzB was found to accelerate oxygen consumption and might also act as a synthase. However, since no other information is available about the process of phenazine biosynthesis in this organism, apart from the phenazine compounds produced, more detailed studies are needed to be able to gain more insight both into the function of this enzyme as well as the mechanism of phenazine biosynthesis in *B. cepacia*.

7.1 Suggestions for Future work

This study has successfully answered a number of questions about phenazine biosynthesis in *Pseudomonas fluorescens 2-79*. It has however, also raised some interesting questions. Chief among them is the apparent lack of activity of PhzA, the activity of PhzB and the presence of two of these enzymes in all phenazine biosynthesis pathways of Pseudomonads. Further efforts towards the solution of the structure of PhzB will help answer some of these questions.

From the interaction studies, an indication of interacting proteins was obtained, with the strong interactions between PhzA and B pointing towards these proteins forming a potential hetero-dimer. The formation of hetero-dimer by PhzA and B would be a particularly interesting point of investigation and would help justify the role of PhzA as a protein which helps transfer the unstable intermediates from PhzF to PhzB and G as proposed by this study.

Experiments towards determining the mode of action of PhzG and the detection of the formation of H_2O_2 during catalysis of this enzyme will help provide comprehensive data about PhzG and its functioning in the phenazine biosynthesis pathway.

Another angle of investigation would be towards prove the structures of the intermediates with methods other than mass-spectroscopy. Towards this end, studies incorporating HPLC coupled to NMR would shed more light into the exact structures of the intermediates hypothesised here and thus further clarify the function of the participating enzymes.

8.0 Zusammenfassung

Die Biosynthese der Phenazine, einer wichtigen Klasse von Sekundärmetaboliten in vielen Mikroorganismen, ist in ihren Einzelheiten nicht geklärt, obwohl sie bereits mehrfach zum Gegenstand wissenschaftlicher Untersuchungen gemacht worden ist. Dies liegt zum Teil darin begründet, dass die Struktur der an diesem Biosyntheseweg beteiligten Enzyme bisher nicht bestimmt wurde. Ziel der vorliegenden Arbeit ist die Strukturaufklärung von PhzA, B und G aus dem Phenazin-Biosyntheseoperon von *Pseudomonas fluorescens* 2-79 sowie eine Analyse der Intermediate, die während der Biosynthese von Phenazin-1-Carbonsäure (PCA) gebildet werden.

Im Verlauf dieser Arbeit wurden die Strukturen von PhzA und PhzG in Apo-Form und im Komplex mit PCA bestimmt und analysiert. Zudem wurde die Struktur eines zu PhzA/B homologen Enzyms, BcepA aus *Burkholderia cepacia*, ebenfalls in der Apo-Form und im Komplex mit einem synthetischen Inhibitor aufgeklärt.

Die Strukturuntersuchungen an PhzA und BcepA haben interessante Eigenschaften dieser beiden Enzyme hervorgebracht. Sie gehören zur Faltungsfamilie der Ketosteroidisomerasen, deren Struktur sich durch eine α/β-Topologie auszeichnet. BcepA ist dabei der erste Vertreter dieser Familie, bei dem eine „Armaustausch-Dimerisierung“ beobachtet wird. Unter den Familienmitgliedern finden sich Proteine mit unterschiedlichsten Funktion, z.B. Kerntransportfaktoren, Isomerasen, Hydrolasen oder Oxidasen. Dies deutet auf eine divergente Evolution innerhalb der Faltungsfamilie hin und ist der Grund dafür, dass es nicht möglich ist, PhzA bzw. BcepA ausschließlich mit Kenntnis ihrer Struktur funktionell einzuordnen.

Das Enzym PhzG besitzt eindeutige Sequenzverwandtschaft mit Pyridoxamin-5’-Phosphatoxidase aus *E. coli*, einem FMN-abhängigen Protein. Diese Verwandtschaft konnte durch die Aufklärung der Struktur von PhzG bestätigt werden. Die Struktur des Enzyms im Komplex mit PCA liefert zudem einen Hinweis darauf, dass PhzG als eine terminale Oxidase bei der Phenazinbiosynthese fungiert.

Um einen über die Strukturen von PhzA und PhzG hinausgehenden Einblick in die Biosynthese von Phenazinen zu erhalten, wurden weitergehende Experimente mit einem bakteriellen 2-Hybrid-System, APCI-Massenspektrometrie und einer Clark-Sauerstoffelektrode durchgeführt. Eine quantitative APCI-MS-Methode wurde

angewendet, um Intermediate des Phenazinbiosyntheseweges aufzuspüren und ihren Auf- bzw. Abbau zu beobachten. So wurden zwei Moleküle mit einem Molekulargewicht von 274 bzw. 228 Da entdeckt. Außerdem konnte so die Reihenfolge festgestellt werden, mit der die Enzyme bei der Phenazinbiosynthese wirken, nämlich als PhzE, D, F, B, G und A, wobei für letzteres Enzym jedoch kein eindeutiger Effekt festgestellt werden konnte. Dies ist insofern überraschend, als das PhzB, das zu 70 % identisch zu PhzA ist, durch APCI-MS und Sauerstoffmessungen mit der Clark-Elektrode als Synthase für das Intermediat mit dem Molekulargewicht 274 identifiziert werden konnte. PhzG agiert als Oxidase des Intermediats mit Molekulargewicht 228 („teilweise aromatisiertes PCA“) zum Endprodukt des Phenazinbiosyntheseweges in *P. fluorescens*, PCA.

Im Rahmen dieser Arbeit wurde zum ersten Mal die Phenazinbiosynthese von *Burkholderia cepacia* untersucht. BcepA, wie PhzB, beschleunigt den Sauerstoffverbrauch bei der enzymkatalysierten Synthese von Phenazinen und könnte demnach ebenfalls eine Synthase für das Intermediat mit Molekulargewicht 274 sein. Weitergehende Studien sind nötig, um mehr Einblicke in den Phenazinbiosyntheseweg dieses Organismus zu erhalten.

Materials and Methods

Read the directions and directly you will be
directed in the right direction.
- Doorknob (Alice in wonderland, Lewis Carroll)

9.1 Materials

9.1.1 Chemicals & Enzymes

Chemicals from the following companies were used:
Amersham-Pharmacia (Freiburg), Baker (Deventer, Holland), Fluka (Neu-Ulm), GERBU (Gaiberg), Merck (Darmstadt), Pharma-Waldhof (Düsseldorf), Qiagen (Hilden), Roche (Mannheim), Roth (Karlsruhe), Serva (Heidelberg) und Sigma-Aldrich (Deisenhofen).
All restriction and DNA modifying enzymes were from Fermentas (St.Leon-Rot) unless otherwise stated.

9.1.2 Materials

Sterile filter FP 030/3 0,2 µm and ME 24 0,2 µm (Schleicher and Schuell, Dassel) Ultrafiltration device VIVASPIN 10, 30 (Vivascience (Lincoln, USA)
0.2µM and 0.45µM sterile filters (Schleicher and Schuell)
Nickel-NTA-Agarose Superflow (Qiagen, Hilden)
Superdex 75 and 200 (Amersham Pharmacia, Freiburg)
Linbro 24 flat bottom well tissue culture plate (ICN Biomedicals, Inc, Ohio)
Gernier™ 96-well flat bottom sitting-drop crystallisation plates.

9.1.3 Kits

QIAprep Spin Miniprep Kit Qiagen (Hilden)
QIAquick Gel Extraction Kit Qiagen (Hilden)
BigDye Terminator Sequencing Kit Applied Biosystems (Langen)
Perfect 1kb-DNA standard Invitrogen (Karlsruhe)
Wide Range, SDS7 protein marker Sigma (Deisenhofen)
1Kb ladder for Agarose gels (Gibco)
Crystal Screen, 2 ™, Index Screen ™ (Hampton Research, California, USA)
Nextal Classic, PEG ion, (Nextal,)

Äkta Prime FPLC system was used throughout for chromatography.

9.1.4 Microorganisms

E. coli BL21 (DE3)	*B, F-, hsdSB (rB-, mB-), gal, dcm, ompT, λ(DE3)* (Novagen)
Rosetta pLysS	containing the tRNA genes *argU*, *argW*, *ileX*, *glyT*, *leuW*, *proL, metT, thrT, tyrU, and thru* (Novagen)
XL1 Blue	*recA1, endA1*, *gyrA96*, thi-1, *hsdR17*, *supE44*, *relA1*, *lac* [F´, *proAB*, *lacIq*ZΔM15, *Tn10* (Tetr)] (Stratagene)
BTH101	F^-, cya^-99, araD139, galE15, galK16, rpsL1 (Str^r), hsdR2, mcrA1, mrcB1 (Bacterial two-hybrid kit)

9.1.5 Plasmid vectors

pET 15b, pET 3a (Novagen). pET 15b is a plasmid containing the 6x Histidine sequence for use in Nickel chromatography for protein purification.

9.1.6 Media and antibiotics

Luria-Bertani (LB): 10 g l^{-1} Bactotryptone, 10 g l^{-1} NaCl, 5 mM NaOH, 5 g l^{-1} yeast extract.

Terrific Broth (TB): 12 g l^{-1} Bactotryptone, 24 g l^{-1} Bacto-yeast-extract, 4 g l^{-1} glycerol, 17 mM KH_2PO4, 72 mM K_2HPO4.

SeMet - Medium: Prepared according to (Van Duyne et al., 1993). It is a minimal medium excluding methionine but containing high concentrations (250 mg l^{-1}) of the amino acids V, L, I, K, T, F and 50 mg/ml of the other amino acids to aid suppression of bacterial methionine biosynthesis.

Antibiotics from GERBU (Gaiberg) were used in following concentrations:
Ampicillin 125 mg l^{-1} or 100 mg l^{-1}; Chloramphenicol 34 mg l^{-1};
Kanamycin 50 mg l^{-1}

2.1.7 Buffers

Deionised and sterile water (Millipore ^{TM}) was used for all buffer preparation. pH values were adjusted at room temperature unless otherwise stated. The composition of buffers used is tabulated overleaf.

Method	Buffer composition
Nickel affinity chromatography	Buffer A 50 mM Na_2HPO_4, 300 mM NaCl (pH 8.0). Buffer B Buffer A with 1M Imidazole, pH 8.0.
Gel filtration chromatography	20 mM Tris/HCL (pH 8.0), 150 mM NaCl
ITC measurements	20 mM Tris/HCL (pH 8.0), 150 mM NaCl (+/- 10% glycerol)
ESI-MS/APCI-MS measurements	50 mM Tris/HCL (pH 7.5)

Table 9.1: Buffers used during the course of this work.

9.2 Molecular Biology Methods

9.2.1 Agarose gels

Agarose gels were prepared and run according to standard procedures (Sambrook, 1989).

9.2.2 Isolation of plasmid DNA

DNA purified by agarose gel electrophoresis was isolated using QIAprep Spin Miniprep Kit from Qiagen (Hilden) according to the manufacturer's protocol.

9.2.3 Polymerase chain reaction (PCR)

Amplification of DNA fragments was carried out using *Pfu* polymerase or *Pwo* polymerase according to standard procedures (Sambrook, 1989). Fragments were digested (see 9.2.4) and purified using the QIAquick Gel Extraction Kit according to the manufacturer's protocol.

9.2.4 DNA digestion

DNA was digested using enzymes from Fermentas, according to the manufacturer's protocol.

9.2.5 Preparation of Competent cells

Competent expression (Rosetta PLys-S) or amplification (XL1-Blue) cells were prepared as follows: 100ml LB media was inoculated with a single colony of *Escherichia coli* cells and grown overnight at 37^{o}C with continuous shaking. 5 ml culture from this preculture was diluted with 500 ml LB media and grown to an optical density (OD_{600}) of 0.6. The cells were harvested by

centrifugation at 3000×g for 15 minutes. The pellet was washed with 500 ml sterile H_2O at 4^oC, twice, and then with 10 ml 10% glycerol and recentrifuged. The resulting cell pellet was resuspended in approximately 2.5 ml GYT media, aliquoted into 75 µl portions, flash frozen in liquid nitrogen and stored at -80^oC till further use.

9.2.6 Ligation

Vector (digested, linearised plasmid) and insert DNA were quantified using agarose gels using digested λ-marker as a reference. 10 ng of vector was ligated with a six fold molar excess of insert by overnight incubation at 16 °C using T4 ligase according to the manufacturer's protocol.

9.2.7 Transformation

The heat shock method was used according to the standard protocol (Sambrook, 1989).

9.2.8 Glycerol Stocks

30% glycerol was added to a bacterial preculture and the stock labelled and stored at -80°C.

9.2.9 DNA sequencing

DNA sequencing was carried out according to Sanger et al. (1992) using the Big Dye terminator kit. A sequencing reaction contained 500 ng DNA, 4 µl terminator mix, 3.2 pmol sequencing primer in a volume of 10 µl. Sequencing PCR and DNA precipitation was carried out according to manufacturer's protocol. Analysis of the sequencing products was done in-house on an ABI PRISM 3700 DNA analyzer.

9.2.10 Cloning of phzA, bcepA, B and G.

The gene encoding enzymes PhzA, BcepA, B and G investigated in this work, were cloned into the pET15b plasmid (Novagen). This plasmid contains N-terminal 6xHis-tag and the genes were inserted into the circular DNA of the plasmid by using the restriction enzymes sites of NdeI and BamHI, and the following primers:

phzA

phzA-up 5'-ACT GCA TAT GCC CGG TTC G-3'

phzA-low 5'-CTA GGA TCC ATG TTC AAT CTC CAA T-3'

BcepA

phzABcep_up 5' TTT TTC ATA TGT CAG ACG TCG AAT CC 3'

phzABcep_low 5' TTT TTG GAT CCA TTG GGT ATG CGT TAG 3'

phzB

phzB-up 5'-TTT CAT ATG CCT GAT AGC ACA GTG-3'

phzB-low 5'-TTT GGA TCC ATG ATG CGA TTG CT-3'

phzG

phzG-up 5' TTT TCA TAT GAA CGG CTC AAT ACA AGG 3'

phzG-low 5' TTT GGA TCC ACA TTT GAC CGA GAT GG 3'

These clones were transformed into Rosetta PLysS competent cells (Novagen). Initial expression tests were carried out to determine the optimal conditions of growth and expression.

9.3 Biochemical Methods

9.3.1 Growth and harvest of protein expressing bacteria

All constructs were transformed into E.*coli Rosseta-Plys-S* cells. The transformed cells were grown in a 37°C shaker at 180 rpm to an OD_{600} of 0.6. Proteins were expressed as 6xHis fusion proteins upon overnight induction with 1 mM Isopropyl-β-D-thiogalactoside at 20°C where the proteins were most soluble. After incubation, the induced cells were pelleted at 1500 g for 20 min, 4°C. The pellet was washed in buffer A and stored at –80°C.

To investigate optimal conditions of growth and protein solubility, all proteins were initially expressed under varying temperature conditions (ranging from 18°C to 30°C), different IPTG concentrations (50 µM to 1 mM) and varying times of induction (4h to overnight).

9.3.2 Protein purification (Ni-NTA chromatography

The frozen cell pellet was resuspended in ice-cold buffer A containing 1 mM protease inhibitor PMSF (Phenylmethylsulfonyl fluoride). The cells were then disrupted in a microfluidiser (Microfluidics Corporation, USA) at a pressure of 600 kPa. The soluble fraction was cleared by ultracentrifugation (150000 g, 45 min, 277 K) and loaded onto a nickel-chelation column (Ni-NTA, Quiagen) equilibrated in buffer A. After washing with a few column volumes with buffer A, the bound protein was eluted on a 10-500 mM Imidazole gradient. Protein containing fractions were identified by analysis on 15% SDS-PAGE and pooled.

9.3.3 SDS-PAGE

Separation of proteins of different molecular weight was performed according to Laemmli (1970) using denaturing 15% SDS-polyacrylamide gel electrophoresis (SDS-PAGE) according to standard protocol (Sambrook, 1989)

9.3.4 Removal of 6xHis-tag and Size exclusion chromatography

Thrombin at a concentration of 1U/20 mg protein was added to the protein obtained at the conclusion of Ni-chromatography and dialysed overnight against gel filtration buffer.

The cleaved protein was then subjected to size exclusion chromatography as a further purification procedure to obtain pure protein for crystallisation purposes. The protein was concentrated prior to loading on a pre-equilibrated Superdex 75 size exclusion column (Amersham Pharmacia Biotech). FPLC was then carried out at a flow-rate of 2 ml/min and 3 ml fractions were collected. The fractions containing pure protein were identified using SDS-PAGE and pooled.

9.3.5 Determination of protein concentration

Protein concentration was determined according to Bradford (1976) using the Biorad protein assay solution. This solution was calibrated prior to use by bovine serum albumin (BSA).

9.3.6 Final concentration and storage of protein

On conclusion of the purification protocol, protein was concentrated using an Amicon chamber with a 10 kDa cut off membrane. The concentrated protein was then aliquoted to 50-100 µl fractions, flash frozen and stored at -80°C.

9.3.7 Seleno-L-methionine labelled protein

For the purpose of structural solution using SAD (Single-wavelength Anomalous Diffraction)/MAD (Multi-wavelength Anomalous Diffraction), inhibition of methionine biosynthesis in synthetic media (Doublie, 1978) was undertaken to incorporate seleno-L-methionine in the protein. *E. coli* Rosetta pLysS cells bearing the pET-15b plasmid incorporating 6xHis-tagged protein were grown overnight in LB media supplemented with ampicillin and chloramphenicol. The cells were then pelleted and resuspended in M9 media containing 50 μg ml^{-1} ampicillin and 17 μg ml^{-1} chloramphenicol. This culture was grown at 37°C to OD_{600} of 0.8 and the amino acids - lysine, phenylalanine and threonine (to a concentration of 100 mg l^{-1}) and isoleucine, leucine and valine (50 mg l^{-1}) were added. The culture was then supplemented with 60 mg l^{-1} seleno-L-methionine and allowed to cool to 20°C before induction with 1 mM IPTG and incubated at 20 °C overnight, with continuous shaking. The protein purification protocol remained identical to that for the native protein. Incorporation of selenium was confirmed by MALDI-TOF mass spectrometry.

9.3.8 Bacterial two hybrid system

The Bacterial two hybrid system developed by Karimova *et al.* was used in this work to explore the interactions between the seven proteins of the phenazine biosynthesis operon.

The bacterial two hybrid system is based on the reconstitution of the artificial cAMP signal transduction pathway in an *Escherichia coli* adenylate cyclase-deficient strain (the *cya*$^-$ strain). It exploits the fact that the catalytic domain of adenylate cyclase from *Bordutella pertussis* consists of two complementary fragments, T18 and T25 which are inactive when physically separated. Thus, when two interacting proteins are fused to these two fragments, they come in physical proximity of each other, resulting in a functional complementation and

induction of cAMP synthesis. The cAMP so produced binds to CAP (Catabolite Activator Protein) forming a pleotropic gene transcription regulator cAMP/CAP in *E.coli* (Figure 9.1). This complex then induces expression of the 'lac' and 'mal' operons involved in lactose and maltose metabolism respectively. Thus the bacteria become capable of utilizing lactose or maltose as unique carbon source and can easily distinguished on indicator or selective agar. MacConkey agar media was the indicator agar used for this work. MacConkey media makes use of pH differences between colonies metabolizing different carbohydrates. The *cya*$^{-}$ strain unable to utilize either lactose or maltose form pink-white colonies while the *cya*$^{+}$ colonies (with reconstituted adenylate cyclase signalling due to protein interaction) form red colonies.

The complementation of the seven enzymes was tested with each other making for a set of 51 possible combinations, including the negative and positive controls. For controls, plasmids provided with this kit were used.

The genes of all seven enzymes were cloned into both pKT25 plasmid and the pUT18 plasmid using the restriction sites of XbaI and BamHI. The primers used for this purpose are mentioned below.

1) Gene: phzA
Upper primer: phzA-Xba
5' TT TTT CTA GAG CCC GGT TCG CTT TCA 3'
Lower primer: phzA_ BamHI
5' CTA GGA TCC ATG TTC AAT CTC CAA T 3'

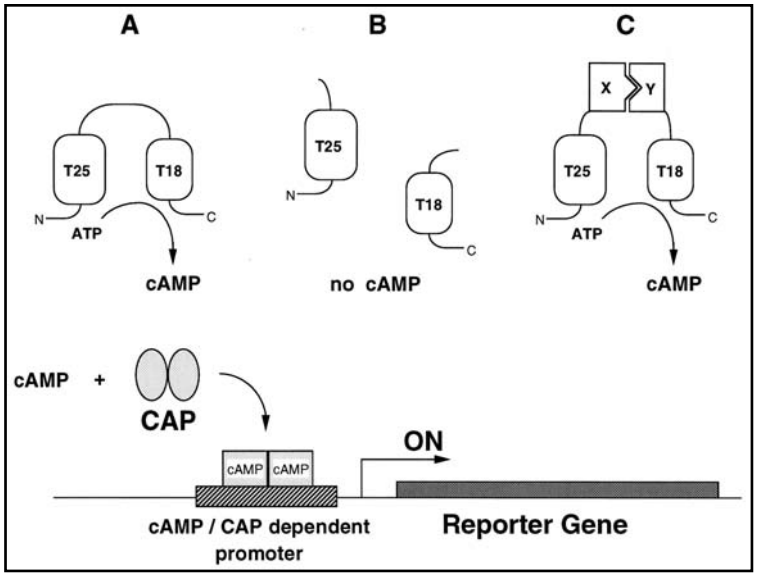

Figure 9.1: Schematic depiction of the bacterial two hybrid system (Karimova *et.al.*1998,)

2) Gene: phzB
Upper primer: phzB-Xba
5' TT TTT CTA GAG CCT GAT AGC ACA GTG 3'
Lower primer: phzB_BamHI
5' TTT GGA TCC ATG ATG CGA TTG CT 3'

3) Gene: phzC
Upper primer: phzC-Xba
5' AA TTT CTA GAG GAA GAC TTA CTG AAA C 3'
Lower primer: phzC_low (BamHI)
5' ACA GGA TCC AGT CAA AGG GAA AC 3'

4) Gene: phzD
Upper primer: phzD-Xba
5' TT TTT CTA GAG ACC GGC ATT CCA TCG 3'

Lower primer: phzD_BamHI
5' TTA GGA TCC TCA TAG CAC CAC CTC A 3'

5) Gene: phzE
Primer: phzE-Xba
5' TT TTT CTA GAG AGC CAA GCC GCC GCC 3'
Lower primer: phzE_ BamHI
5' TTT GGA TCC GTA GTT GTG CAT GGT 3'

6) Gene: phzF
Upper primer: phzF-Xba
5' TT TTT CTA GAG CAC AAC TAC GTC ATT 3'
Lower primer: phzF_BamHI
5' TTT GGA TCC TTG TAT TGA GCC GTT 3'

7) Gene: phzG
Upper primer: phzG-Xba
5' TT TTT CTA GAG AAC GGC TCA ATA CAA G 3'
Lower primer: phzG-BamHI
5' TTT GGA TCC ACA TTT GAC CGA GAT GG 3'

Varying combinations of the pKT25-phz-gene and pUT18-phz-gene were transformed simultaneously into *E.coli* BTH101 cells, which can accept two plasmids. The transformed cells were then grown at 37 °C for one hour, plated on agar plates and incubated overnight. A 5 ml culture was grown from single colonies by incubation in LB media supplemented with kanamycin (50 mg l^{-1}) And ampicillin (100 mg l^{-1}). Glycerol stocks were prepared from 1 ml of this culture and stored at -80 °C till further use.

For analysis of complementation and hence interaction between the enzymes, a swab of cells from the frozen glycerol stocks were used to plate on a nutrient agar plate containing the suitable antibiotics. A single colony from this plate was picked and streaked on the MacConkey agar and allowed to grow at 20 °C overnight. The colouration of the colonies (pink-white/red) was then observed and noted.

9.3.10 Liquid β-Galactosidase activity assay.

This assay was used to quantify the protein-protein interaction studied with the bacterial two hybrid system. The β-Galactosidase activity assay was performed as per the protocol by McDonald (Methods in Molecular Biology, Humana Press, 1998).

9.3.11 High Pressure Liquid Chromatography (HPLC)

The HPLC separations were run under following conditions: Agilent 1100 HPLC equipped with degasser, auto-sampler, two binary pumps, diode array detector connected on-line to a Finnigan LCQ Advantage mass spectrometer; C18 Nautilus column, 250x4 mm, 5 µm, MN, Germany; flow rate 1 ml/min; solvent A: 0.1 % formic acid in water, solvent B 0.1 % formic acid in acetonitrile; gradient: 0-1 min 0 % B, 1-15 min 0-50 % B 15-25 min 50-100 % B, re-equilibration of the column in 5 min; positive ion mode detection.

9.3.12 Mass Spectroscopy

Mass spectrometry is an analytical tool used for measuring the Molecular Weight (Mw) of samples. The following mass spectroscopic instruments and methods were used in this work.

9.3.12.1 MALDI-TOF MS

In **M**atrix **A**ssisted **L**aser **D**esorption **I**onisation **T**ime of **F**light **M**ass **S**pectroscopy (MALDI-TOF MS) analysis, the analyte is first co-crystallized with a large molar excess of a matrix compound, usually a UV-absorbing weak organic acid which absorbs efficiently at the laser wavelength. The matrix allows the energy from the laser to be dissipated and also assists with the ionisation of sample molecules

through electron transfer and chemical processes. This analyte-matrix mixture thus results in the vaporization of the matrix which carries the analyte with it. The matrix therefore plays a key role by strongly absorbing the laser light energy and causes, indirectly, the analyte to vaporize. It also serves as a proton donor and receptor, acting to ionize the analyte in both positive and negative ionization modes, respectively. The correct preparation and deposition of MALDI samples onto the sample plate is thus critical to the success of the method.

MALDI-TOF MS was used to confirm the molecular weight of proteins. Protein solution was diluted with water to an approximate concentration of 10 nanograms and mixed 1:1 with the selected matrix (for proteins > 10 kDa: saturated sinapinic acid in acetonitrile and 0.2% TFA). This solution was allowed to dry on a special sample plate and data acquired on a Voyager DE Pro (Applied Biosystems).

9.3.12.2 ESI-MS

Electrospray ionisation (ESI) as the name suggests, involves the spraying of solvent to be analysed (usually an aqueous or aqueous + organic solvent system), which is first passed through a needle held at a high voltage (typically 4-5 kV) relative to some counter electrode. The spray emerges as a fine mist of droplets at the needle tip and these droplets possess a net positive or a net negative charge, determined by the polarity of the needle and are attracted to the entrance of the mass analyser. The droplets emerge from what is known as the ‘Taylor cone’ (Figure 9.1) is formed by the elongation of the electrolyte solution at the needle tip as like-charged ions, which are repelled from the needle. The application of a ‘counter-current’ of dry gas passing in a direction opposite to that of the needle flow aids droplet evaporation and leads to the ionisation of the molecules present in the solvent. As the droplets evaporate, the ions within this droplet move closer together. Eventually, sufficient Coulombic repulsive forces build up, which help the ions to overcome surface tension forces, resulting in the production of smaller droplets that continue to undergo the same process. Finally, solvent-

free ions are produced, that are passed through the mass analyser and detected (Figure 9.1).

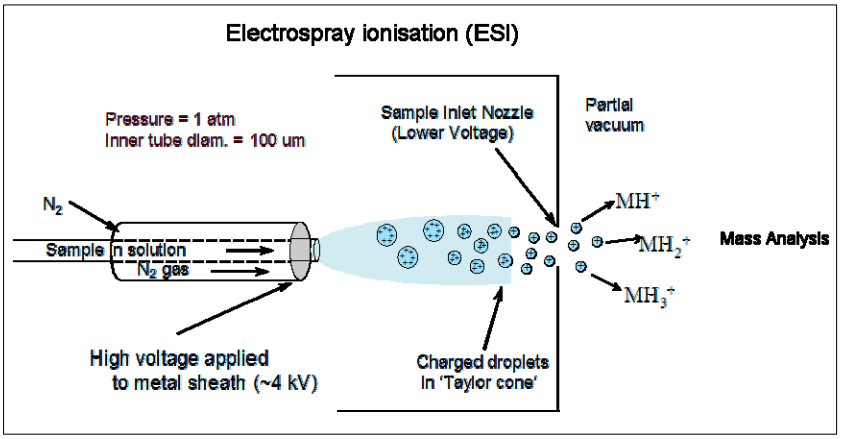

Figure 9.1: Schematic diagram of ESI-MS

Electrospray ionisation mass spectroscopy was used to follow the reaction catalysed by the enzymes PhzA, B, F and G in the presence of the substrate, DHHA. In a glass vial (Agilent Technologies) 1 mM DHHA in Tris buffered (50 mM; pH 8.5) solution was prepared and 10 µl of this solution injected directly into the spectrometer and analysed to get a time zero (t=0; blank reading). After this, 1 µM of PhzF was added to initiate the reaction i.e. the conversion of DHHA, along with the enzyme/s for which the reaction was to be analysed. A spectrum was recorded every 10 minutes for a period of 260 m. The manufacturer's software 'Xcalibur' (Voyager Mass Spectroscopy Systems) was used for data analysis and Excel (Microsoft) for representation of the data.

9.3.12.3 APCI-MS

In a technique similar to electrospray ionization (ESI), liquid effluent is introduced directly into the source of an Atmospheric Pressure Chemical Ionization (APCI) mass spectrometer. The APCI source contains a heated vaporizer which facilitates rapid desolvation/vaporization of the droplets. Vaporized sample molecules are carried through an ion-molecule reaction region at atmospheric pressure. The ionization occurs by a corona discharge and is mediated by chemical processes and hence is termed chemical ionisation. The method of ionisation is where APCI differs from ESI. This mode of

chemical ionisation is related to electron impact method of ESI, except that ionisation of a reagent gas rather than the sample molecule itself occurs first. This is followed by the transfer of charge to the sample molecule by a chemical process. One of the most common reagent gases is methane. When subjected to electron impact, a molecule of methane can ionise to form CH_4^+ by electron loss. This ion can react with a second molecule of methane, to form CH_5^+, as shown in the equation below

$$CH_4^+ + CH_4 \longrightarrow CH_5^+ + CH_3$$

The ion CH_5^+ is an efficient proton donor, so that a sample molecule 'S' also present in the ionisation chamber can be ionised according to the following equation:

$$S + CH_5^+ \longrightarrow [S + H]^+ + CH_4$$

To prevent the direct ionisation of the molecule 'S', methane is present in the ion source at a much higher concentration than the sample. Because of this, a chemical ionisation source operates at a much higher pressure (0.1 to 1 Pa), thus the name of this method, Atmospheric Pressure Chemical Ionisation (APCI). The main advantages of using APCI include the fact that gas-phase ionization in APCI is more effective than ESI for analyzing less-polar species, it offers an excellent LC/MS (liquid chromatography/mass spectroscopy) interface and is readily compatible with MS/MS methods, which was of importance while analysing the nature of the various intermediates formed during the course of this investigation of the phenazine biosynthesis pathway.

APCI was coupled to High Pressure liquid Chromatography (HPLC) to follow the reaction catalysed by PhzA, B, F and G and to detect the various intermediates formed as a part of the reaction by mass analysis. Samples prepared in a manner identical to those for ESI-MS measurement were supplemented with marker molecule caffeine (concentration 1 mM) and a spectrum was collected with 1 µl of injected sample every 8 m for a total of 360 min. An 'Atlantis' (Waters)

column was used for HPLC with buffers and flow-rate identical to those described in section 9.3.11. The use of HPLC allowed better separation of molecules and the inclusion of caffeine allowed a comparison of the various spectra obtained during the course of this work. Spectral analysis was done using the 'XCalibur' program and data analysis and representation using Excel (Microsoft).

9.3.13 Measurements with Clarke's Electrode.

The Clarke's electrode was employed to measure the speed of oxygen consumption during the reaction consisting of the conversion of DHHA to PCA, and to examine the effect of various enzymes on the same. The apparatus used for this purpose is depicted in the figure below:

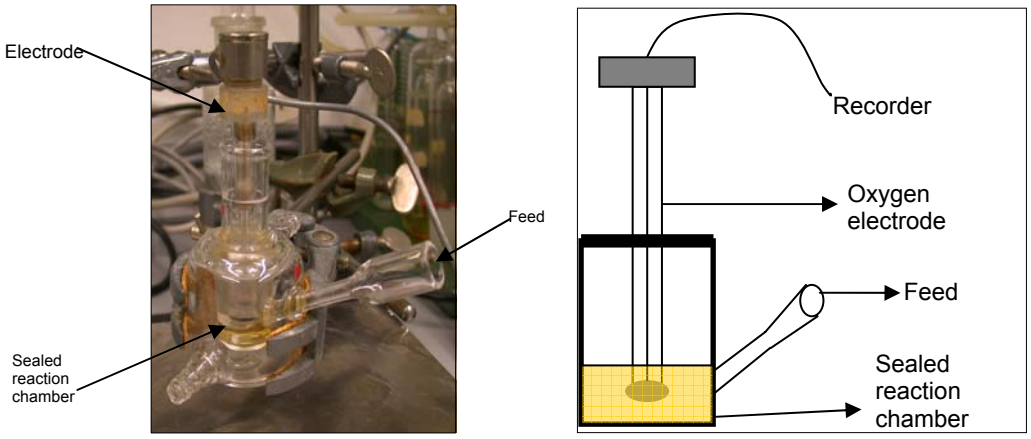

Figure 9.2: The set-up of the apparatus for oxygen measurements with the Clarke's electrode; Shown both as photograph and schematically.

At the initiation of the measurements, the electrode was flushed with nitrogen, to calibrate the electrode. 1 mM DHHA dissolved in 50 mM Tris buffer (pH 7.5) was then added and the chamber sealed. After this, enzymes dissolved in buffer were introduced into the chamber using a syringe and in various combinations and concentrations. The concentration of PhzF was kept constant at 1 µM for all readings. The chamber was then sealed again, allowed to stabilise and the readings recorded.

9.4 Crystallographic methods

The soluble state of macromolecules is characterized by randomness of motion and orientation. Crystallisation induces the molecule to adopt one or

few identical orientations, forming a three dimensional, orderly array of molecules held together by non-covalent interactions - the crystalline state.

Protein crystallisation can be achieved by a slow, controlled precipitation from aqueous solution under non-denaturing conditions. This is mainly a trial and error procedure in which impurities, crystallisation nuclei and other unknown factors all play a role. As a rule of thumb, however, there are a few pre-requisites of protein crystallisation:

- Protein purity – It is imperative to start with a highly (97-99%) pure protein.
- Starting environment of the protein – The protein should be dissolved in a suitable solution of either buffer or water with/without organic solvents, so that it is stable and does not form precipitates while in solution.
- Initiation of supersaturation – A gradual increase in the level of saturation is required to induce proteins to separate from solution and to start producing a solid (crystalline) state.

Supersaturation is thus the key to crystallisation and can be achieved with careful addition of precipitants in the form of salts and/or water soluble polymers like polyethylene glycol (PEGs) etc. (Figure 9.2). In practice, various pre-formulated

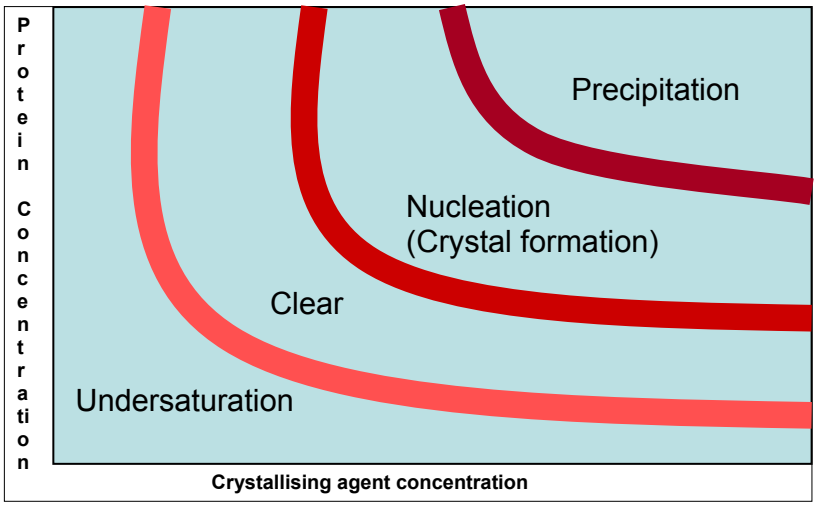

Figure 9.3: Typical solubility curve for a protein as a function of precipitant concentration.

combinations of precipitants at a range of pHs and concentrations are now available and these are used as initial screens for protein crystallisation.

There are various techniques of crystallisation, like batch crystallisation, dialysis, vapour-diffusion and liquid-liquid diffusion.

9.4.1 Crystallisation by Vapour-diffusion.

Vapour diffusion is the most widely used method of crystallisation and was also employed in this work. In this method, a drop containing protein, precipitant and buffer is equilibrated against a reservoir of precipitant in a sealed container. Due to the uneven concentration of precipitants in the drop and reservoir, equilibration initiates until the vapour pressure in the drop equals that of the reservoir. During this process, the concentration of all constituents in the drop increases, which in turns leads to nucleation in the drop. Once nucleation is achieved, actual crystal growth can begin. The variations of vapour-diffusion used in this work are the 'hanging drop' and 'sitting drop' methods (Figure 9.3).

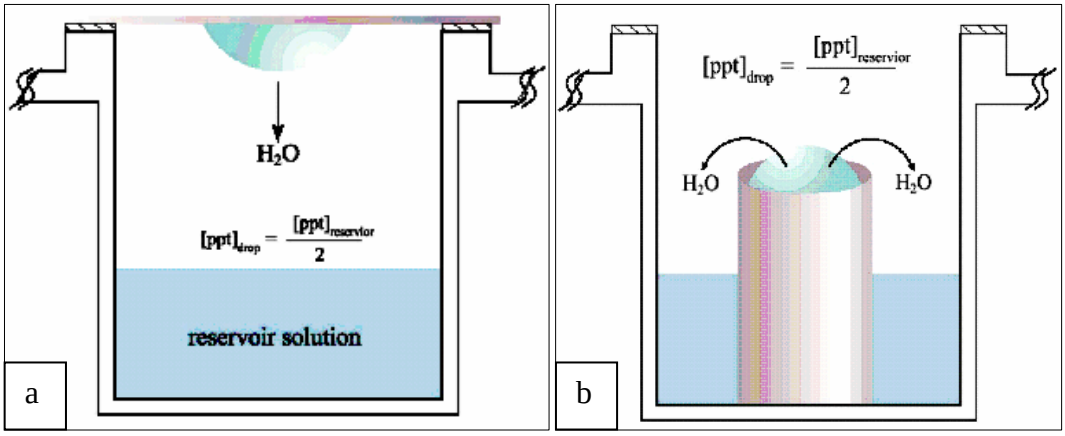

Figure 9.4: A schematic drawing of the hanging drop (a) and sitting drop (b) method. (From Rhodes, G 2001)

Crystallisation trials for all proteins were initiated using Crystal Screen, Crystal Screen 2 and Index Screen from Hampton Research, Nextal Classic from Nextal, by the sitting drop vapour diffusion method. Crystallisation robot 'Mosquito' (TTP Labtech, UK) was used to setup crystallization using the sitting drop method in 96 well plates (Garnier). The reservoir was filled with 70 µl screen solution and drops contained 70 nl protein mixed with 70 nl of the screen solution. These plates were then sealed and incubated at 20° C. Conditions yielding crystals in 96 well plates were further optimised in Linbro™ cell culture plates with 500 µl of reservoir solution and drop size

varying from 2-4 µl. Hanging drop method of crystallisation was used in this step.

9.4.2 Crystal Soaking

Macromolecular crystals typically have a high solvent content (27% to 95%; Stout, 1989). This solvent content can be classified in two parts, the 'bound solvent' (typically 10%) which is tightly associated with the protein and occupies well-defined positions in the crystal structure. This solvent forms well-defined channels through the crystals and allows the diffusion of small molecules. Soaking experiments are done by adding, inhibitors, activators, substrates, products, cryo-protectants and heavy atoms to the bathing solutions.

PhzG-PCA complex crystals were obtained by this method of crystal soaking. Crystals of native PhzG were transferred in mother liquor containing no FMN for 24 hrs, to ensure the removal of excess FMN. Thereafter, the crystals were transferred to a fresh drop of mother liquor containing 10 mM PCA. The crystals were tested after being allowed to soak in this solution for at least 24h.

9.3.1 PhzA

The initial screening of PhzA yielded long needle shaped crystals which appeared in 0.8 M sodium/potassium tartrate and 0.1 M sodium HEPES pH 7.5. These crystals were tested on the home source and found to diffract upto 6.9 Å. They were sent to the synchrotron light source and a dataset of 6 Å was collected. However, the very long axis of the asymmetric unit of the crystals interfered with optimal data collection and further work on this crystal form was stopped. Further screening yielded another crystal form which appeared in the drop containing 1.6 M magnesium sulphate and 0.1 M MES in the pH range 6.0-6.5. This crystal form was used for data collection and structure elucidation.

9.3.2 PhzB

The initial screening of PhzB yielded two conditions with micro-crystals, but despite repeated efforts, these micro-crystals could not be optimized to better

crystals. Crystallisation trials were repeated in the presence of a variety of ligands and also without the removal of the 6xHis tag, however, no diffraction quality crystals were obtained.

9.3.3 BcepA

The screening solution from Nextal PEG setup containing 0.2 M Ammonium acetate and 20% (w/v) PEG 3350 yielded flat triangular crystals which were used for data collection and structure determination.

9.3.4 PhzG

Initial screening PhzG was performed both in the presence (10 mM) and absence of FMN. The condition of 0.2 M ammonium sulfate, 0.1 M Bis-Tris (pH 6.5), 25% PEG-3350 and 10 mM FMN yielded yellow-coloured crystals of a good size and quality.

9.3.5 Complex of PhzG with PCA

The crystals of native PhzG were transferred into mother liquor containing no FMN and allowed to soak for at least 24 h. This step ensured washing away all extra FMN from proximity of the crystal. After this washing step, the crystals were transferred into a mother liquor solution supplemented with 10 mM phenazine-1-carboxylic acid (PCA) or PDC and allowed to incubate at 20°C for 24 h. The crystals tested for the presence of bound PCA/PDC at the home source were used for data collection at the synchrotron. All crystals of Seleno-L-methionine labeled protein were obtained from the same conditions as those for the native protein.

9.4.3 Cryocrystallography

Protein crystals undergo radiation damage when exposed to x-rays. The high energy x-ray photons cause the formation of solvent-derived free radicals in the crystal which lead to subsequent chemical degradation of protein molecules and thus a gradual destruction of crystalline order. Thus several crystals would be needed for collecting a complete dataset at room temperature.

However, it has been found that radiation damage is arrested to an appreciable degree when the crystals are flash cooled, e.g. by liquid nitrogen,

to very low temperatures, thus enabling a complete data set to be collected from a single crystal. The low temperatures inhibit the heating of the crystals when exposed to x-rays and thus slows-down the process of radical formation. For cryocrystallography, crystals are soaked in crystallisation buffer containing cryo-protecting solutions like low freezing point methyl pentanediol (MPD), isopropanol etc., and mounted on a cryo-nylon loop. These crystals are then flash cooled in liquid nitrogen to prevent the formation of ice crystals.
PhzA crystals were cryo-protected by soaking in mother liquor supplemented with sugars (10% xylitol + 10% sucrose). The increase in concentration of PEG (3350) from 20% to 30% in case of BcepA (protein similar to PhzA, from *Burkholderia cepacia*) and from 25% to 30% for PhzG was found to be sufficiently cryoprotecting and the crystals were washed in this solution before flash-freezing in liquid nitrogen.

9.4.4 Data collection

All cryoprotected crystals were initially tested at home source - a copper rotating anode with osmic mirrors (λ = 1.5419 Å, 50 kV, 100 mA, 0.1 mm collimator) at 100 K. Final datasets were then obtained at various synchrotron sources chiefly, the ESRF at Grenoble, France and the SLS at Basel, Switzerland.

9.4.5 Data Processing

The central experiment of data measurement is the positioning of a protein crystal into an x-ray beam, then, through the combination of scattering and interference a diffraction pattern is generated, which is recorded on an x-ray sensitive device. The diffraction experiment is described by Bragg's law, represented in the following equation:

$$n\lambda = 2d \sin\theta$$

Where, d = distance between two parallel reflecting planes of the crystal,

λ = the wavelength and

n = an integral number

In order to collect X-ray diffraction data the crystal is rotated around an axis perpendicular to the beam in steps of 0.5 – 1.0 degree over a range typically of 90°- 180°. One diffraction image per rotation step is recorded and all reflections from all diffraction images ("frames") combine to constitute one complete data set. This raw data is subsequently processed by a series of steps (Rossman et al., 1999), which include,

(i) Indexing. This requires a peak-picking procedure, followed by an analysis of the position of the peaks to determine unit-cell dimensions, Bravais lattice and crystal orientation.

(ii) Pre-refinement of the camera parameters (crystal-to-detector distance, scanning direction relative to oscillation direction, detector tilt away from being normal to the X-ray beam), crystal orientation and effective mosaic spread (actual mosaic spread convoluted with beam divergence).

(iii) Intensity integration by profile fitting, assuming reflection position as calculated from the pre-refined camera and crystal parameters. [Error estimates can be made for each reflection; overlap and overloaded (non-linear response of detector) corrections can be applied; partiality of reflections can be computed.]

(iv) Lorentz and polarization corrections, followed by reduction to a unique asymmetric unit in reciprocal space (this is a Laue-group-dependent step). The reflections then need to be sorted on the basis of their indices and reduced to an asymmetric unit in reciprocal space. This permits ready comparison of symmetry-related reflections which will be adjacent in the reflection list.

(v) Scaling and merging of images onto a common scale.

Data processing was carried out using the program XDS (Kabsch, 1993), which incorporates all of the above-mentioned steps. Other parameters affecting data processing like mosaicity, Matthew's coefficient etc., were also calculated.

The regular repetition of the unit cells is normally interrupted by lattice defects. The diffraction pattern of a crystal is infact the sum of diffraction patterns originating from mosaic blocks with slightly different orientations. Mosaicity values were checked to ensure that the lattice defects are moderate (between 0.2°- 0.5°).

Typically, 30-80% of the unit cell volume is occupied by solvent. Based on the volume of asymmetric unit (determined by x-ray measurements) and molecular weight of the protein one can estimate the number of protein molecules present in a unit cell by calculating Matthew's coefficient (V_M) via the equation:

$$V_M = \frac{V}{Mw \times Z}$$

Where,

V = Volume of the asymmetric unit ($Å^3$) .

Mw = Molecular weight of the protein (k Da).

Z = Number of molecules in the asymmetric unit.

The average Matthew coefficient for a protein crystal is 2.5 $Å^3$/Da which corresponds to a unit cell solvent content of 50% (Matthews, 1968).

9.4.6 Determination of Phases

In a diffraction experiment, the intensities of waves scattered from a plane (denoted by *h, k, and l*) in the crystal are measured. Calculation of electron density at a position (*xyz*) in the unit cell of a crystal requires a summation over all the structure factors (*hkl*) which can be expressed in as:

$$p(xyz) = 1/V \sum |F_{hkl}| \exp(i\alpha_{hkl}) \exp(-2\pi i hx + ky + Iz)$$

where, V = volume of the unit cell.

α_{hkl} = the phase associated with the structure-factor amplitude $|F_{hkl}|$.

F_{hkl} is a periodic function and possesses amplitude, frequency and phase (α_{hkl}). This is diffracted and thus has the same frequency as that of the x-ray source. Moreover, the amplitude of F_{hkl} is proportional to the square root of the reflection intensity (I_{hkl}). Thus structure amplitudes are obtained directly from the measured reflection intensities. However, there is no such direct relationship between amplitudes and phases. Thus, phases are not directly obtainable from a single measurement of reflection intensities. This is known as the phase problem in crystallography.

There are four principle methods for determining the phase angle α and thus solving the phase problem. However, each of these four methods requires a particular type of information to be available beforehand (Table 9.2) (Taylor, 2003). Single wavelength anomalous diffraction method (SAD) has been used for this work.

Phasing Method	Necessary Prior Knowledge
Direct Methods	$\rho \geq 0$, discrete atoms
Molecular Replacement (MR)	Homology model
Isomorphous Replacement (MIR, SIRAS)	Heavy atom substructure
Anomalous Scattering (MAD, SAD)	Anomalous atom substructure

Table 9.2: Phasing methods and information required for application.

Scattering of X-rays is generally considered to be due to valence electrons of atoms which can be considered effectively free. Hence in this case, the scattered

beam differs in phase by exactly 180° with respect to the incident beam. Thus pairs of structure factors F_{hkl} and F_{-h-k-l} (called Friedel pairs) have equal and opposite value, i.e. $|F_{hkl}| = |F_{-h-k-l}|$ and hence it follows that the amplitudes, $\alpha_{hkl} = -\alpha_{-h-k-l}$ (Friedel's law, Friedel, 1913).

However, the inner electrons of the atom are more strongly bound to the nucleus, a fact which is especially true for heavy atoms (e.g. Selenium), which have a high nuclear charge. As a consequence, the phase difference between the incident beam and the beam scattered by such electrons is different (i.e. not exactly 180°). This property is called 'anomalous scattering' and is characterised by Friedel pairs having unequal intensities and different absolute values for phase α (Figure 9.5).

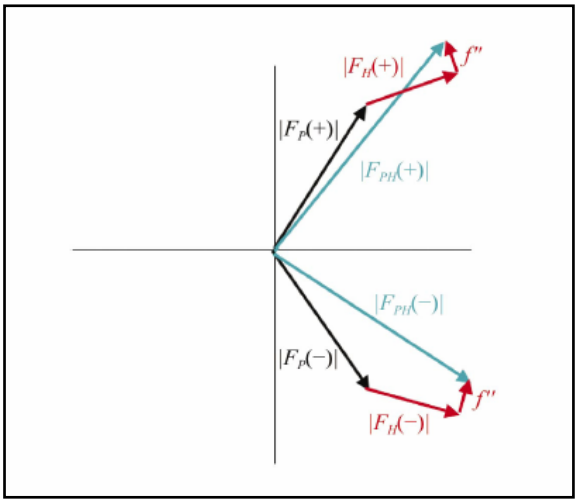

Figure 9.5: Vector diagram for structure factors of normally and anomalously scattering atoms clarifying the breakdown of Friedel's law in the presence of an anomalous scatterer. ($F_{hkl} \neq F_{-h-k-l}$)

The anomalous effect only becomes of importance if the core electrons contribute significantly to the scattering and this only occurs at X-ray wavelengths

close to the absorption edges of the inner electrons. Another characteristic of anomalous diffraction is therefore its wavelength dependence. There will be a sufficiently large contribution to the overall scattering (to be useful for phase determination) only if there is a relatively heavy atom present in the structure and the wavelengths chosen are tuned to the absorption edges of this heavy atom. An example of this is depicted in Figure 9.6 which shows the variation in anomalous scattering at the K edge of Selenium (0.0989 Å)

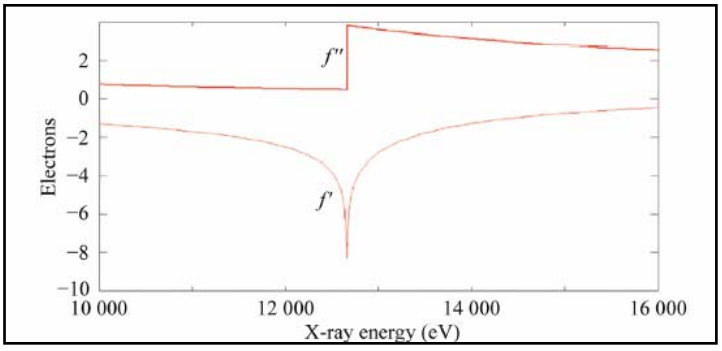

Figure 9.6: Fluorescence scan for detection of peak and inflection of Selenium for MAD/SAD data collection.

Mathematically, anomalous scattering can be expressed by the following equation:

$$|F|^2 = |F_{BA}|^2 + p|F_A|^2 + |F_{BA}| \times |F_A| \times [q \cos(\alpha_{BA} - \alpha_A) + r \sin(\alpha_{BA} - \alpha_A)]$$

with

$$p = \frac{(\Delta f)^2 + (f'')^2}{{f_0}^2},\ q = 2\frac{\Delta f}{f_0} \text{ and } r = 2\frac{f''}{f_0}$$

where, F_A = non-anomalous contribution of the anomalously scattering atoms

F_B = contribution to the structure factor by the non-anomalously scattering atom

F_{BA} = the complete non-anomalous part

α_A = phase angle of vector F_A

α_{BA} = phase angle of F_{BA}

Δf = vector representing the real part of anomalous scattering

if" = vector representing the imaginary part of anomalous scattering

f_0 = vector representing atomic scattering of a completely free electron

p, q and *r* are functions of λ (wavelength) and are known from atomic scattering factor curves. $|F|^2$ values are different for the Friedel mates and can be determined experimentally. The unknown quantities are $|F_{BA}|$, $|F_A|$ and $(\alpha_{BA} - \alpha_A)$ which are independent of λ and equal for Freidel mates, except for the sign of $(\alpha_{BA} - \alpha_A)$. Therefore, a dataset for one value of λ gives two sets of equations for these unknowns. Measurements at two different wavelengths are thus sufficient to find $|F_{BA}|$, $|F_A|$ and $(\alpha_{BA} - \alpha_A)$ for each reflection.

In practice, selenium is one of the most widely used heavy atoms for SAD/MAD phasing and was used for labeling proteins for this work. This approach was undertaken after unsuccessful molecular replacement trials using closely related structures. Anomalous datasets of crystals of SeMet labeled PhzA and PhzG proteins were collected at x-ray energies corresponding to peak, inflection and one high-energy remote point of the K-edge of Se (λ of the X-ray tuned to 0.979147Å). From these datasets, estimates for the full structure-factor amplitudes of the anomalous scatterers, the so-called F_A values, were derived using the programme XPREP (version 6.09, Bruker Analytical X-ray Solutions, 2001). These F_A values were then used as input for the programme SHELXD (Schneider and Sheldrick, 2002),

which determines the position of the selenium atoms using Patterson methods.

Seleno-L-methionine labelled PhzA and BcepA contain three each and PhzG five Selenium atoms per monomer. All Se atoms of PhzA and BcepA and three out of five Se atoms of PhzG were successfully located by the programme SHELXD. Position of these selenium atoms was further refined and successfully used for generating initial phases using SHARP (delaFortelle and Bricogne, 1997). These initial phases were then improved through solvent flattening using the programme SOLOMON (Abrahams and Leslie, 1998) and DM (Cowtan, 1994) from the CCP4 suite (Bailey, 1994).

9.4.7 Refinement

The initial structural model contains errors that can be minimised through iterative model refinement. This is a process of adjustment of the atomic coordinates of the model in order to minimise the difference between experimentally observed structure factor amplitudes (F_{obs}) and those calculated from the model (F_{calc}). The progress of refinement was monitored using the conventional crystallographic index 'R factor' and 'R-free'. The R factor is defined by the equation:

$$\text{R-factor} = \sum_{hkl} \left| |F_{obs}\, hkl| - |F_{calc}\, hkl| \right| \Big/ \sum_{hkl} |F_{obs}\, hkl|$$

An acceptable value for the R-factor depends on the resolution of the structure. For structures determined at high resolution (<2.0 Å) the value of the final R-factor is expected to be below 0.2 or 20%. Given the low observations-to-parameters ratio for protein structures the R-factor can be artificially lowered at the expense of the stereochemistry of the model. To avoid this type of error, Brunger (1992) introduced a new methodology in the refinement process (cross validation) where approximately 5% of the data (a test group of reflections 'T') is isolated from the remainder (the working group) and not used for the purposes of refinement). Instead the refinement is performed by using only the reflections belonging to the working group. At each cycle of refinement the structure factors are calculated for both groups.

Whilst the working group is used for the calculation of the R-factor as defined above, the test group is used to calculate a new parameter, R-free, in an exactly analogous manner.

$$\text{R-free} = \sum_{hkl \subset T} \left| |F_{obs}\, hkl| - |F_{calc}\, hkl| \right| \Big/ \sum_{hkl \subset T} |F_{obs}\, hkl|$$

The fundamental difference between these two discordance indices is that the refinement procedure `knows' about the working group (as it is used for the very refinement process) but it has never `seen' the test group. The great advantage of the R-free is that it is a sensitive indicator of over-refinement, that is, a refinement protocol which attempts to extract more information than the data is capable of providing.

The refinement program REFMAC 5 (Murshudov et al., 1997) was used for refinement and the model further adjusted by hand using the graphics program O or COOT (Emsley et al., 2000).

9.4.8 Validation

The model was validated by the programs ‘Procheck’ (Laskowski et al., 1993) and ‘Whatcheck’ (Hooft et al., 1996). Contacting amino acids in the dimer interfaces of all the structures were identified using the CCP4 program Contact (Bailey, 1994) and plotted using the program ‘Ligplot’ (Wallace et al., 1995). The area of buried surface between two monomers also determined using the programme AREAIMOL (CCP4 suite). The structure alignments throughout this work were performed using the programs LSQMAN, MOLEMAN2 and COOT.

9.4.9 Representation of structures

All figures were prepared using the program PYMOL (DeLano Scientific LLC) and adjusted for final printing with the help of PHOTOSHOP (Adobe Corporation).

References

If you don't know where you are going, any road will take you there.
- Alice in wonderland, Lewis Carroll

10.0 References

Aarons, S., A. Abbas, et al. (2000). "A regulatory RNA (PrrB RNA) modulates expression of secondary metabolite genes in Pseudomonas fluorescens F113." J Bacteriol 182(14): 3913-9.

Abken, H. J., M. Tietze, et al. (1998). "Isolation and characterization of methanophenazine and function of phenazines in membrane-bound electron transport of methanosarcina mazei go1." J Bacteriol 180(8): 2027-32.

Abrahams, J. P. and R. A. De Graaff (1998). "New developments in phase refinement." Curr Opin Struct Biol 8(5): 601-5.

Abrahams,J.P. and Leslie, A.G.W. (1996). Methods used in the structure determination of bovine mitochondrial F-1 ATPase. Acta Crystallographica Section D-Biological Crystallography, 52, 30-42.

Ahmed, K., T. C. Dai, et al. (1993). "Neutrophil response to Pseudomonas aeruginosa in respiratory infection." Microbiol Immunol 37(7): 523-9.

Allen, L., D. H. Dockrell, et al. (2005). "Pyocyanin production by Pseudomonas aeruginosa induces neutrophil apoptosis and impairs neutrophil-mediated host defenses in vivo." J Immunol 174(6): 3643-9.

Altschul, S.F., Gish, W., Miller, W., Myers, E.W. & Lipman, D.J. (1990) "Basic local alignment search tool." J. Mol. Biol. 215:403-410.

Altschul, S.F., Madden, T.L., Schäffer, A.A., Zhang, J., Zhang, Z., Miller, W. & Lipman, D.J. (1997) "Gapped BLAST and PSI-BLAST: a new generation of protein database search programs." Nucleic Acids Res. 25:3389-3402.

Amitani, R., R. Wilson, et al. (1991). "Effects of human neutrophil elastase and Pseudomonas aeruginosa proteinases on human respiratory epithelium." Am J Respir Cell Mol Biol 4(1): 26-32.

Aoyagi, T., H. Tobe, et al. (1978). "Amastatin, an inhibitor of aminopeptidase a, produced by actinomycetes." J Antibiot (Tokyo) 31(6): 636-8.

Arima, M., S. Kamoshita, et al. (1964). "Genetical studies of wilson's disease. 3. Genetical and epidemiological studies of wilson's disease in mikura island." Paediatr Univ Tokyo 10: 5-10.

Bailey,S. (1994). The CCP4 Suite - Programs for Protein Crystallography. Acta Crystallographica Section D-Biological Crystallography, 50, 760-763

Bakker, P. A., D. C. Glandorf, et al. (2002). "Effects of Pseudomonas putida modified to produce phenazine-1-carboxylic acid and 2,4-diacetylphloroglucinol

on the microflora of field grown wheat." Antonie Van Leeuwenhoek 81(1-4): 617-24.

Balinsky D., Davies D. D., (1961) " Aromatic biosynthesis in higher plants. 2. Mode of attachment of shikimic acid and dehydroshikimic acid to dehydroshikimic reductase." Biochem J.80:296-300.

Ballard RW, Palleroni NJ,Doudoroff M, Stanier RY, Mandel M. (1970) "Taxonomy of the aerobic pseudomonads: Pseudomonas cepacia, P. marginata, P. alliicola and P. caryophylli." J Gen Microbiol.60(2):199-214.

Barger G, Dale HH. (1907) "Ergotoxine and some other Constituents of Ergot." BiochemJ.2(5-6):240-99.

Baron,S.S. and Rowe,J.J. (1981). Antibiotic Action of Pyocyanin. Antimicrobial Agents and Chemotherapy, 20, 814-820.

Barry, V. C. and M. L. Conalty (1958). "Antituberculosis activity in the phenazine series. II. N3-substituted anilinoaposafranines (rimino-compounds) and some derivatives." Am Rev Tuberc 78(1): 62-73.

Bassett, D. J. and A. B. Fisher (1976). "Stimulation of rat lung metabolism with 2,4-dinitrophenol and phenazine methosulfate." Am J Physiol 231(3): 898-902.

Bergdoll,M., Remy,M.H., Cagnon,C., Masson,J.M., and Dumas,P. (1997). Proline-dependent oligomerization with arm exchange. Structure, 5, 391-401.

Berger, S., J. Fiedler, et al. (2004). "Metal vs ligand reduction in complexes of dipyrido[3,2-a:2',3'-c]phenazine and related ligands with [(C5Me5)ClM]+ (M = Rh or Ir): evidence for potential rather than orbital control in the reductive cleavage of the metal-chloride bond." Inorg Chem 43(4): 1530-8.

Blankenfeldt, W., A. P. Kuzin, et al. (2004). "Structure and function of the phenazine biosynthetic protein PhzF from Pseudomonas fluorescens." Proc Natl Acad Sci U S A 101(47): 16431-6.

Blankenfeldt,W., Kuzin,A.P., Skarina,T., Korniyenko,Y., Tong,L., Bayer,P., Janning,P., Thomashow,L.S., and Mavrodi,D.V. (2004). Structure and function of the phenazine biosynthetic protein PhzF from Pseudomonas fluorescens. Proc. Natl. Acad. Sci. U. S. A, 101, 16431-16436.

Bradford, MM. "A rapid and sensitive for the quantitation of microgram quantitites of protein utilizing the principle of protein-dye binding." Analytical Biochemistry 72: 248-254. 1976.

Brisbane, P. G., L. J. Janik, et al. (1987). "Revised structure for the phenazine antibiotic from Pseudomonas fluorescens 2-79 (NRRL B-15132)." Antimicrob Agents Chemother 31(12): 1967-71.

Britton G. (1983). “Biochemistry of Natural Pigments”. Cambridge, UK: Cambridge Univ. Press. 366 pp

Bull, C. T., B. Duffy, et al. (2001). "Characterization of spontaneous gacS and gacA regulatory mutants of Pseudomonas fluorescens biocontrol strain CHAO." Antonie Van Leeuwenhoek 79(3-4): 327-36.

BU'LOCK,J.D. (1961). Intermediary metabolism and antibiotic synthesis. Adv. Appl. Microbiol., 3, 293-342.

Byng,G.S., Eustice,D.C., and Jensen,R.A. (1979). Biosynthesis of phenazine pigments in mutant and wild-type cultures of Pseudomonas aeruginosa. J. Bacteriol., 138, 846-852.

Calhoun, D. H. and R. A. Jensen (1972). "Significance of altered carbon flow in aromatic amino acid synthesis: An approach to the isolation of regulatory mutants in pseudomonas aeruginosa." J Bacteriol 109(1): 365-72.

Carter C.H., (1961) “4,7-Phenanthroline-5,6-quinone, a new agent for amebiasis.” Antibiot Chemother.

Cao,H., Krishnan,G., Goumnerov,B., Tsongalis,J., Tompkins,R., and Rahme,L.G. (2001). A quorum sensing-associated virulence gene of Pseudomonas aeruginosa encodes a LysR-like transcription regulator with a unique self-regulatory mechanism. Proceedings of the National Academy of Sciences of the United States of America, 98, 14613-14618.

Cerecetto, H., M. Gonzalez, et al. (2004). "1, 2, 4-triazine n-oxide derivatives: Studies as potential hypoxic cytotoxins. Part iii." Arch Pharm (Weinheim) 337(5): 271-80.

Chang, P. C. and A. C. Blackwood (1968). "Simultaneous biosynthesis of pyocyanine, phenazine-1-carboxylic acid, and oxychloroaphine from labelled substrates by Pseudomonas aeruginosa Mac 436." Can J Biochem 46(8): 925-9.

Cheung, A. T., R. B. Moss, et al. (1992). "Chronic Pseudomonas aeruginosa endobronchitis in rhesus monkeys: I. Effects of pentoxifylline on neutrophil influx." J Med Primatol 21(7-8): 357-62.

Chin,A.W.T., van den,B.D., de Voer,G., van der Drift,K.M., Tuinman,S., Thomas-Oates,J.E., Lugtenberg,B.J., and Bloemberg,G.V. (2001). Phenazine-1-carboxamide production in the biocontrol strain Pseudomonas chlororaphis PCL1391 is regulated by multiple factors secreted into the growth medium. Mol. Plant Microbe Interact., 14, 969-979.

Chin-A-Woeng TFC, Bloemberg GV, Lugtenberg BJJ. (2003). “Phenazines and their role in biocontrol by Pseudomonas bacteria.” New Phytol. 157:503–23

Chin-A-Woeng TFC, Bloemberg GV, van der Bij AJ, van der Drift KMGF, Schripsema J, et al. (1998). “Biocontrol by phenazine-1-carboxamide-producing Pseudomonas chlororaphis PCL1391 of tomato root rot caused by Fusarium oxysporum f. sp. radicis-lycopersici.” Mol. Plant-Microbe Interact. 11:1069–77

Cole, N., S. Bao, et al. (2003). "Pseudomonas aeruginosa keratitis in IL-6-deficient mice." Int Arch Allergy Immunol 130(2): 165-72.

Collaborative Computational Project, Number 4. (1994). "The CCP4 Suite: Programs for Protein Crystallography". Acta Cryst. D50, 760-763

Colovos,C. and Yeates,T.O. (1993). Verification of Protein Structures - Patterns of Nonbonded Atomic Interactions. Protein Science, 2, 1511-1519.

Cowtan,K. (1994). 'dm': An automated procedure for phase improvement by density modification. Joint CCP4 and ESF-EACBM Newsletter on Protein Crystallography, 31, 34-38.

Cox, C. D. (1985). "Iron transport and serum resistance in Pseudomonas aeruginosa." Antibiot Chemother 36: 1-12.

Cudney,B., Patel,S., Weisgraber,K., and Newhouse,Y. (1994). Screening and Optimization Strategies for Macromolecular Crystal-Growth. Acta Crystallographica Section D-Biological Crystallography, 50, 414-4123.

Daly, J. A., R. Boshard, et al. (1984). "Differential primary plating medium for enhancement of pigment production by Pseudomonas aeruginosa." J Clin Microbiol 19(6): 742-3.

Dekkers, L. C., I. H. Mulders, et al. (2000). "The sss colonization gene of the tomato-Fusarium oxysporum f. sp. radicis-lycopersici biocontrol strain Pseudomonas fluorescens WCS365 can improve root colonization of other wild-type pseudomonas spp.bacteria." Mol Plant Microbe Interact 13(11): 1177-83.

delaFortelle,E. and Bricogne,G. (1997). Maximum-likelihood heavy-atom parameter refinement for multiple isomorphous replacement and multiwavelength anomalous diffraction methods. Macromolecular Crystallography, Pt A, 276, 472-494.

Delaney,S.M., Mavrodi,D.V., Bonsall,R.F., and Thomashow,L.S. (2001). phzO, a gene for biosynthesis of 2-hydroxylated phenazine compounds in Pseudomonas aureofaciens 30-84. J. Bacteriol., 183, 318-327.

DeLano WL. 2002. The PyMOL molecular graphics system. http://www.pymol.org

Denning GM, Railsback MA, Rasmussen GT, Cox CD, Britigan BE. (1998). “Pseudomonas pyocyanine alters calcium signaling in human airway epithelial cells.” Am. J. Physiol. 274:L893–900

Denning GM, Wollenweber LA, Railsback MA, Cox CD, Stoll LL, et al. (1998). “Pseudomonas pyocyanin increases interleukin-8 expression by human airway epithelial cells.” Infect. Immun. 66:5777–84

Denning, G. M., S. S. Iyer, et al. (2003). "Phenazine-1-carboxylic acid, a secondary metabolite of Pseudomonas aeruginosa, alters expression of immunomodulatory proteins by human airway epithelial cells." Am J Physiol Lung Cell Mol Physiol 285(3): L584-92.

di Salvo, M. L., M. K. Safo, et al. (2003). "Structure and mechanism of escherichia coli pyridoxine 5'-phosphate oxidase." Biochim Biophys Acta 1647(1-2): 76-82.

Dietrich, L. E., A. Price-Whelan, et al. (2006). "The phenazine pyocyanin is a terminal signalling factor in the quorum sensing network of Pseudomonas aeruginosa." Mol Microbiol.

DiMango, E., H. J. Zar, et al. (1995). "Diverse Pseudomonas aeruginosa gene products stimulate respiratory epithelial cells to produce interleukin-8." J Clin Invest 96(5): 2204-10.

Drenth J. (1999) “Principles of Protein X-Ray Crystallography.” Springer-Verlag Inc. NY

Doublie,S. (1997). Preparation of selenomethionyl proteins for phase determination. Macromolecular Crystallography, Pt A, 276, 523-530.

Doyle, R. P., P. E. Kruger, et al. (2001). "Phenazine-2,3-diamine." Acta Crystallogr C 57(Pt 1): 104-5.

Du Buy, H. G. and J. Showacre (1959). "Enzymes catalyzing sequential reactions in mouse brain and liver supernatant fractions: I. Differential use of Janus green B and phenazine methosulfate." J Histochem Cytochem 7: 361-9.

Dunn, M. M. and D. W. Kamp (1987). "Pulmonary clearance of Pseudomonas aeruginosa in neutropenic mice. Effects of systemic immunization." Am Rev Respir Dis 135(6): 1294-9.

Eftink,M.R. (1997). Fluorescence methods for studying equilibrium macromolecule-ligand interactions. Fluorescence Spectroscopy, 278, 221-257.

Emsley P, Cowtan K "Coot: model-building tools for molecular graphics" (2004) Acta Crystallographica Section D-Biological Crystallography 60: 2126-2132 Part 12.

Endo, H., M. Tada, et al. (1969). "Studies on antitumor activity of phenazine derivatives against S 180 in mice. 8." Sci Rep Res Inst Tohoku Univ [Med] 16(1): 18-26.

Erickson, D. L., J. L. Lines, et al. (2004). "Pseudomonas aeruginosa relA contributes to virulence in Drosophila melanogaster." Infect Immun 72(10): 5638-45.

Essar DW, Eberly L, Hadero A, Crawford IP. (1990) “Identification and characterization of genes for a second anthranilate synthase in Pseudomonas aeruginosa: interchangeability of the two anthranilate synthases and evolutionary implications.” J Bacteriol. 172(2):884-900.

Evans, K., L. Passador, et al. (1998). "Influence of the MexAB-OprM multidrug efflux system on quorum sensing in Pseudomonas aeruginosa." J Bacteriol 180(20): 5443-7.

Fernandez, D. U., R. Fuchs, et al. (2001). "The structure of a pyoverdine produced by a pseudomonas tolaasii-like isolate." Biometals 14(1): 81-4.

Fordos J. 1859. Rec. Trav. Soc. Emul. Sci. Pharm. 3:30

Friedheim EA. (934). “The effect of pyocyanine on the respiration of some normal tissues and tumours.” Biochem J. 1;28(1):173-9.

Fujii, T., J. Kadota, et al. (1995). "Long term effect of erythromycin therapy in patients with chronic Pseudomonas aeruginosa infection." Thorax 50(12): 1246-52.

Fuqua C, Parsek MR, Greenberg EP. (2001). “Regulation of gene expression by cell-to-cell communication: acyl-homoserine lactone quorum sensing.” Annu. Rev. Genet. 35:439–68

Galbraith, M. D., S. R. Giddens, et al. (2004). "Role of glutamine synthetase in phenazine antibiotic production by Pantoea agglomerans Eh1087." Can J Microbiol 50(10): 877-81.

Gallagher, L. A., S. L. McKnight, et al. (2002). "Functions required for extracellular quinolone signaling by Pseudomonas aeruginosa." J Bacteriol 184(23): 6472-80.

Gamage, S. A., G. W. Rewcastle, et al. (2006). "Phenazine-1-carboxamides: structure-cytotoxicity relationships for 9-substituents and changes in the H-bonding pattern of the cationic side chain." Bioorg Med Chem 14(4): 1160-8.

Gardner, P. R. and C. W. White (1996). "Failure of tumor necrosis factor and interleukin-1 to elicit superoxide production in the mitochondrial matrices of mammalian cells." Arch Biochem Biophys 334(1): 158-62.

Gardner, P. R., D. D. Nguyen, et al. (1996). "Superoxide scavenging by mn(ii/iii) tetrakis (1-methyl-4-pyridyl) porphyrin in mammalian cells." Arch Biochem Biophys 325(1): 20-8.

Garfield, H. J. (1980). "Safe use of phenazine methosulfate." Clin Chem 26(2): 357-8.

Ge, Y., X. Huang, et al. (2004). "Phenazine-1-carboxylic acid is negatively regulated and pyoluteorin positively regulated by gacA in Pseudomonas sp. M18." FEMS Microbiol Lett 237(1): 41-7.

Geller, D. M. (1969). "The effects of phenazine dyes and N,N,N',N'-tetramethyl-p-phenylenediamine upon light-induced absorbance changes and photophosphorylation in Rhodospirillum rubrum extracts." J Biol Chem 244(3): 971-80.

Georgakopoulos, D. G., M. Hendson, et al. (1994). "Analysis of Expression of a Phenazine Biosynthesis Locus of Pseudomonas aureofaciens PGS12 on Seeds with a Mutant Carrying a Phenazine Biosynthesis Locus-Ice Nucleation Reporter Gene Fusion." Appl Environ Microbiol 60(12): 4573-79.

Gerber NN, Lechevalier MP. (1964). “Phenazines and phenoxazinones from Waksmania aerata sp. nov. and Pseudomonas iodina.” Biochemistry 35:598–602

Gibson, J. S., M. C. Muzyamba, et al. (2003). "Effect of phenazine methosulphate on K+ transport in human red cells." Cell Physiol Biochem 13(6): 329-36.

Giddens, S. R., Y. Feng, et al. (2002). "Characterization of a novel phenazine antibiotic gene cluster in Erwinia herbicola Eh1087." Mol Microbiol 45(3): 769-83.

Goh, E. B., Yim, G., Tsui, W., McClure, J., Surette, M. G. & Davies, J. (2002) Proc Natl Acad Sci U S A 99, 17025-30.

Graebsch A., (2006). “Synthese und untersuchung von liganden und inhibitoren der an der phenazine biosynthese beteiligten enzyme” Diplomarbeit, Univerity of Dortmund.

Gurusiddaiah, S., D. M. Weller, et al. (1986). "Characterization of an antibiotic produced by a strain of Pseudomonas fluorescens inhibitory to Gaeumannomyces graminis var. tritici and Pythium spp." Antimicrob Agents Chemother 29(3): 488-95.

Haas D, Blumer C, Keel C. (2000) “Biocontrol ability of fluorescent pseudomonads genetically dissected: importance of positive feedback regulation.” Curr Opin Biotechnol. (3):290-7.

Haley, T. J. and F. Stolarsky (1950). "A study of in vitro neutralization of heparin by thiazine, oxazine, phenazine, and other dyes." J Am Pharm Assoc Am Pharm Assoc 39(2): 76-81.

Haley, T. J. and F. Stolarsky (1951). "A study of the acute and chronic toxicity of toluidine blue and related phenazine and thiazine dyes." Stanford Med Bull 9(2): 96-100.

Halliwell, B. (1977). "Hydroxylation of aromatic compounds by reduced nicotinamide-adenine dinucleotide and phenazine methosulphate requires hydrogen peroxide and hydroxyl radicals, but not superoxide." Biochem J 167(1): 317-20.

Handelsman, J. and E. V. Stabb (1996). "Biocontrol of soilborne plant pathogens." Plant Cell 8(10): 1855-69.

Harman, J. W. and M. C. Macbrinn (1963). "The Effect of Phenazine Methosulphate, Pyocyanine and Edta on Mitochondrial Succinic Dehydrogenase." Biochem Pharmacol 12: 1265-78.

Hassan, H. M. and I. Fridovich (1980). "Mechanism of the antibiotic action pyocyanine." J Bacteriol 141(1): 156-63.

Hassett, D. J., H. P. Schweizer, et al. (1995). "Pseudomonas aeruginosa sodA and sodB mutants defective in manganese- and iron-cofactored superoxide dismutase activity demonstrate the importance of the iron-cofactored form in aerobic metabolism." J Bacteriol 177(22): 6330-7.

Hassett, D. J., L. Charniga, et al. (1992). "Response of Pseudomonas aeruginosa to pyocyanin: mechanisms of resistance, antioxidant defenses, and demonstration of a manganese-cofactored superoxide dismutase." Infect Immun 60(2): 328-36.

Hassett,D.J., Charniga,L., Bean,K., Ohman,D.E., and Cohen,M.S. (1992). Response of Pseudomonas-Aeruginosa to Pyocyanin - Mechanisms of Resistance, Antioxidant Defenses, and Demonstration of A Manganese-Cofactored Superoxide-Dismutase. Infection and Immunity, 60, 328-336.

Hassett,D.J., Schweizer,H.P., and Ohman,D.E. (1995). Pseudomonas-Aeruginosa Soda and Sodb Mutants Defective in Manganese-Cofactored and Iron-Cofactored Superoxide-Dismutase Activity Demonstrate the Importance of the Iron-Cofactored Form in Aerobic Metabolism. Journal of Bacteriology, 177, 6330-6337.

Henderson, B. (1982). "The sensitivity to light of solutions of phenazine methosulphate: a quantitative cytochemical study." Histochem J 14(4): 649-53.

Hendrickson, E. L., J. Plotnikova, et al. (2001). "Differential roles of the Pseudomonas aeruginosa PA14 rpoN gene in pathogenicity in plants, nematodes, insects, and mice." J Bacteriol 183(24): 7126-34.

Herbert, R. B. and F. G. Holliman (1969). "Pigments of pseudomonas species. Ii. Structure of aeruginosin b." J Chem Soc [Perkin 1] 18: 2517-20.

Hernandez, M. E., A. Kappler, et al. (2004). "Phenazines and other redox-active antibiotics promote microbial mineral reduction." Appl Environ Microbiol 70(2): 921-8.

Hoiby, N., S. S. Pedersen, et al. (1990). "Immunology of Pseudomonas aeruginosa infection in cystic fibrosis." Acta Univ Carol [Med] (Praha) 36(1-4): 16-21.

Holliman, F. G. (1969). "Pigments of pseudomonas species. I. Structure and synthesis of aeruginosin a." J Chem Soc [Perkin 1] 18: 2514-6.

Hollstein, U. and D. A. McCamey (1973). "Biosynthesis of phenazines. II. Incorporation of (6-14C)-D-shikimic acid into phenazine-1-carboxylic acid and iodinin." J Org Chem 38(19): 3415-7.

Hollstein, U. and L. G. Marshall (1972). "Biosynthesis of phenazines." J Org Chem 37(22): 3510-4.

Hooft, R. W., G. Vriend, et al. (1996). "Errors in protein structures." Nature 381(6580): 272.

Ikehara, T., H. Yamaguchi, et al. (1985). "Phenazine methosulfate stimulation of ouabain-sensitive Rb+ uptake by HeLa cells: effects of respiratory inhibitors, anaerobiosis, and ascorbate." J Cell Biochem 28(4): 273-80.

Imamura,N., Nishijima,M., Takadera,T., Adachi,K., Sakai,M., and Sano,H. (1997). New anticancer antibiotics pelagiomicins, produced by a new marine bacterium Pelagiobacter variabilis. J. Antibiot. (Tokyo), 50, 8-12.

Jacobs,M.A., Alwood,A., Thaipisuttikul,I., Spencer,D., Haugen,E., Ernst,S., Will,O., Kaul,R., Raymond,C., Levy,R., Liu,C.R., Guenthner,D., Bovee,D., Olson,M.V., and Manoil,C. (2003). Comprehensive transposon mutant library of Pseudomonas aeruginosa. Proceedings of the National Academy of Sciences of the United States of America, 100, 14339-14344.

Jancarik,J. and Kim,S.H. (1991). Sparse-Matrix Sampling - A Screening Method for Crystallization of Proteins. Journal of Applied Crystallography, 24, 409-411.

Jankowski, W. and M. Gdaniec (2002). "The beta-polymorph of phenazine." Acta Crystallogr C 58(Pt 3): o181-2.

Jensen, E. T., A. Kharazmi, et al. (1992). "Some bacterial parameters influencing the neutrophil oxidative burst response to Pseudomonas aeruginosa biofilms." Apmis 100(8): 727-33.

Jensen, P. O., C. Moser, et al. (2004). "Faster activation of polymorphonuclear neutrophils in resistant mice during early innate response to Pseudomonas aeruginosa lung infection." Clin Exp Immunol 137(3): 478-85.

Jones, G. P., D. G. Lewis, et al. (1988). "Structure of the pseudomonad fungal antibiotic phenazine-1-carboxylic acid." Acta Crystallogr C 44 (Pt 12): 2220-2.

Jones, G. R. (1968). "Quantitative cytochemical studies of the stimulation of rat-liver succinate-neotetrazolium reductase by phenazine methosulphate and quinones, and of inhibition by neotetrazolium, with observations on altered formazan localisation." Exp Cell Res 49(2): 251-65.

Jones,G., Willett,P., and Glen,R.C. (1995). Molecular Recognition of Receptor-Sites Using A Genetic Algorithm with A Description of Desolvation. Journal of Molecular Biology, 245, 43-53.

Jones,G., Willett,P., Glen,R.C., Leach,A.R., and Taylor,R. (1997). Development and validation of a genetic algorithm for flexible docking. Journal of Molecular Biology, 267, 727-748.

Jones,S., Marin,A., and Thornton,J.M. (2000). Protein domain interfaces: characterization and comparison with oligomeric protein interfaces. Protein Engineering, 13, 77-82.

Jones,T.A., Zou,J.Y., Cowan,S.W., and Kjeldgaard (1991). Improved methods for building protein models in electron density maps and the location of errors in these models. Acta Crystallogr. A, 47 (Pt 2), 110-119.

Kabsch,W. (1993). Automatic Processing of Rotation Diffraction Data from Crystals of Initially Unknown Symmetry and Cell Constants. Journal of Applied Crystallography, 26, 795-800.

Karimova, G., J. Pidoux, et al. (1998). "A bacterial two-hybrid system based on a reconstituted signal transduction pathway." Proc Natl Acad Sci U S A 95(10): 5752-6.

Karimova, G., A. Ullmann, et al. (2000). "A bacterial two-hybrid system that exploits a camp signaling cascade in escherichia coli." Methods Enzymol 328: 59-73.

Karimova, G., A. Ullmann, et al. (2000). "Bordetella pertussis adenylate cyclase toxin as a tool to analyze molecular interactions in a bacterial two-hybrid system." Int J Med Microbiol 290(4-5): 441-5.

Kawano,Y., Kumagai,T., Muta,K., Matoba,Y., Davies,J., and Sugiyama,M. (2000). The 1.5 angstrom crystal structure of a bleomycin resistance determinant from bleomycin-producing Streptomyces verticillus. Journal of Molecular Biology, 295, 915-925.

Kearns,L.P. and Hale,C.N. (1995). Incidence of bacteria inhibitory to Erwinia amylovora from blossoms in New Zealand apple orchards. Plant Pathology, 44, 918-924.

Kearns,L.P. and Mahanty,H.K. (1998). Antibiotic production by Erwinia herbicola Eh1087: its role in inhibition of Erwinia amylovora and partial characterization of antibiotic biosynthesis genes. Appl. Environ. Microbiol., 64, 1837-1844.

Kellen, J. and V. Krcmery (1966). "Determination of lactic and malic dehydrogenase activity in microorganisms by means of phenazine metosulphate." J Hyg Epidemiol Microbiol Immunol 10(1): 1-7.

Kelley L. A., MacCallum R. M., Sternberg M. J., (2000). “Enhanced genome annotation using structural profiles in the program 3D-PSSM.” Mol Biol. 299(2):499-520.

Kerber, N. L., N. L. Pucheu, et al. (1978). "Phenazine methosulfate mediated photoinactivation of some energy linked reactions in Rhodospirillum rubrum." Biochem Biophys Res Commun 81(2): 667-71.

Kerr, J. R., G. W. Taylor, et al. (1999). "Pseudomonas aeruginosa pyocyanin and 1-hydroxyphenazine inhibit fungal growth." J Clin Pathol 52(5): 385-7.

Kerr,J.R. (2000). Phenazine Pigments: antibiotics and virulence factors. Infect Dis Rev, 2, 184-194.

Khan SR, Mavrodi DV, Jog GJ, Suga H, Thomashow LS, et al. (2005). “Activation of the phz operon of Pseudomonas fluorescens 2-79 requires the LuxR homolog PhzR, N-(3-OH-hexanoyl)-L-homoserine lactone produced by the LuxI homolog PhzI, and a cis-acting phz box.” J. Bacteriol. 187:6517–27

Kharami, A., Z. Bibi, et al. (1989). "Effect of Pseudomonas aeruginosa rhamnolipid on human neutrophil and monocyte function." Apmis 97(12): 1068-72.

Kidani, Y. (1954). "Studies on phenazines. VIII. Some observations in the phenazine synthesis by the improved Wohl-Aue reaction." Pharm Bull 2(3): 292-4.

Kiprianova, E. A. and A. S. Rabionvich (1969). "[Production of phenazine-1-carboxylic acid by Pseudomonas fluorescens]." Mikrobiologiia 38(2): 224-7.

Kitahara, M., H. Nakamura, et al. (1982). "Saphenamycin, a novel antibiotic from a strain of streptomyces." J Antibiot (Tokyo) 35(10): 1412-4.

Kitahara, M., T. Takeda, et al. (1982). "Treatment of meniere's disease with isosorbide." ORL J Otorhinolaryngol Relat Spec 44(4): 232-8.

Kleywegt,G. and Jones,T.A. (1994). Halloween...Masks and Bones. In Bailey,S., Hubbard,R., and Waller,D. (Eds.), From First Map to Final Model, . SERC Daresbury Laboratory, pp. 59-66.

Kleywegt,G., Zou,J.Y., Kjeldgaard,M., and Jones,T.A. (2001). Around O. In Rossmann,M.G. and Arnold,E. (Eds.), International Tables for Crystallography, Vol. F. Crystallography of Biological Macromolecules, . Kluwer Academic Publishers, pp. 353-367.

Kleywegt,G.J. (1996). Use of non-crystallographic symmetry in protein structure refinement. Acta Crystallographica Section D-Biological Crystallography, 52, 842-857.

Konig, B., M. Ceska, et al. (1995). "Effect of Pseudomonas aeruginosa on interleukin-8 release from human phagocytes." Int Arch Allergy Immunol 106(4): 357-65.

Konig, B., M. L. Vasil, et al. (1997). "Role of haemolytic and non-haemolytic phospholipase C from Pseudomonas aeruginosa in interleukin-8 release from human monocytes." J Med Microbiol 46(6): 471-8.

Korth H, Romer A, Budzikiewicz H, Pulverer G. (1978). “4,9-Dihydroxyphenazine-1,6-dicarboxylic acid dimethylester and the "missing link" in phenazine biosynthesis.” J. Gen. MicroBiol. 104:299–303

Kumagai,T., Hibino,R., Kawano,Y., and Sugiyama,M. (1999). Mutation of the N-terminal proline 9 of BLMA from Streptomyces verticillus abolishes the binding affinity for bleomycin. Febs Letters, 450, 227-230.

Laemmli,U.K. (1970). Cleavage of structural proteins during the assembly of the head of bacteriophage T4. Nature, 227, 680-685.

Laskowski,R.A., Macarthur,M.W., Moss,D.S., and Thornton,J.M. (1993). Procheck - A Program to Check the Stereochemical Quality of Protein Structures. Journal of Applied Crystallography, 26, 283-291.

Lau,G.W., Goumnerov,B.C., Walendziewicz,C.L., Hewitson,J., Xiao,W.Z., Mahajan-Miklos,S., Tompkins,R.G., Perkins,L.A., and Rahme,L.G. (2003). The Drosophila melanogaster toll pathway participates in resistance to infection by the gram-negative human pathogen Pseudomonas aeruginosa. Infection and Immunity, 71, 4059-4066.

Lau,G.W., Ran,H.M., Kong,F.S., Hassett,D.J., and Mavrodi,D. (2004). Pseudomonas aeruginosa pyocyanin is critical for lung infection in mice. Infection and Immunity, 72, 4275-4278.

Laursen, J. B. and J. Nielsen (2004). "Phenazine natural products: biosynthesis, synthetic analogues, and biological activity." Chem Rev 104(3): 1663-86.

LeBlanc, C. M., R. Bortolussi, et al. (1982). "Opsonization of mucoid and non-mucoid Pseudomonas aeruginosa by serum from patients with cystic fibrosis assessed by a chemiluminescence assay." Clin Invest Med 5(2-3): 125-8.

Lee, H. J., J. S. Kim, et al. (2004). "Synthesis and cytotoxicity evaluation of 6,11-dihydro-pyridazo- and 6,11-dihydro-pyrido[2,3-b]phenazine-6,11-diones." Bioorg Med Chem 12(7): 1623-8.

Lee, H., V. Richards, et al. (1961). "Effect of phenazine di-N-oxide and phenazine on total cellular dry mass of mouse Ehrlich ascites cells as measured by interference microscopy." J Natl Cancer Inst 26: 435-43.

Leisinger T, Margraff R. (1979) “Secondary metabolites of the fluorescent pseudomonads.” Microbiol Rev.;43(3):422-42.

Levitch, M. E. (1970). "Regulation of aromatic amino acid biosynthesis in phenazine-producing strains of Pseudomonas." J Bacteriol 103(1): 16-9.

Levitch, M. E. and E. R. Stadtman (1964). "Study of the Biosynthesis of Phenazine-1-Carboxylic Acid." Arch Biochem Biophys 106: 194-9.

Li, Z., X. Wang, et al. (1995). "Inhibitory action of metabolites of Pseudomonas aeruginosa against gram-negative bacteria." Kansenshogaku Zasshi 69(8): 924-7.

Lin, T. J., R. Garduno, et al. (2002). "Pseudomonas aeruginosa activates human mast cells to induce neutrophil transendothelial migration via mast cell-derived IL-1 alpha and beta." J Immunol 169(8): 4522-30.

Liu, H., D. Dong, et al. (2006). "Genetic diversity of phenazine- and pyoluteorin-producing pseudomonads isolated from green pepper rhizosphere." Arch Microbiol 185(2): 91-8.

Longley, R. P. and D. Perlman (1972). "Conversion of l-sorbose to 5-keto-d-fructose by pseudomonads." Biotechnol Bioeng 14(5): 843-6.

Longley, R. P., J. E. Halliwell, et al. (1972). "The branchpoint of pyocyanine biosynthesis." Can J Microbiol 18(9): 1357-63.

Look, A. T. (2005). "Molecular pathogenesis of mds." Hematology (Am Soc Hematol Educ Program): 156-60.

Look, D. C., L. L. Stoll, et al. (2005). "Pyocyanin and its precursor phenazine-1-carboxylic acid increase il-8 and intercellular adhesion molecule-1 expression in human airway epithelial cells by oxidant-dependent mechanisms." J Immunol 175(6): 4017-23.

Lugtenberg BJ, Dekkers LC. (1999) “What makes Pseudomonas bacteria rhizosphere competent?” Environ Microbiol. Feb;1(1):9-13.

Lundqvist, K., H. Herwald, et al. (2004). "Heparin binding protein is increased in chronic leg ulcer fluid and released from granulocytes by secreted products of Pseudomonas aeruginosa." Thromb Haemost 92(2): 281-7.

Mahajan-Miklos,S., Tan,M.W., Rahme,L.G., and Ausubel,F.M. (1999). Molecular mechanisms of bacterial virulence elucidated using a Pseudomonas aeruginosa Caenorhabditis elegans pathogenesis model. Cell, 96, 47-56.

Martin,T.W., Dauter,Z., Devedjiev,Y., Sheffield,P., Jelen,F., He,M., Sherman,D.H., Otlewski,J., Derewenda,Z.S., and Derewenda,U. (2002). Molecular basis of mitomycin C resistance in Streptomyces: Structure and function of the MRD protein. Structure, 10, 933-942.

Maruyama,M., Kumagai,T., Matoba,Y., Hayashida,M., Fujii,T., Hata,Y., and Sugiyama,M. (2001). Crystal structures of the transposon Tn5-carried bleomycin resistance determinant uncomplexed and complexed with bleomycin. Journal of Biological Chemistry, 276, 9992-9999.

Matlola, N. M., H. C. Steel, et al. (2001). "Antimycobacterial action of B4128, a novel tetramethylpiperidyl-substituted phenazine." J Antimicrob Chemother 47(2): 199-202.

Matsuura, S., N. Sunagawa, et al. (1969). "Antitumor activity of phenazine di-N-oxides. II." Sci Rep Res Inst Tohoku Univ [Med] 16(1): 15-7.

Matthews,B.W. (1968). Solvent Content of Protein Crystals. Journal of Molecular Biology, 33, 491-&.

Maul C, Sattler I, Zerlin M, Hinze C, Koch C, Maier A, Grabley S, Thiericke R.(1999) “Biomolecular-chemical screening: a novel screening approach for the discovery of biologically active secondary metabolites. III. New DNA-binding metabolites.” J Antibiot;52(12):1124-34

Mavrodi, D. V., B. M. Chatuev, et al. (1997). "[A genetic locus controlling biosynthesis of phenazine antibiotic in Pseudomonas fluorescens strain 2-79]." Dokl Akad Nauk 352(1): 117-20.

Mavrodi, D. V., N. Bleimling, et al. (2004). "The purification, crystallization and preliminary structural characterization of PhzF, a key enzyme in the phenazine-

biosynthesis pathway from Pseudomonas fluorescens 2-79." Acta Crystallogr D Biol Crystallogr 60(Pt 1): 184-6.

Mavrodi, D. V., R. F. Bonsall, et al. (2001). "Functional analysis of genes for biosynthesis of pyocyanin and phenazine-1-carboxamide from Pseudomonas aeruginosa PAO1." J Bacteriol 183(21): 6454-65.

Mavrodi, D. V., W. Blankenfeldt, et al. (2006). "Phenazine Compounds in Fluorescent Pseudomonas Spp. Biosynthesis and Regulation." Annu Rev Phytopathol.

Mavrodi, D. V., V. N. Ksenzenko, et al. (1998). "A seven-gene locus for synthesis of phenazine-1-carboxylic acid by Pseudomonas fluorescens 2-79." J Bacteriol 180(9): 2541-8.

Mavrodi,D.V., Bonsall,R.F., Delaney,S.M., Soule,M.J., Phillips,G., and Thomashow,L.S. (2001). Functional analysis of genes for biosynthesis of pyocyanin and phenazine-1-carboxamide from Pseudomonas aeruginosa PAO1. J. Bacteriol., 183, 6454-6465.

Mavrodi,D.V., Ksenzenko,V.N., Bonsall,R.F., Cook,R.J., Boronin,A.M., and Thomashow,L.S. (1998). A seven-gene locus for synthesis of phenazine-1-carboxylic acid by Pseudomonas fluorescens 2-79. J. Bacteriol., 180, 2541-2548.

Mazzola, M., R. J. Cook, et al. (1992). "Contribution of phenazine antibiotic biosynthesis to the ecological competence of fluorescent pseudomonads in soil habitats." Appl Environ Microbiol 58(8): 2616-24.

McClellan, S. A., X. Huang, et al. (2003). "Macrophages restrict Pseudomonas aeruginosa growth, regulate polymorphonuclear neutrophil influx, and balance pro- and anti-inflammatory cytokines in BALB/c mice." J Immunol 170(10): 5219-27.

McDonald, M., D. V. Mavrodi, et al. (2001). "Phenazine biosynthesis in Pseudomonas fluorescens: branchpoint from the primary shikimate biosynthetic pathway and role of phenazine-1,6-dicarboxylic acid." J Am Chem Soc 123(38): 9459-60.

McDonald,M., Wilkinson,B., Van't Land,C.W., Mocek,U., Lee,S., and Floss,H.G. (1999). Biosynthesis of phenazine antibiotics in Streptomyces antibioticus: Stereochemistry of methyl transfer from carbon-2 of acetate. Journal of the American Chemical Society, 121, 5619-5624.

Messenger, A. J. and J. M. Turner (1978). "Phenazine-1,6-dicarboxylate as the common precursor of other bacterial phenazines [proceedings]." Biochem Soc Trans 6(6): 1326-8.

Millican R C. (1963) “Thiobarbituric acid assay for shikimic acid.” Anal Biochem. 6:181-92A

Mittal, R., S. Sharma, et al. (2006). "Contribution of quorum-sensing systems to virulence of Pseudomonas aeruginosa in an experimental pyelonephritis model." J Microbiol Immunol Infect 39(4): 302-9.

Mohanty, P., B. Z. Braun, et al. (1973). "Light-induced slow changes in chlorophyll a fluorescence in isolated chloroplasts: effects of magnesium and phenazine methosulfate." Biochim Biophys Acta 292(2): 459-76.

Mosher, C. W., D. Y. Lee, et al. (1979). "A phenazine analogue of actinomycin D." J Med Chem 22(8): 918-22.

Muhlradt, P. F., H. Tsai, et al. (1986). "Effects of pyocyanine, a blue pigment from Pseudomonas aeruginosa, on separate steps of T cell activation: interleukin 2 (IL 2) production, IL 2 receptor formation, proliferation and induction of cytolytic activity." Eur J Immunol 16(4): 434-40.

Muller, M. (1995). "Scavenging of neutrophil-derived superoxide anion by 1-hydroxyphenazine, a phenazine derivative associated with chronic Pseudomonas aeruginosa infection: relevance to cystic fibrosis." Biochim Biophys Acta 1272(3): 185-9.

Muller, M. and T. C. Sorrell (1995). "Inhibition of the human platelet cyclooxygenase response by the naturally occurring phenazine derivative, 1-hydroxyphenazine." Prostaglandins 50(5-6): 301-11.

Muller, M., K. Sztelma, et al. (1994). "Inhibition of platelet eicosanoid metabolism by the bacterial phenazine derivative pyocyanin." Ann N Y Acad Sci 744: 320-2.

Muller, P. K., K. Krohn, et al. (1989). "Effects of pyocyanine, a phenazine dye from Pseudomonas aeruginosa, on oxidative burst and bacterial killing in human neutrophils." Infect Immun 57(9): 2591-6.

Murshudov G., Vagin A., Dodson E., (1996) “Application of Maximum Likelihood Refinement" in the Refinement of Protein structures, Proceedings of Daresbury Study Weekend.

Murshudov G.N., Lebedev A., Vagin A.A., Wilson K.S.,.Dodson E.J (1999) "Efficient anisotropic refinement of Macromolecular structures using FFT" Acta Cryst. section D55, 247-255.

Murshudov G.N., Vagin A.A., Dodson E.J., (1997) "Refinement of Macromolecular Structures by the Maximum-Likelihood Method" in Acta Cryst. D53, 240-255.

Murshudov,G.N., Vagin,A.A., and Dodson,E.J. (1997). Refinement of macromolecular structures by the maximum-likelihood method. Acta Crystallographica Section D-Biological Crystallography, 53, 240-255.

O'Malley YQ, Reszka KJ, Spitz DR, Denning GM, Britigan BE. (2004(. “Pseudomonas aeruginosa pyocyanin directly oxidizes glutathione and decreases its levels in airway epithelial cells.” Am. J. Physiol. 287L:94–103

Ozaki, T., M. Maeda, et al. (1989). "Role of alveolar macrophages in the neutrophil-dependent defense system against Pseudomonas aeruginosa infection in the lower respiratory tract. Amplifying effect of muramyl dipeptide analog." Am Rev Respir Dis 140(6): 1595-601.

Pannu N.J., Murshudov G.N., Dodson E.J., Read R.J. (1998) "Incorporation of Prior Phase Information Strengthen Maximum-Likelihood Structure Refinemen" Acta Cryst. section D54, 1285-1294.

Parsons, J. F., F. Song, et al. (2004). "Structure and function of the phenazine biosynthesis protein PhzF from Pseudomonas fluorescens 2-79." Biochemistry 43(39): 12427-35.

Parsons,J.F., Song,F., Parsons,L., Calabrese,K., Eisenstein,E., and Ladner,J.E. (2004). Structure and function of the phenazine biosynthesis protein PhzF from Pseudomonas fluorescens 2-79. Biochemistry, 43, 12427-12435.

Patel, M., V. Hegde, et al. (1984). "A novel phenazine antifungal antibiotic, 1,6-dihydroxy-2-chlorophenazine. Fermentation, isolation, structure and biological properties." J Antibiot (Tokyo) 37(9): 943-8.

Perrakis,A., Morris,R., and Lamzin,V.S. (1999). Automated protein model building combined with iterative structure refinement. Nature Structural Biology, 6, 458-463.

Pesci EC, Pearson JP, Seed PC, Iglewski BH. (1997). “Regulation of las and rhl quorum sensing in Pseudomonas aeruginosa.” J. Bacteriol. 179:3127–32

Phillips, I. (1969). "Identification of Pseudomonas aeruginosa in the clinical laboratory." J Med Microbiol 2(1): 9-16.

Pierson, L. S., 3rd and L. S. Thomashow (1992). "Cloning and heterologous expression of the phenazine biosynthetic locus from Pseudomonas aureofaciens 30-84." Mol Plant Microbe Interact 5(4): 330-9.

Pierson, L. S., 3rd, T. Gaffney, et al. (1995). "Molecular analysis of genes encoding phenazine biosynthesis in the biological control bacterium. Pseudomonas aureofaciens 30-84." FEMS Microbiol Lett 134(2-3): 299-307.

Pierson, L. S., 3rd, V. D. Keppenne, et al. (1994). "Phenazine antibiotic biosynthesis in Pseudomonas aureofaciens 30-84 is regulated by PhzR in response to cell density." J Bacteriol 176(13): 3966-74.

Pitt, T. L. (1986). "Biology of Pseudomonas aeruginosa in relation to pulmonary infection in cystic fibrosis." J R Soc Med 79 Suppl 12: 13-8.

Price-Whelan, A., L. E. Dietrich, et al. (2006). "Rethinking 'secondary' metabolism: physiological roles for phenazine antibiotics." Nat Chem Biol 2(2): 71-8.

Podojil M, Gerber N. N., (1970) “Biosynthesis of 1,6-phenazinediol 5,10-dioxide (iodinin). Incorporation of shikimic acid.“ Biochemistry. Nov 10;9(23):4616-8

Raaijmakers J. M., Weller D. M., (2001). “Exploiting genotypic diversity of 2,4-diacetylphloroglucinol-producing Pseudomonas spp.: characterization of superior root-colonizing P. fluorescens strain Q8r1-96.” Appl. Environ. MicroBiol. 67:2545–54

Raaijmakers J. M., Vlami M., de Souza J. T., (2002). ”Antibiotic production by bacterial biocontrol agents.” Antonie Van Leeuwenhoek 81:537–47

Rabaey, I., W. Ossieur, et al. (2005). "Continuous microbial fuel cells convert carbohydrates to electricity." Water Sci Technol 52(1-2): 515-23.

Rabaey, K., P. Clauwaert, et al. (2005). "Tubular microbial fuel cells for efficient electricity generation." Environ Sci Technol 39(20): 8077-82.

Rahme, L. G., M. W. Tan, et al. (1997). "Use of model plant hosts to identify pseudomonas aeruginosa virulence factors." Proc Natl Acad Sci U S A 94(24): 13245-50.

Ran,H.M., Hassett,D.J., and Lau,G.W. (2003). Human targets of Pseudomonas aeruginosa pyocyanin. Proceedings of the National Academy of Sciences of the United States of America, 100, 14315-14320.

Rhodes G. (2000) “Crystallography Made Crystal Clear.” Academic Press. CA.

Rossmann, M. G. and C. G. van Beek (1999). "Data processing." Acta Crystallogr D Biol Crystallogr 55(Pt 10): 1631-40.

Safo, M. K., F. N. Musayev, et al. (2005). "Structure of escherichia coli pyridoxine 5'-phosphate oxidase in a tetragonal crystal form: Insights into the mechanistic pathway of the enzyme." Acta Crystallogr D Biol Crystallogr 61(Pt 5): 599-604.

Safo, M. K., I. Mathews, et al. (2000). "X-ray structure of escherichia coli pyridoxine 5'-phosphate oxidase complexed with fmn at 1.8 a resolution." Structure 8(7): 751-62.

Saiki,R.K., Scharf,S., Faloona,F., Mullis,K.B., Horn,G.T., Erlich,H.A., and Arnheim,N. (1985). Enzymatic amplification of beta-globin genomic sequences and restriction site analysis for diagnosis of sickle cell anemia. Science, 230, 1350-1354.

Sambrook J, Fritsch E, Maniatis T (1989) “Molecular Cloning: a Laboratory Manual”, 2nd edn. Cold Spring Harbor Laboratory Press, New York.

Sato,A., Takahashi,S., Ogita,T., Sugano,M., and Kodama,K. (1995). Marine Natural Product. Annu Rep Sankyo Res Lab, 47, 1-58.

Schmidt, W. and W. Gabler (1973). "The influence of phenazine methosulphate on the histochemical demonstration of steroid dehydrogenases." Folia Morphol (Praha) 21(2): 172-4.

Schneider,T.R. and Sheldrick,G.M. (2002). Substructure solution with SHELXD. Acta Crystallographica Section D-Biological Crystallography, 58, 1772-1779.

Schwartz, M. (1967). "Wavelength-dependent quantum yields of chloroplast phosphorylation catalyzed by phenazine methosulphate." Biochim Biophys Acta 131(3): 548-58.

Schroth, M. N., Hancock, J. G. (1982) “Disease suppressive soil and root colonizing bacteria.” Science 216:1337-81

Sheldon,P.J., Johnson,D.A., August,P.R., Liu,H.W., and Sherman,D.H. (1997). Characterization of a mitomycin-binding drug resistance mechanism from the producing organism, Streptomyces lavendulae. Journal of Bacteriology, 179, 1796-1804.

Sheldon,P.J., Mao,Y.Q., He,M., and Sherman,D.H. (1999). Mitomycin resistance in Streptomyces lavendulae includes a novel drug-binding-protein-dependent export system. Journal of Bacteriology, 181, 2507-2512.

Shindyalov,I.N. and Bourne,P.E. (1998). Protein structure alignment by incremental combinatorial extension (CE) of the optimal path. Protein Engineering, 11, 739-747.

Shoji, J., R. Sakazaki, et al. (1988). "Isolation of a new phenazine antibiotic, DOB-41, from Pseudomonas species." J Antibiot (Tokyo) 41(5): 589-94.

Singh, M. P., A. T. Menendez, et al. (1997). "Biological and mechanistic activities of phenazine antibiotics produced by culture LL-14I352." J Antibiot (Tokyo) 50(9): 785-7.

Slininger, P. J. and M. A. Shea-Wilbur (1995). "Liquid-culture pH, temperature, and carbon (not nitrogen) source regulate phenazine productivity of the take-all

biocontrol agent Pseudomonas fluorescens 2-79." Appl Microbiol Biotechnol 43(5): 794-800.

Slininger, P. J., K. D. Burkhead, et al. (2000). "Isolation, identification, and accumulation of 2-acetamidophenol in liquid cultures of the wheat take-all biocontrol agent Pseudomonas fluorescens 2-79." Appl Microbiol Biotechnol 54(3): 376-81.

Smirnov V, Kiprianova E. (1990). “Bacteria of Pseudomonas genus.” Kiev: Naukova Dumka. 264 pp. (In Russian)

Sorensen, R. U. and J. D. Klinger (1987). "Biological effects of Pseudomonas aeruginosa phenazine pigments." Antibiot Chemother 39: 113-24.

Stout, J. and Jensen, L. H., (1988) “X-ray structure determination”. Wiley Interscience.

Sugiyama,M., Kumagai,T., Hayashida,M., Maruyama,M., and Matoba,Y. (2002). The 1.6-A crystal structure of the copper(II)-bound bleomycin complexed with the bleomycin-binding protein from bleomycin-producing Streptomyces verticillus. Journal of Biological Chemistry, 277, 2311-2320.

Tan,M.W., Mahajan-Miklos,S., and Ausubel,F.M. (1999). Killing of Caenorhabditis elegans by Pseudomonas aeruginosa used to model mammalian bacterial pathogenesis. Proceedings of the National Academy of Sciences of the United States of America, 96, 715-720.

Tanaka, E., Y. Yuba, et al. (1994). "Effects of the beige mutation on respiratory tract infection with Pseudomonas aeruginosa in mice." Exp Lung Res 20(4): 351-66.

Taylor, G. (2003). "The phase problem." Acta Crystallogr D Biol Crystallogr 59(Pt 11): 1881-90.

Terashima, T., M. Kanazawa, et al. (1995). "Neutrophil-induced lung protection and injury are dependent on the amount of Pseudomonas aeruginosa administered via airways in guinea pigs." Am J Respir Crit Care Med 152(6 Pt 1): 2150-6.

Thomashow, L. S. and D. M. Weller (1988). "Role of a phenazine antibiotic from Pseudomonas fluorescens in biological control of Gaeumannomyces graminis var. tritici." J Bacteriol 170(8): 3499-508.

Thomashow, L. S., D. M. Weller, et al. (1990). "Production of the Antibiotic Phenazine-1-Carboxylic Acid by Fluorescent Pseudomonas Species in the Rhizosphere of Wheat." Appl Environ Microbiol 56(4): 908-12.

Mavrodi D.V., Blankenfeldt W., Thomashow L.S., “Phenazine Compounds in Fluorescent Pseudomonas Spp. Biosynthesis and Regulation.” (2006)Annu Rev Phytopathol. [Epub ahead of print]

Timms-Wilson, T. M., R. J. Ellis, et al. (2000). "Chromosomal insertion of phenazine-1-carboxylic acid biosynthetic pathway enhances efficacy of damping-off disease control by Pseudomonas fluorescens." Mol Plant Microbe Interact 13(12): 1293-300.

Timms-Wilson,T.M., Ellis,R.J., Renwick,A., Rhodes,D.J., Mavrodi,D.V., Weller,D.M., Thomashow,L.S., and Bailey,M.J. (2000). Chromosomal insertion of phenazine-1-carboxylic acid biosynthetic pathway enhances efficacy of damping-off disease control by Pseudomonas fluorescens. Mol. Plant Microbe Interact., 13, 1293-1300.

Toohey J. I., Nelson C. D., Krotkov G., (1965). ”Toxicity of phenazine carboxylic acids in some bacteria, algae, higher plants, and animals.” Can. J. Bot. 43:1151–55

Turner,J.M. and Messenger,A.J. (1986). Occurrence, biochemistry and physiology of phenazine pigment production. Adv. Microb. Physiol, 27, 211-275.

Umezawa, H. and T. Takeuchi (1951). "Nitrosporin, antibiotic from streptomyces nitrosporeus active to gram positive bacteria." Jpn J Med 4(3): 173-9.

Umezawa, H., T. Tazaki, et al. (1951). "An antiviral substance, abikoviromycin, produced by streptomyces species." Jpn J Med 4(5): 331-46.

Usher, L. R., R. A. Lawson, et al. (2002). "Induction of neutrophil apoptosis by the Pseudomonas aeruginosa exotoxin pyocyanin: a potential mechanism of persistent infection." J Immunol 168(4): 1861-8.

Wallace,A.C., Laskowski,R.A., and Thornton,J.M. (1995). Ligplot - A Program to Generate Schematic Diagrams of Protein Ligand Interactions. Protein Engineering, 8, 127-134.

van den Broek, D., A. W. T. F. Chin, et al. (2003). "Biocontrol traits of Pseudomonas spp. are regulated by phase variation." Mol Plant Microbe Interact 16(11): 1003-12.

van den Broek, D., A. W. T. F. Chin, et al. (2005). "Molecular nature of spontaneous modifications in gacS which cause colony phase variation in Pseudomonas sp. strain PCL1171." J Bacteriol 187(2): 593-600.

van den Broek, D., G. V. Bloemberg, et al. (2005). "The role of phenotypic variation in rhizosphere Pseudomonas bacteria." Environ Microbiol 7(11): 1686-97.

van Rij E. T., Girard G., Lugtenberg B. J. J., Bloemberg G. V.,(2005). ”Influence of fusaric acid on phenazine-1-carboxamide synthesis and gene expression of Pseudomonas chlororaphis strain PCL1391.” Microbiology 151:2805–14

van Rij, E. T., G. Girard, et al. (2005). "Influence of fusaric acid on phenazine-1-carboxamide synthesis and gene expression of Pseudomonas chlororaphis strain PCL1391." Microbiology 151(Pt 8): 2805-14.

van Rij, E. T., M. Wesselink, et al. (2004). "Influence of environmental conditions on the production of phenazine-1-carboxamide by Pseudomonas chlororaphis PCL1391." Mol Plant Microbe Interact 17(5): 557-66.

Vantland,C.W., Mocek,U., and Floss,H.G. (1993). Biosynthesis of the Phenazine Antibiotics, the Saphenamycins and Esmeraldins, in Streptomyces-Antibioticus. Journal of Organic Chemistry, 58, 6576-6582.

Wallace, A. C., R. A. Laskowski, et al. (1995). "Ligplot: A program to generate schematic diagrams of protein-ligand interactions." Protein Eng 8(2): 127-34.

Watanabe, T., T. Hirayama, et al. (1989). "Phenazine derivatives as the mutagenic reaction product from o- or m-phenylenediamine derivatives with hydrogen peroxide." Mutat Res 227(3): 135-45.

Watanabe, T., T. Kasai, et al. (1996). "Genotoxicity in vivo of phenazine and aminophenazines assayed in the wing spot test and the DNA-repair test with Drosophila melanogaster." Mutat Res 369(1-2): 75-80.

Whistler, C. A. and L. S. Pierson, 3rd (2003). "Repression of phenazine antibiotic production in Pseudomonas aureofaciens strain 30-84 by RpeA." J Bacteriol 185(13): 3718-25.

White, J. R. and H. H. Dearman (1965). "Generation of free radicals from phenazine methosulfate, streptonigrin, and riboflavin in bacterial suspensions." Proc Natl Acad Sci U S A 54(3): 887-91.

Villavicencio RT. (1998) “The history of blue pus.”J Am Coll Surg. 187(2):212-6

Wilson R., Sykes D. A., Watson D., Rutman A., Taylor G. W., Cole P. J., (1988). “Measurement of Pseudomonas aeruginosa phenazine pigments in sputum and assessment of their contribution to sputum sol toxicity for respiratory epithelium.” Infect. Immun. 56:2515–17

Vining LC. (1990).”Functions of secondary metabolites.” Annu Rev Microbiol; 44:395-427

Winn M., Isupov M., Murshudov G.N. (2001) "Use of TLS parameters to model anisotropic displacements in macromolecular refinement" Acta Cryst. D57, 122-133

Wood D.W., Pierson L.S., (1996). “The phzI gene of Pseudomonas aureofaciens 30-84 is responsible for the production of a diffusible signal required for phenazine antibiotic production.” Gene 168:49–53

Woodruff, A. W., B. Bisseru, et al. (1966). "Infection with animal helminths as a factor in causing poliomyelitis and epilepsy." Br Med J 5503: 1576-9.

Yang, E. S. and V. Schirch (2000). "Tight binding of pyridoxal 5'-phosphate to recombinant escherichia coli pyridoxine 5'-phosphate oxidase." Arch Biochem Biophys 377(1): 109-14.

Yang, F., L. H. Wang, et al. (2005). "Quorum quenching enzyme activity is widely conserved in the sera of mammalian species." FEBS Lett 579(17): 3713-7.

Yang, H., P. M. Johnson, et al. (2005). "Cloning, characterization and expression of escapin, a broadly antimicrobial fad-containing l-amino acid oxidase from ink of the sea hare aplysia californica." J Exp Biol 208(Pt 18): 3609-22.

Yang, W., L. Shi, et al. (2005). "Evaluation of the biofilm-forming ability and genetic typing for clinical isolates of pseudomonas aeruginosa by enterobacterial repetitive intergenic consensus-based pcr." Microbiol Immunol 49(12): 1057-61.

Zhang Z., Pierson L.S., (2001). “A second quorum-sensing system regulates cell surface properties but not phenazine antibiotic production in Pseudomonas aureofaciens.” Appl. Environ. MicroBiol. 67:4305–15

Acknowledgements

'I can no other answer make, but, thanks, and thanks.'
- William Shakespeare

Acknowledgements

I would like to take this opportunity to convey my heartfelt thanks to the following people,

First and foremost, my sincere gratitude to my supervisors, **Dr. Roger Goody and Dr. Wulf Blankenfeldt**. They have always been very generous with their time, knowledge, ideas and encouragement, not just in things science related, but life in general. Their support has been an immense source of strength and hope. Thank You!

Dr. Roland Winter, my third supervisor and committee member of the IMPRS-CB graduate school, for taking time to offer words of encouragement and for his helpful comments on my thesis.

Dr. Petra Janning, for her invaluable help with all mass spectroscopic work. Without her guidance and patience, this work would not have been accomplished with such precision and speed.

Dr. Linda Thomashow and Dr. Dimitri Mavrodi, our collaborators for their constant support and excellent guidance into the world of phenazines.

Petra Herde, for the best technical support anyone could ever hope for and for being such a wonderful friend, always patient and supportive.

Nathalie Bleimling for being my German teacher and for never being too busy to answer a multitude of question in or out of the lab.

Thanks are also due to the past and present members of **AG Blankenfeldt**, my **colleagues** and the **X-ray community** at the Max Planck for a wonderful and friendly atmosphere at work.

My parents and brothers, I thank for their patience and support and their desire to seek out the best for me, always.

My friends both in and outside Max Planck have made these three years a truly enriching and happy time, without them, life would not have had as much colour as it does. Many Thanks to you all!

A special ‘Dhanyavad’ to **Helen Chapelle, Tammy Woo, Dr. Sussane Eschenburg, Dr. Cristina Hartmann-Fatu** and **Dr. Ljiljana Fruk**, for sharing with me, every stumble and leap, on this journey called life.